Biochemistry & Molecular Biology of Plants, B. Buchanan, W. Gruissem, R. Jones, Eds.

CHAPTER 2

The Cell Wall

Nicholas Carpita
Maureen McCann

The protoplast is the cell's way of making more wall.
—*Joe Varner*

CHAPTER OUTLINE

Introduction

The shape of a plant cell is dictated largely by its cell wall. When a living plant cell is treated with cell-wall–degrading enzymes to remove the wall, the resulting membrane-bound **protoplast** is invariably spherical (Fig. 2.1). In living cells, the cell wall constrains the rate and direction of cell growth, exerting a profound influence on plant development and morphology. Cell walls contribute to the functional specialization of cell types. Within *Zinnia* leaves, for example, the shape of spongy parenchyma cells maximizes both the volume of the intercellular spaces and the surface area available for gas exchange (Fig. 2.2A), whereas the branched structure of trichomes (Fig. 2.2D) may be adapted for sending mechanical stimuli. In contrast, the papillae-shaped epidermal cells of a snapdragon petal reflect light, attracting the attention of pollinators (Fig. 2.2B). In some cells, including tracheary elements (Fig. 2.2C), the protoplast disintegrates during development, and the mature cell consists entirely of cell wall.

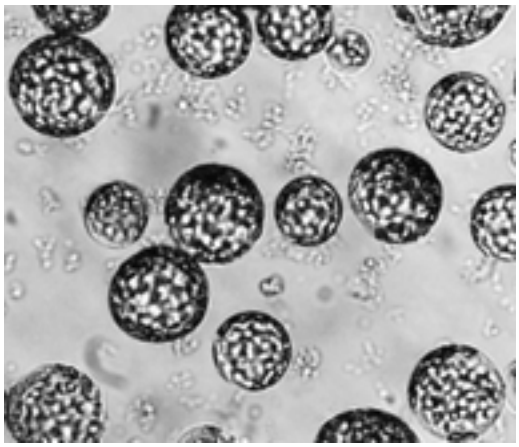

Figure 2.1
Without its wall, a protoplast adopts a spherical form.

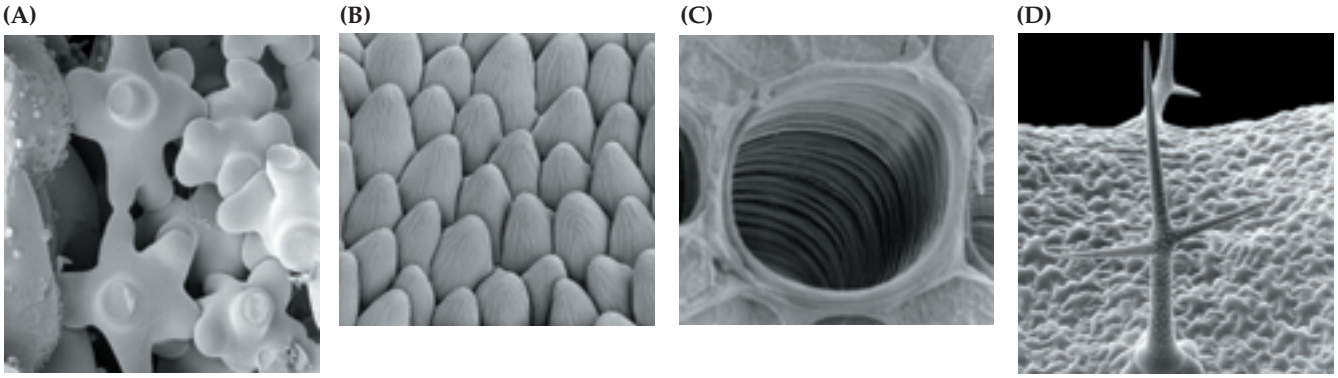

Figure 2.2
A developing cell can change its wall architecture to provide myriad forms. (A) The spongy parenchyma of a *Zinnia* leaf minimizes cell contact and maximizes cell surface for gas exchange. (B) The specialized shapes of these epidermal cells reflect light to enrich the colors of a snapdragon petal. (C) The secondary thickenings of a tracheid prevent collapse of the wall from the tension created by the transpirational pull. (D) An *Arabidopsis* trichome is an exquisitely branched modified epidermal cell.

The plant cell wall is a dynamic compartment that changes throughout the life of the cell. The new **primary cell wall** (Fig. 2.3) is born in the cell plate during cell division (see Chapter 5) and rapidly increases in surface area during cell expansion, in some cases by more than a hundred-fold. The **middle lamella** forms the interface between the primary walls of neighboring cells. Finally, at differentiation, many cells elaborate within the primary wall a **secondary cell wall** (Fig. 2.4), building complex structures uniquely suited to the cell's function.

The plant cell wall is a highly organized composite of many different polysaccharides, proteins, and aromatic substances. Some structural molecules act as fibers, others as a cross-linked matrix, analogous to the glass-fibers-and-plastic matrix in fiberglass. The molecular composition and arrangements of the wall polymers differ among species, among tissues of a single species, among individual cells, and even among regions of the wall around a single protoplast (Fig. 2.5).

Not all specialized functions of cell walls are structural. Some cells walls contain molecules that affect patterns of development and mark a cell's position within the plant. Walls contain signaling molecules that participate in cell–cell and wall–nucleus communication. Fragments of cell wall polysaccharides may elicit the secretion of defense molecules, and the wall may become impregnated with protein and lignin to armor it against invading fungal and bacterial pathogens (Fig. 2.6;

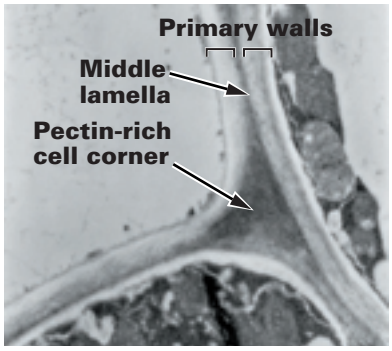

Figure 2.3
The primary walls of cells are capable of expansion. The middle lamella is formed during cell division and grows coordinately during cell expansion. Contact between certain cells is maintained by the middle lamella, and the cell corners are often filled with pectin-rich polysaccharides. In older cells (not shown), the material in the cell corners is sometimes degraded and an air space forms.

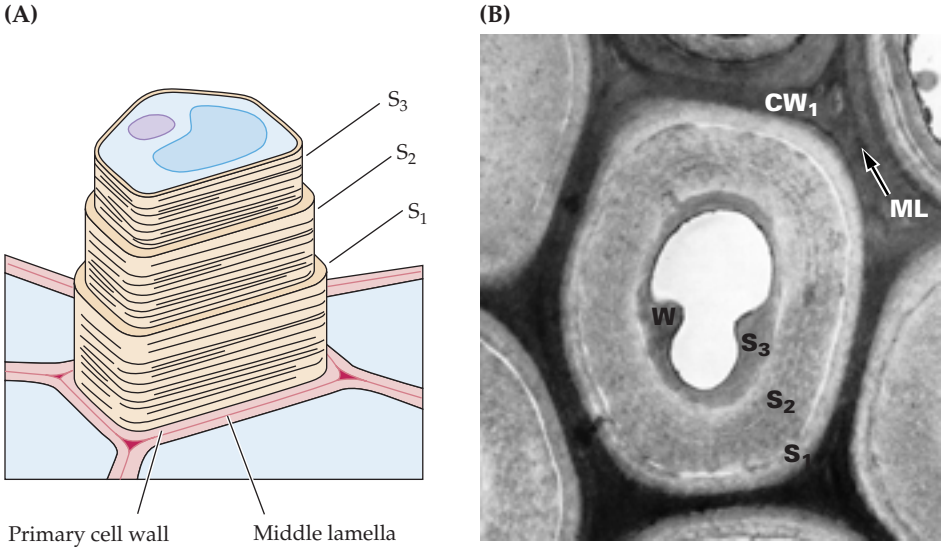

Figure 2.4
When they have achieved their final size and shape, some cells elaborate a multilayered secondary wall within the primary wall. In the diagram (A), the lumen of the cell is sometimes surrounded by several distinct kinds of secondary walls (here, S_1–S_3), with the original primary wall (CW_1) and the middle lamella (ML) constituting the outermost layers. As shown in this example of a fiber cell from a young stem of a locust tree, fibers may also contain "warts" (W), which are a last stage of wall thickening before the protoplast disintegrates (B).

see also Chapters 21 and 24). In other instances, the walls participate in early recognition of symbiotic nitrogen-fixing bacteria (see Chapter 16). Surface molecules on cell walls also allow plants to distinguish their own cells from foreign cells in pollen-style interactions (Fig. 2.7; see also Chapter 19).

2.1 Sugars: building blocks of the cell wall

Polysaccharides, polymers of sugar, are the principal components of the cell wall and form its main structural framework. Polysaccharides are long chains of sugar molecules

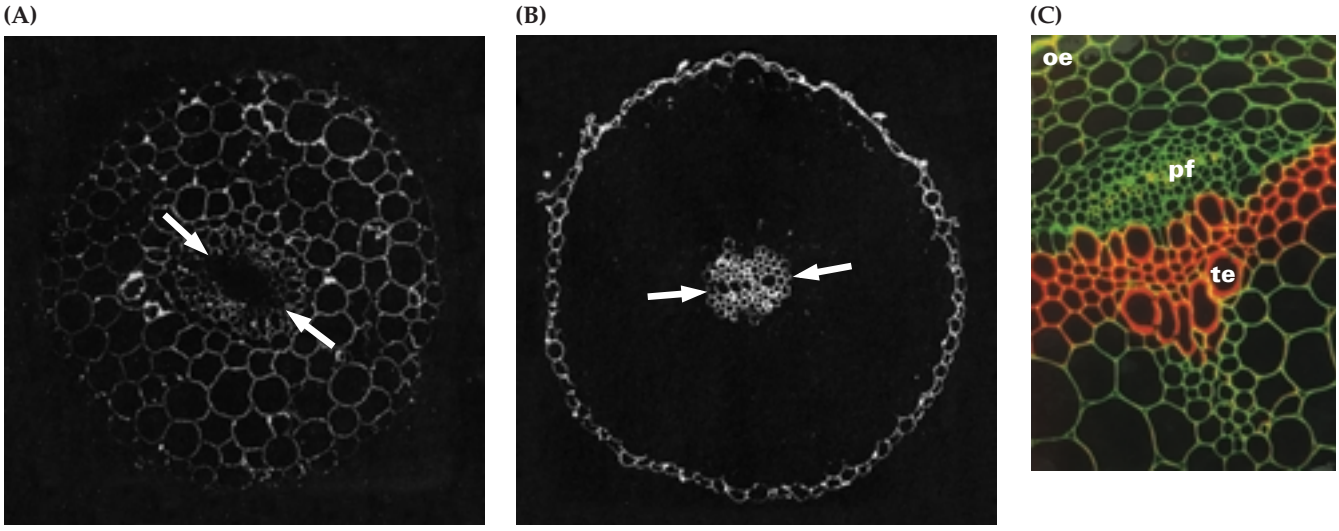

Figure 2.5
The production of complex, chemically diverse molecules within cell walls is developmentally regulated. (A, B) Staining walls of the oat root with two antibodies against arabinogalactan proteins demonstrates that different members of this class of molecules occur in specific tissues. One epitope is present only in cortical cell walls (A), whereas a second epitope is present only in walls of the vascular cylinder (arrows) and epidermis (B). (C) Antibodies against methyl-esterified pectin and unesterified pectins show that these epitopes are enriched not only in different cells but also in different regions of the walls of a single cell. In this cross-section of an *Arabidopsis* stem, domains enriched in methyl-esterified pectin are labeled in green, whereas deesterified pectins, shown in yellow, are found in specialized cells, such as the outer epidermal wall (oe), fiber cells of phloem (pf), some cell corners and cross-walls, and tracheary elements of the xylem (te). The autofluorescence of lignin is shown in red.

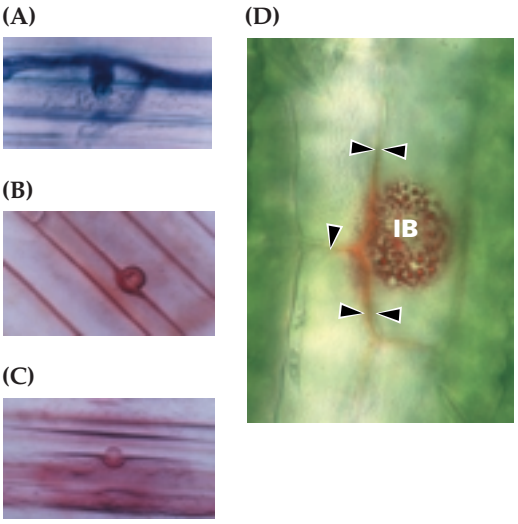

Figure 2.6
Cells often respond to potential pathogens and symbionts through alterations in their cell wall. In response to the attempt of a fungal hypha of *Colletotrichum,* stained with lactophenol-cotton Blue (A), to penetrate a maize cell, the cell produces a wall apposition called a papilla. Largely composed of callose, the papilla also accumulates lignin, as shown by staining with phloroglucinol (B) and by staining with syringaldehyde to detect laccase activity (C). (D) In its response to *Colletotrichum* invasion, an infected cell of sorghum accumulates phytoalexins in inclusion bodies (IB), and the neighboring cells armor their walls with the reddish phenylpropanoids (arrowheads).

covalently linked at various positions, some being decorated with side chains of various lengths. Familiarity with the chemistry and nomenclature of sugars will greatly facilitate understanding of the many biological functions of the cell wall polysaccharides.

Sugars represent a vast spectrum of polyhydroxyl aldehydes **(aldoses)** and ketones **(ketoses)** that can be grouped according to their chemical formula, configuration, and stereochemical conformation. Almost all cell wall sugars are aldoses. Many sugars have the empirical formula $(CH_2O)_n$, from which the term **carbohydrate** is derived.

Numerical prefixes define how many carbons a sugar contains. For example, a triose has three carbon atoms, a pentose five, and a hexose six. All sugar molecules can assume a straight-chain conformation, and those containing four carbons or more can also rearrange into heterocyclic rings (Fig. 2.8). Sugars that adopt a five-membered ring configuration (four carbons and an oxygen) are called **furanoses,** whereas those forming six-membered rings (five carbons and an oxygen) are **pyranoses.** The ring conformation a sugar adopts is not defined by the number of carbons: Both pentoses and hexoses can occur in either ring form.

Pyranose and furanose rings can be diagrammed by using either flat **Haworth projections** or conformational models (Fig. 2.8). The pyranose sugars assume the so-called "chair" conformation, whereas the furanose sugars are a "puckered" five-membered ring. The five tetrahedral carbon atoms forming a pyranose ring project the hydrogen and hydroxyl groups either in **equatorial** positions away from the ring or in **axial** positions above and below the ring. Pyranoses adopt one of two possible "chair" forms that will place as many hydroxyl or other bulky groups as possible in the equatorial position. For the common cell wall D-sugars, such as D-glucose, the $^4C_1$ conformation is more favorable, but for the deoxysugars L-fucose and L-rhamnose, the $^1C_4$-chair is the more favorable conformation (Fig. 2.9).

In aldoses, including the hexose glucose and the pentose arabinose, the C-1 is the **anomeric carbon,** the only carbon bound to two oxygen atoms. The other carbons are

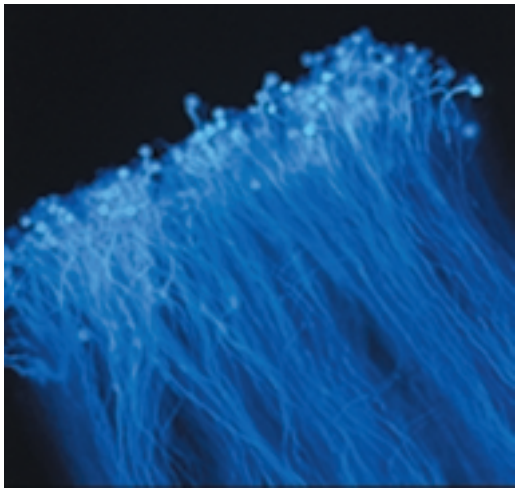

Figure 2.7
In a self-incompatibility response, growth of pollen tubes is terminated coincident with swelling of the pollen tube tips and formation of callose plugs, as observed here by staining with analine blue.

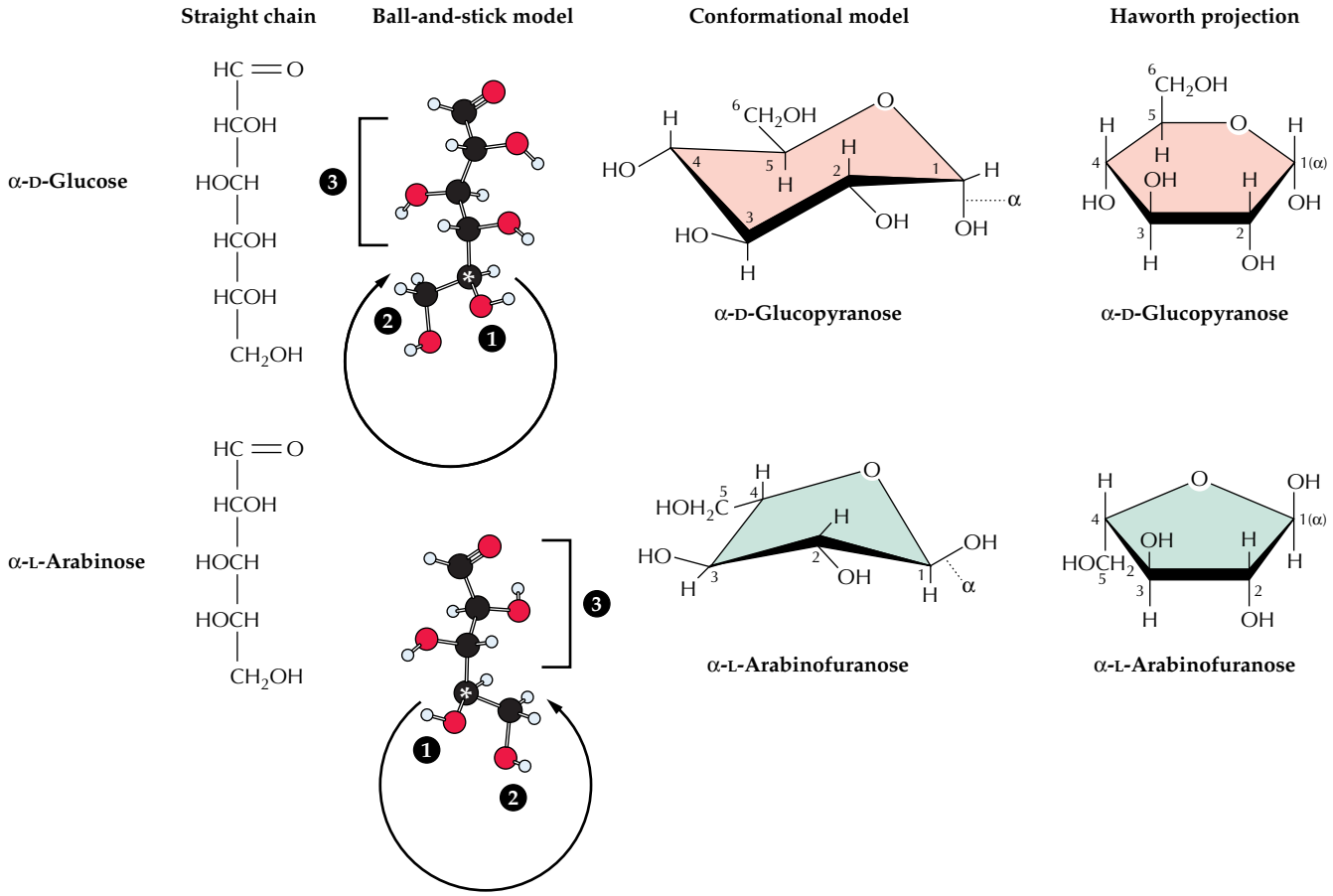

Figure 2.8
Sugar nomenclature. Both D-glucose and L-arabinose are shown (from left to right) in straight-chain models, ball-and-stick models, conformational models, and Haworth projections. The ball-and-stick model demonstrates the convention whereby the last asymmetric carbon (marked with an asterisk) is oriented with its hydrogen group to the rear. The three asymmetric groups are labeled numerically, 1 being the smallest and 3 the largest. The size of the three asymmetric groups increases clockwise for D-sugars or counterclockwise for L-sugars. The conformational model distinguishes the relative axial and equatorial positions of the hydroxyl groups around the ring structure of pyranoses. α-D-Glucose is the most stable of the hexoses because every hydroxyl group of the ring and the C-6 primary alcohol group are in the equatorial position, which is energetically more favorable than other orientations. By convention, the α configuration of L-arabinofuranose is in the "up" equatorial position.

numbered sequentially around the ring. The hydroxyl group of the anomeric carbon can be in (α) or (β) position. In solution, the hydroxyl group of the anomeric carbon will **mutarotate,** flip-flopping between the α and β configurations as the ring spontaneously opens and closes (see Chapter 13, Fig. 13.11). However, the hydroxyl becomes locked into a specific configuration when the anomeric carbon becomes linked to another molecule.

The designation D or L should always accompany reference to an α or β configuration. The D or L designation refers to the position of the hydroxyl group on the asymmetric **(chiral)** carbon farthest from the C-1 (i.e., the C-5 of hexoses and the C-4 of pentoses). An asymmetric carbon is one in which all four substituent groups are different, so that **enantiomers** (mirror images) of the structures cannot be superimposed. The D-configuration means that when viewed in a **ball and stick model,** the three larger groups of the last asymmetric carbon increase in size clockwise, whereas in the L-configuration they increase in size counterclockwise (see Fig. 2.8). Note that D and L do not correlate to the (+) or (–) designations for **dextrorotatory** or **levorotatory** optical rotation, which define as clockwise or counterclockwise, respectively, the direction in which a chemical species rotates plane-polarized light.

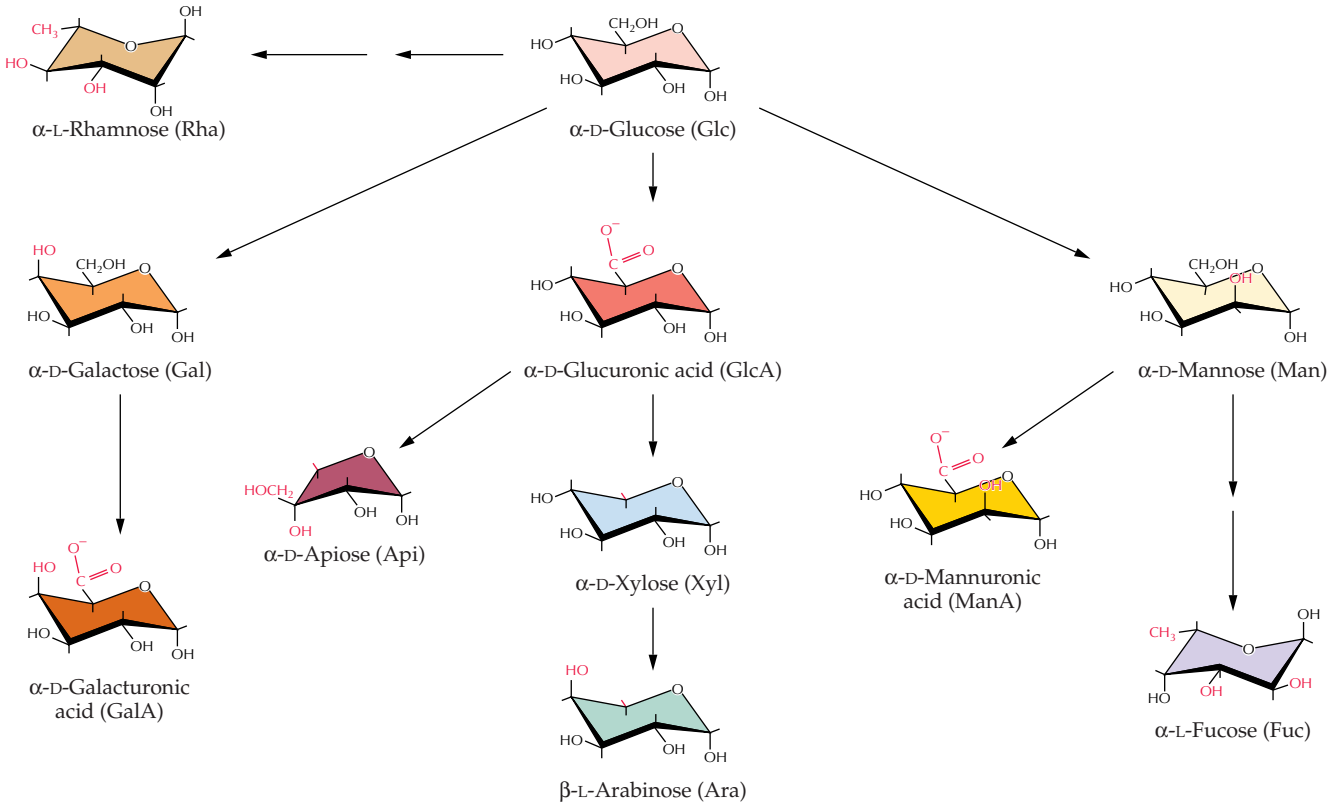

Figure 2.9
The common sugars of plant cell walls and their interconversion. The modifications needed to convert D-Glc into the other sugars are shown in red. L-Rha and L-Fuc adopt an alternative ring form to accommodate as many of the bulkier side groups as possible in the equatorial position. By convention, the "up" axial position is now the α configuration. The abbreviations of each of these sugars are specified by IUPAC-IUBMB convention and should be used exclusively. Note that L-Ara can assume both the α-furanose conformation shown in Fig. 2.8 and the β-pyranose conformation shown here.

2.1.1 The monosaccharides in cell wall polymers are derived from glucose.

D-Mannose (Man) and **D-galactose** (Gal) are **epimers** of D-glucose (Glc) made by converting the C-2 and C-4 hydroxyl groups, respectively, from the equatorial to the axial positions (Fig. 2.9). The C-6 primary alcohols of these three sugars can be oxidized to a carboxylic acid group to form **D-mannuronic acid** (ManA), **D-galacturonic acid** (GalA), or **D-glucuronic acid** (GlcA). Enzymatic removal of the carboxyl group from D-glucuronic acid forms the pentapyranose **D-xylose** (Xyl), a sugar in which all of the carbons are part of the heterocyclic ring. A rare branched sugar, **D-apiose** (Api), also is formed from D-GlcA. The C-4 epimer of D-xylose is **L-arabinose** (Ara). The D to L conversion occurs because, in this instance, the epimerization occurs at C-4, the last asymmetric carbon.

Carbon 6 of some hexapyranoses also can be dehydrated to methyl groups, creating deoxysugars. In plants, the two major cell wall deoxysugars are 6-deoxy-L-mannose, called **L-rhamnose** (Rha), and 6-deoxy-L-galactose, called **L-fucose** (Fuc). This spontaneously changes the conformation of L-Rha and L-Fuc from the $^4C_1$-chair conformation to the more favorable $^1C_4$-chair conformation (Fig. 2.9).

2.1.2 Polymers of specific sugars are further defined by their linkage type and the configuration of the anomeric carbon.

Sugars in polymers are always locked in pyranose or furanose rings. During sugar polymerization, the anomeric carbon of one sugar molecule is joined to the hydroxyl group of another sugar, a sugar alcohol, a

hydroxylamino acid, or a **phenylpropanoid** compound in a **glycosidic linkage.** A sugar can be attached to D-glucose at O-2, O-3, O-4, or O-6, that is, to the hydroxyl oxygens on C-2, C-3, C-4, or C-6. Only the O-5 position is unavailable, because it constitutes part of the ring structure.

A disaccharide can be described with respect to both linkage and anomeric configuration. For example, cellobiose is β-D-glucosyl-(1→4)-D-glucose: The anomeric linkage forms when the C-1 of one D-glucose residue is replaced by the equatorial hydroxyl at the C-4 position of the other D-glucose (Fig. 2.10). Only one D-glucose is locked in the β configuration; the other D-glucose is undesignated because its anomeric hydroxyl group is free to mutarotate in solution. Because the aldehyde of this sugar is able to reduce copper under alkaline conditions, it classically is described as a **reducing sugar,** and this end of even a very long polymer is called the **reducing end.** Branched polysaccharides will have a **nonreducing sugar** at the end of each side chain and at the terminus of the backbone but only a single reducing end.

Note that in cellobiose the anomeric carbon of one glucose is linked to the hydroxyl group farthest away from the anomeric carbon of the other glucose. For the β-linkage to occur with the C-4 equatorial hydroxyl group, the sugars to be linked must be inverted almost 180° relative to each other; iteration of this linkage produces a nearly linear molecule. In contrast, the units of laminaribiose, or β-D-glucosyl-(1→3)-D-glucose (Fig. 2.10), are linked somewhat askew; iteration of this linkage produces a helical polymer. Polysaccharides are named after the principal sugars that constitute them. Most polysaccharides have a backbone structure, and the composition of this structure is indicated by the last sugar in the polymer's name. For example, xyloglucan has a backbone of C-4–linked glucosyl residues to which xylosyl units are attached, glucuronoarabinoxylan has a backbone of C-4–linked xylosyl residues to which glucosyluronic acid and arabinosyl units are attached, and so forth.

2.1.3 Carbohydrate structures offer great functional flexibility.

What makes sugar subunits such versatile building materials is their ability to form linkages at multiple positions. With 11 different sugars commonly found in plant cell walls (see Fig. 2.9), 4 different linkage positions, and 2 configurations with respect to the oxygen atom, the permutations of pentasaccharide structure exceed 5×10^9! Glucose alone can form almost 15,000 different pentameric structures. Moreover, multiple bonding positions make possible the formation of branched polysaccharides, enormously increasing the number of possible structures. Fortunately for cell wall researchers, the structures of some of the major wall components are relatively conserved among species.

The two major tools that carbohydrate chemists use to elucidate the structure of highly complex polysaccharides are methylation analysis (Box 2.1) and nuclear magnetic resonance (NMR) spectroscopy (Box 2.2).

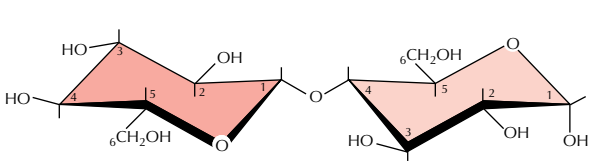

Cellobiose
(β-D-Glucosyl-(1→4)-D-glucose)

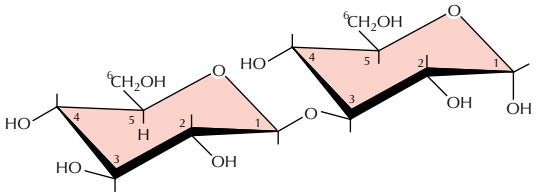

Laminaribiose
(β-D-Glucosyl-(1→3)-D-glucose)

Figure 2.10
Linkage structures of cellobiose and laminaribiose. The (1→4)β-D-linkage of cellobiose inverts the glucosyl unit about 180° with respect to each neighbor, whereas the (1→3)β-D-linkage is only slightly askew. (The shading of the glucose units is used to illustrate the 180° inversion).

Box 2.1 Methylation analysis determines carbohydrate linkage structure.

Strong acids can break the glycosidic linkages of polysaccharides, freeing the individual monosaccharide components. The monosaccharides can then be chemically reduced with borohydride and acetylated with acetic anhydride to make **alditol acetates.** For example, the complex xyloglucan shown in panel A of the figure is hydrolyzed to its four major sugar components. Ketoses (not shown in figure) are reduced to a mixture of C-2 epimers of the equivalent alditols. The alditol acetates derived from different sugars are volatile at different temperatures and can be separated on that basis by **gas–liquid chromatography.** The derivatives are injected onto a thin capillary column coated with a highly polar, waxy, liquid phase to which they adhere. The temperature is then raised to the point at which the interaction with the wax is broken, and the derivatives are swept out of the column by an inert carrier gas to a detector. If a temperature gradient is applied, different sugars will elute at different times (panel B). By comparing these results with the behavior of similarly treated standards, one can determine the molar ratio of each sugar in the original sample. Frequently, the types of sugars present in the sample and their molar ratios will give a good indication of the type of polysaccharide.

However, complex polysaccharides cannot be identified from their derivative content alone. Polymer backbones are built from unit structures of one to a few repeated sugars and linkages but are frequently substituted with appendant sugar units and side chains that may themselves be further branched. Linkage structure of polysaccharides can be deduced indirectly by a method called **methylation analysis.** Polysaccharides are chemically methylated with methyl iodide at every free hydroxyl group. The carbon atoms that participate in glycosidic linkages and in the ring do not have a free hydroxyl group and thus are not methylated. The methylated polysaccharide is hydrolyzed into its components of partly methylated monosaccharides, and then these components are reduced and acetylated as before. However, because linkage analyses of certain derivatives depend on the ability to differentiate the top of the molecule or molecular fragment from its bottom,

(Continued)

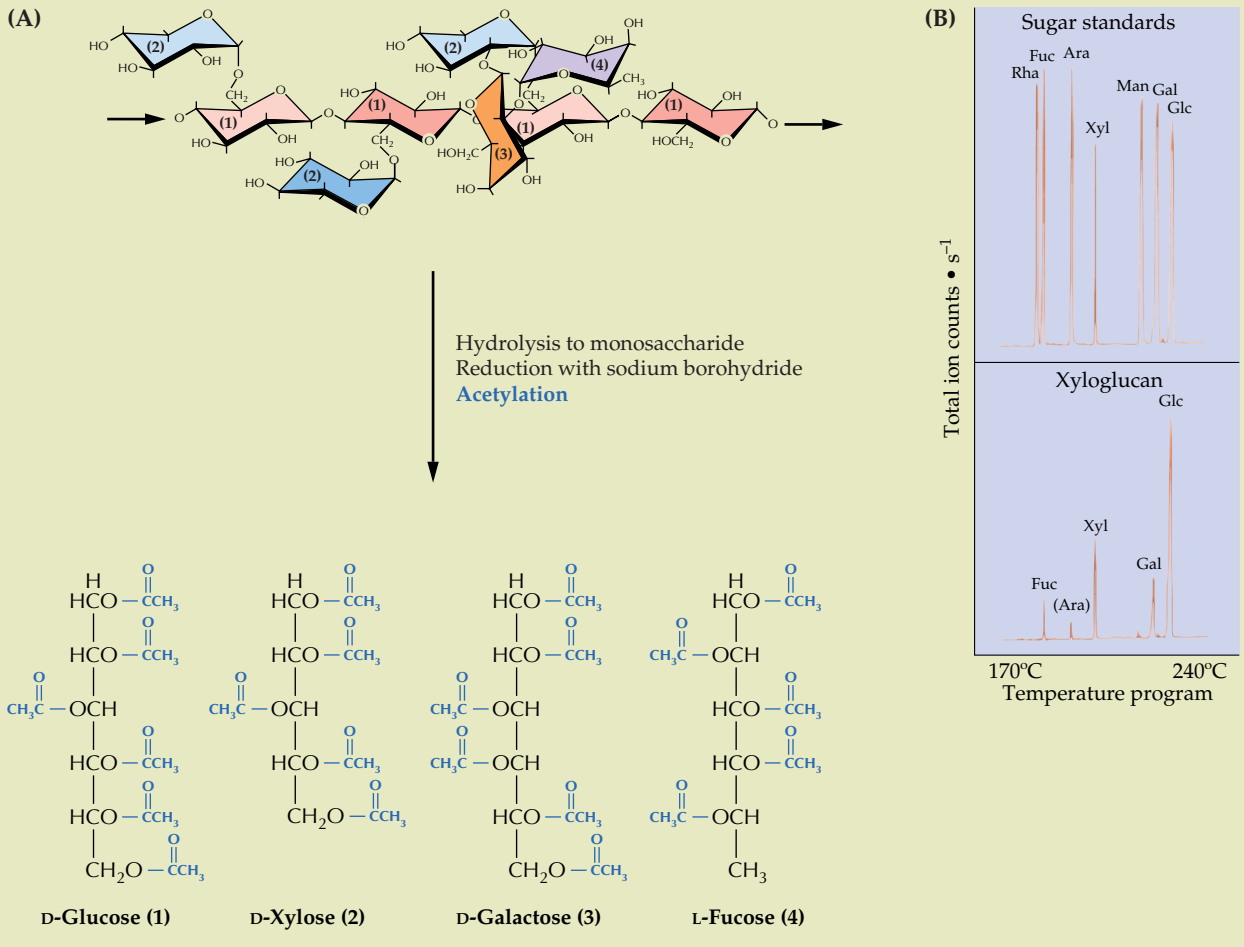

Box 2.1 *(continued)* Methylation analysis determines carbohydrate linkage structure.

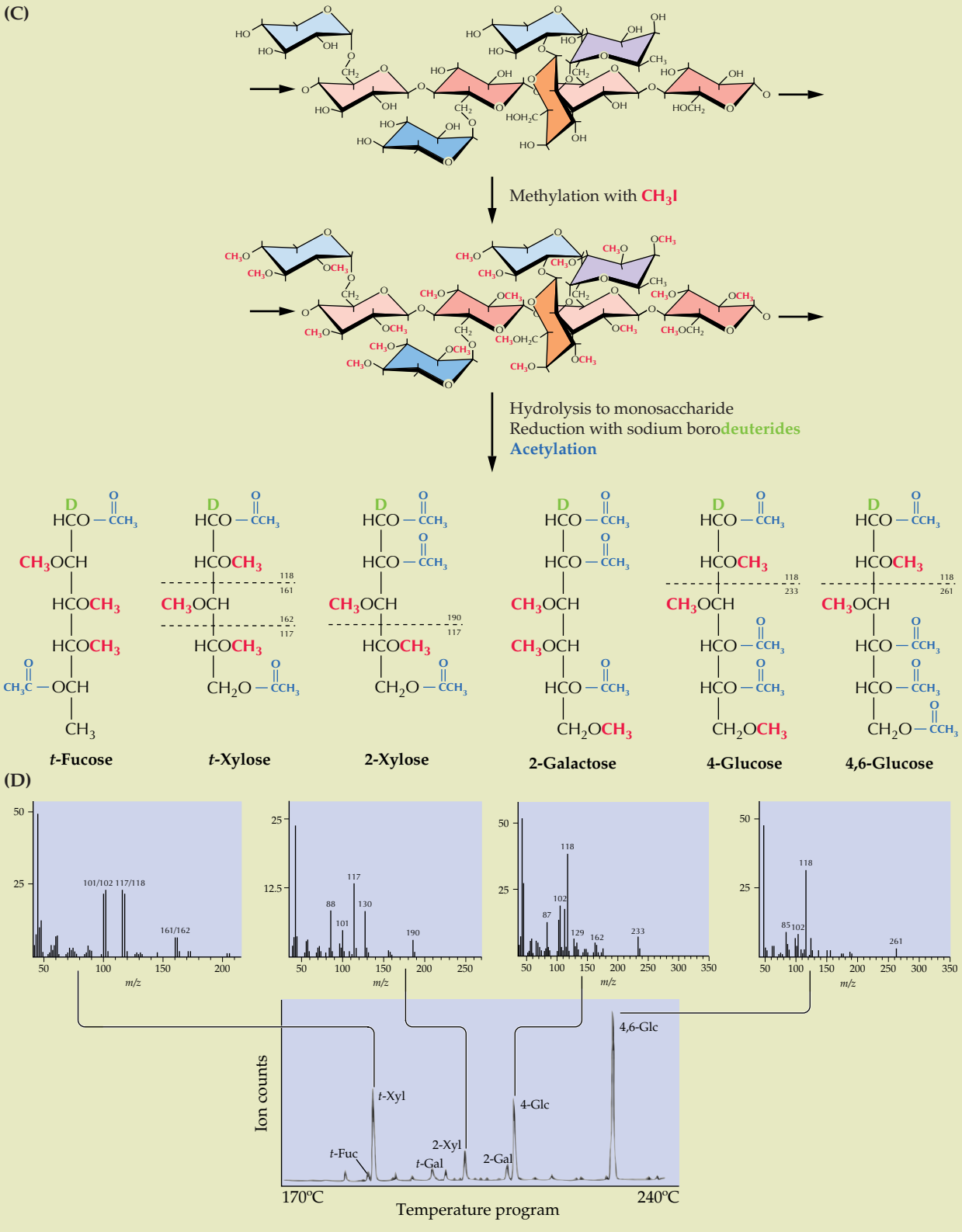

the reducing agent borodeuteride is used to label the C-1 alcohol and thus fix its position in later analyses. These partly methylated alditol acetates are resolved by gas–liquid chromatography. The xyloglucan methylated before hydrolysis yields an array of derivatives (panel C), the nature of which depends on the number and positions of the acetyl groups, which in turn indicate the positions to which another sugar was attached (see arrows). The *t* designation refers to the terminal sugar in a side chain.

Unequivocal determination of the structure is made by **electron-impact mass spectrometry** (EIMS). As the partly methylated alditol acetate derivatives exit the gas chromatograph column, an electron beam breaks each derivative into fragments. The bonds in each derivative have different susceptibilities to breakage, so the molecule breaks into a characteristic set of fragments, which are like the pieces of a jigsaw puzzle. The larger fragments are more diagnostic, but each of these may be broken into still smaller fragments that give added complexity to the spectrum. The relative abundance of the mass of each fragment, in combination with the spectrum of masses for the fragments from a particular derivative, is diagnostic of its structure. Identification of the one or two extra acetyl groups instead of methyl groups indicates which carbons were participating in glycosidic bonds and ring formation. For example (panel D), a C-4–linked glucose unit in xyloglucan gives characteristic mass/charge ratios (*m/z* values) of 118 and 233; the latter fragment indicates the acetyl group at the O-4 position, which was protected from methylation by the linkage of a sugar. Likewise, the 4,6-linked glucose branch point contains yet another acetyl group, increasing the signal for this fragment to *m/z* 261. Note that the presence of the deuterium atom at C-1 is essential for discriminating between 2-Xyl and 4-Xyl, which are symmetrical derivatives. The major fragments from the 2-Xyl derivative are *m/z* 190 and 117, whereas those from 4-Xyl are *m/z* 118 and 189; without the deuterium at the C-1, the results would be *m/z* 117 and 189 for both derivatives, which would thus be indistinguishable.

EIMS of the partly methylated alditol acetates is the main procedure used by carbohydrate biochemists to establish the linkage structure of unknown polymers. New mass spectrometry (MS) techniques, however, greatly extend the mass range that can be analyzed and can provide linkage and sequence information about underivatized oligosaccharides. One such technique is **matrix-assisted laser desorption ionization–time of flight (MALDI-TOF) MS.** Underivatized polymers are mixed with a material that ionizes them on exposure to brief pulses of a laser. The polymeric ions are differentially accelerated in the mass spectrometer, depending on their size, and molecular masses as great as 200 kDa are detected by a finely tuned calculation of the time interval between laser bombardment and contact with the mass spectrometer anode.

2.2 Macromolecules of the cell wall

2.2.1 Cellulose is the principal scaffolding component of all plant cell walls.

Cellulose is the most abundant plant polysaccharide, accounting for 15% to 30% of the dry mass of all primary cell walls and an even larger percentage of secondary walls. Cellulose exists in the form of **microfibrils,** which are paracrystalline assemblies of several dozen (1→4)β-D-glucan chains hydrogen-bonded to one another along their length (Fig. 2.11). In plants, on average, each microfibril is 36 individual chains thick in cross-section, but microfibrils of algae can form either large, round cables or flattened ribbons of several hundred chains. Microfibrils of angiosperms have been measured to be between 5 and 12 nm wide in the electron microscope. Each (1→4)β-D-glucan chain may be just several thousand units (about 2 to 3 μm long), but individual chains begin and end at different places within the microfibril to allow a microfibril to reach lengths of hundreds of micrometers and to contain thousands of individual glucan chains. This structure is analogous to a spool of thread that consists of thousands of individual cotton fibers, each about 2 to 3 cm long.

By electron diffraction, the (1→4)β-D-glucan chains of cellulose are arranged parallel to one another; that is, all of the reducing ends of the chains point in the same direction. Recently, bacterial cellulose was shown to be synthesized by the adding of glucose units to the nonreducing ends of glucan chains.

Callose differs from cellulose in consisting of (1→3)β-D-glucan chains, which can form helical duplexes and triplexes. Callose is made by a few cell types at specific stages of wall development, such as in growing pollen tubes and in the cell plates of dividing cells. It is also made in response to wounding (see Section 2.4.3) or to attempted penetration by invading fungal hyphae (see Fig. 2.6).

Box 2.2

Nuclear magnetic resonance spectroscopy can help determine polymer structure.

Nuclear magnetic resonance (NMR) spectroscopy is a nondestructive method that provides many different kinds of information about the polysaccharides that make up the cell wall. Specific NMR experiments have been developed to probe the chemical structure and composition of polysaccharides, their relative orientation, their mobility, and the nature of their mutual interactions.

An NMR spectrometer consists of a powerful magnet and special electronic circuitry that is designed to measure the magnetic properties of the atomic nuclei contained in a sample, such as a purified polysaccharide. Atomic nuclei are charged particles (panel A) that have an intrinsic angular momentum, sometimes called the "nuclear spin." A spinning charge generates a magnetic field, and many common nuclei, such as ^{1}H and ^{13}C, are magnetic. The nucleus most frequently observed by NMR is the proton (^{1}H), which is the nucleus of virtually all hydrogen atoms. In contrast, the magnetically active carbon isotope ^{13}C represents only 1.1% of all naturally occurring carbon, which makes ^{13}C-NMR much less sensitive than ^{1}H-NMR. Nevertheless, ^{13}C-NMR is sensitive enough to probe the structures of polysaccharides that are available in milligram quantities.

When a magnetic nucleus is placed in the spectrometer's magnetic field, a force is exerted that tends to line up the spin of this nucleus with the applied magnetic field. However, the rules of quantum mechanics do not allow a nucleus to arbitrarily adopt just any orientation. That is, the angular momentum (or spin) of the nucleus is "quantized" (i.e., limited to a few well-defined values). The interplay of the quantized angular momentum and the magnetic force causes the nucleus to "wobble" the way a spinning top does under the influence of gravity (panel B). This motion, called **precession,** has a characteristic "resonance frequency" that depends on the strength of the magnetic field and the magnetic properties of the nucleus.

NMR experiments observe populations of nuclei, rather than individual nuclei. Under most conditions, the precession of a population of nuclei is not "coherent"; that is, the nuclear spins in the sample are tilted in different directions (panel C, left) so the precession cannot be detected. To be observed by NMR, the nuclei must be made to precess coherently. This is accomplished by subjecting the sample to a brief magnetic pulse, called a radiofrequency (RF) pulse, that oscillates at the nuclear resonance frequency. This pulse redistributes the nuclear spin orientations so that they become partially aligned, and the precessing components of nuclear spin can be observed (panel C, right).

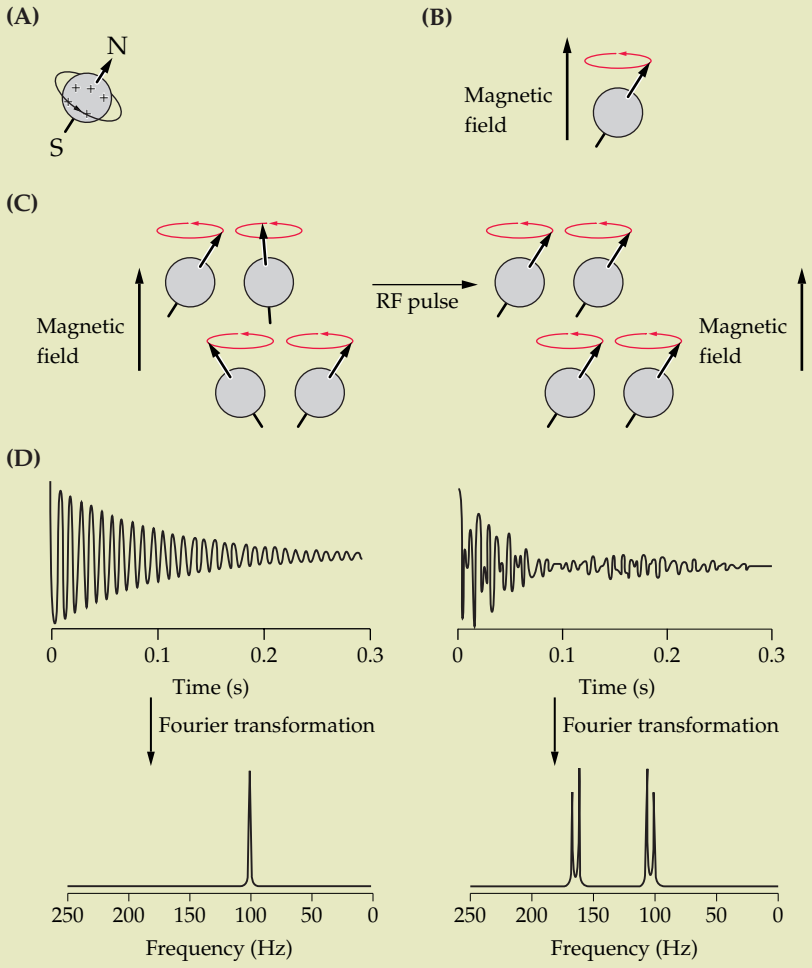

The signal observed as a result of the RF pulse is usually composed of many slightly different resonance frequencies. The RF pulse is thus analogous to ringing a bell to produce a mixture of different audio frequencies. All the frequencies are recorded simultaneously, just as we hear all of the frequencies of a ringing bell simultaneously. A mathematical operation called **Fourier transformation** is used to convert the NMR data into a form (called a frequency-domain spectrum) that makes it easier to distinguish and tabulate signals with different frequencies (panel D).

The different frequencies in the NMR spectrum arise because the electron cloud surrounding each nucleus "shields" it from the applied magnetic field. Neighboring atoms with different degrees of electronegativity surrounding the nucleus being observed produce a change in its resonance frequency called the **chemical shift.** This chemical shift, which is measured in parts per million (ppm) relative to the resonance frequency of a nucleus in a standard compound such as trimethylsilane, provides information about the chemical environment of the nucleus within the molecule. For example, the electron-withdrawing oxygen attached to C6 of glucose decreases the electronic shielding for this nucleus, resulting in a chemical shift of approximately 60 ppm. On the other hand, two electron-withdrawing oxygen atoms are attached to the anomeric carbon (C1) of glucose, which is thus even less shielded than C6 and has a chemical shift of approximately 100 ppm. Chemical shifts can provide specific structural information, as illustrated in the ^{13}C-NMR spectrum of β-methylcellobioside (panel E). Here, the glycosidic bond between two glucosyl residues causes the chemical shift (80.2 ppm) of C4′ (at the point of attachment) to be substantially greater than the chemical shift (71.0 ppm) of C4. This difference, called a **glycosylation effect,** is often used to establish the specific point at which two sugars are joined by a glycosidic bond.

Nuclei that are connected by three or fewer molecular bonds often exhibit an interaction called **scalar coupling.** This coupling leads to the familiar splitting of signals that is a characteristic feature of ^{1}H-NMR spectra. The magnitude of a scalar coupling interaction depends on molecular geometry. For example, the scalar coupling between two protons that are separated by three bonds depends on a geometric parameter called the dihedral angle, which provides a convenient means of determining whether the anomeric configuration of a sugar is α or β. The anomeric (H1) resonance of a typical sugar is split into a doublet by scalar coupling with H2. For a β-linked glucosyl residue (as in cellobiose), the dihedral angle H1–C1–C2–H2 (i.e., the angle between the plane containing H1, C1, and C2 and the plane containing H2, C2, and C1) is approximately 180°, which results in a relatively large H1–H2 scalar coupling of 8.0 Hz. That is, the H1 resonance of a β-linked glucosyl residue is split into a doublet consisting of two signals separated by 8.0 Hz. Conversely, the dihedral angle H1–C1–C2–H2 for an α-linked glucosyl residue (as in maltose) is approximately 60°, which results in a relatively small H1–H2 scalar coupling of 3.6 Hz. Thus, the anomeric configuration of a glucosyl residue can be unambiguously determined simply by measuring the distance (in Hertz) between the two components of the anomeric proton doublet.

As one might predict, the ^{1}H- and ^{13}C-NMR spectra of a polysaccharide can be quite complicated, and it is often difficult to determine the complete primary structure of the polymer by this technique. Nevertheless, the structures of oligosaccharides with 10 or more glycosyl residues can be completely characterized by two- and three-dimensional NMR techniques. NMR analysis is not limited to determining the primary structures of biopolymers. For example, ^{13}C-NMR analysis of the products generated when a plant is fed a ^{13}C-labeled substrate can be used to study biosynthetic pathways in vivo. NMR is an important tool for analyzing the conformational and dynamic properties of oligosaccharides in solution. **Solid-state NMR** techniques can distinguish regions of a polysaccharide that differ in their mobility or conformation, thus facilitating the development of models for the assembly of polysaccharides to form complex, dynamic structures within the cell wall. *Will York, Complex Carbohydrate Research Center, University of Georgia, Athens, contributed this section.*

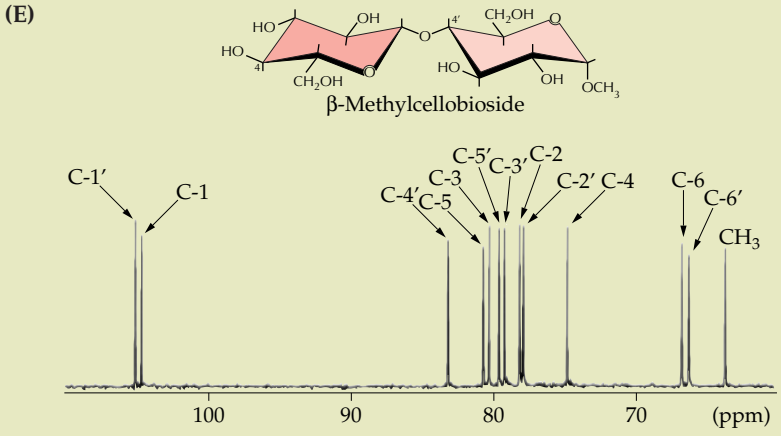

2.2.2 Cross-linking glycans interlock the cellulosic scaffold.

Cross-linking glycans are a class of polysaccharides that can hydrogen-bond to cellulose microfibrils: They may coat microfibrils but are also long enough to span the distance between microfibrils and link them together to form a network. Most cross-linking glycans are often called "hemicelluloses," a widely used but archaic term for all materials extracted from the cell wall with molar concentrations of alkali, regardless of structure.

The two major cross-linking glycans of all primary cell walls of flowering plants are **xyloglucans** (XyGs) and **glucuronoarabinoxylans** (GAXs) (Fig. 2.12). The XyGs cross-link the walls of all dicots and about one-half of the monocots, but in the cell walls of the "commelinoid" line of monocots, which includes bromeliads, palms, gingers, cypresses, and grasses, the major cross-linking glycan is GAX (Fig. 2.13).

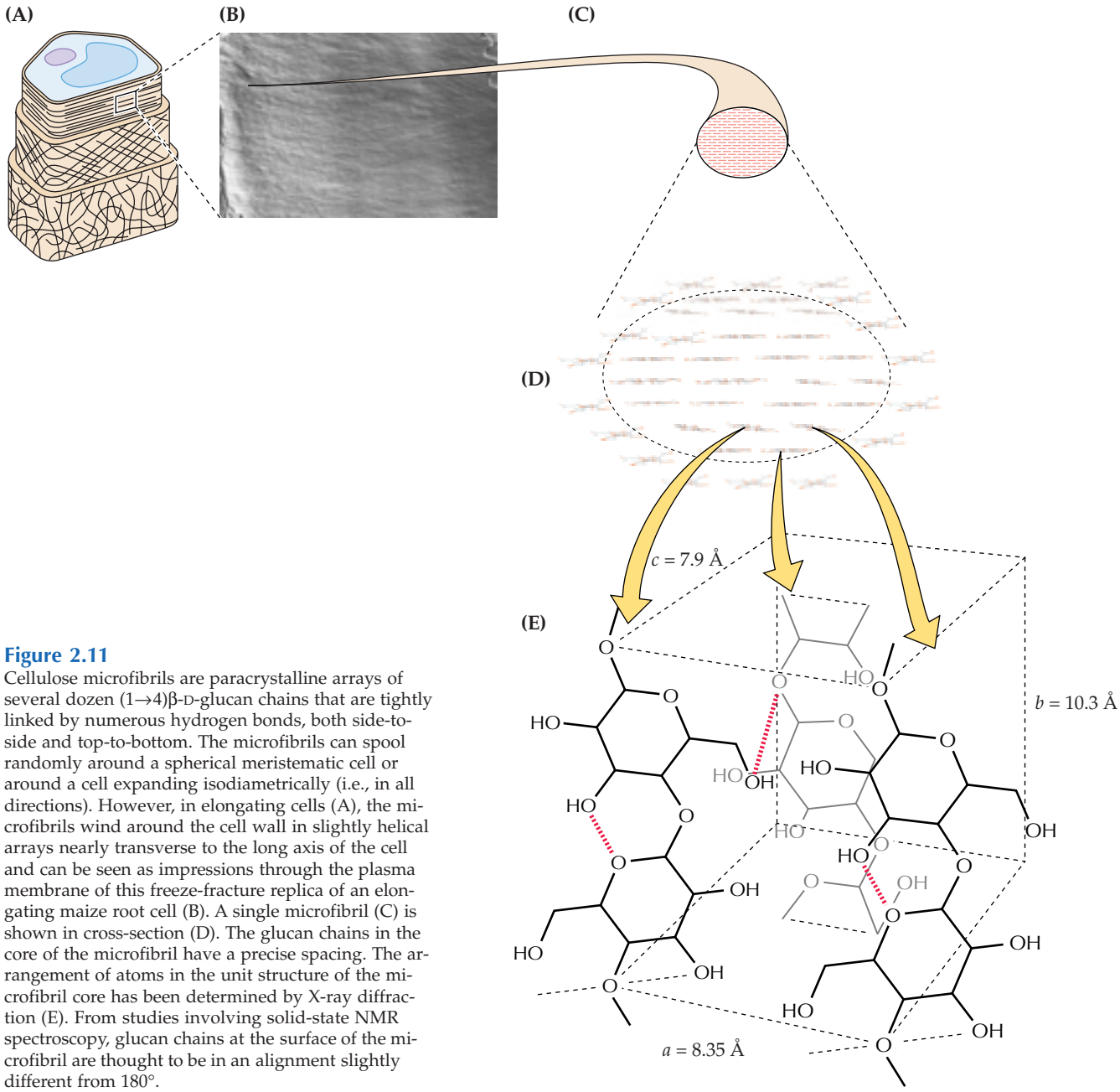

Figure 2.11
Cellulose microfibrils are paracrystalline arrays of several dozen (1→4)β-D-glucan chains that are tightly linked by numerous hydrogen bonds, both side-to-side and top-to-bottom. The microfibrils can spool randomly around a spherical meristematic cell or around a cell expanding isodiametrically (i.e., in all directions). However, in elongating cells (A), the microfibrils wind around the cell wall in slightly helical arrays nearly transverse to the long axis of the cell and can be seen as impressions through the plasma membrane of this freeze-fracture replica of an elongating maize root cell (B). A single microfibril (C) is shown in cross-section (D). The glucan chains in the core of the microfibril have a precise spacing. The arrangement of atoms in the unit structure of the microfibril core has been determined by X-ray diffraction (E). From studies involving solid-state NMR spectroscopy, glucan chains at the surface of the microfibril are thought to be in an alignment slightly different from 180°.

The XyGs consist of linear chains of (1→4)β-D-glucan with numerous α-D-Xyl units linked at regular sites to the O-6 position of the Glc units. Some of the xylosyl units are substituted further with α-L-Ara or β-D-Gal, depending on the species, and sometimes the Gal is substituted further with α-L-Fuc. Sequence-dependent hydrolases are used to elucidate the fine structure of XyGs by cleaving them at specific sites along the glucan backbone into fragments that are small enough to characterize fully (Box 2.3). A convention has been adopted to describe certain ubiquitous side chains of XyG in which the entire subtending side chain along the glucan is designated by a single letter on the basis of its terminal sugar (Table 2.1).

The XyGs are constructed in block-like unit structures containing 6 to 11 sugars, the proportions of which vary among tissues and species. The XyGs can form three major variants of structure. All of the noncommelinoid monocots and most of the dicots are fucogalacto-XyGs (see Fig. 2.12A). The fundamental structure is composed of nearly equal amounts of XXXG and XXFG, but variations can occur, and α-L-Ara is added at some places along the glucan chain. Solanaceous species and peppermint have arabino-XyGs (see Fig. 2.12B), in which only two of every four glucosyl units contains a xylose unit, and the xylosyl units are substituted with either one or two α-L-Ara units to produce a mixture of AXGG, XAGG, and AAGG subunits. Curiously, an acetyl group replaces the third xylosyl unit in the arabino-XyGs. The commelinoid monocots also contain small amounts of XyG, but these include random additions of xylosyl units and rarely any further subtending sugars.

All angiosperms also contain at least small amounts of GAXs, but their structure may vary considerably with respect to the degree of substitution and position of attachment of α-L-Ara residues. In the commelinoid monocots, where GAXs are the major cross-linking polymers, the Ara units are invariably on the O-3 position (Fig. 2.12C). However, in species where XyG is the major cross-linking glycan, the α-L-Ara units are more commonly found at the O-2 position (Fig. 2.12D). In all GAXs, the α-D-GlcA units are attached to the O-2 position.

In the order Poales, which contains the cereals and grasses, a third major cross-linking glycan, called **"mixed-linkage" (1→3),(1→4)β-D-glucans** (β-glucans), distinguishes these species from the other commelinoid species (Fig. 2.14). These unbranched polymers consist of 90% cellotriose and cellotetraose units in a ratio of about 2:1 and connected by (1→3)β-D-linkages. The cellotriosyl and cellotetraosyl units together make up corkscrew-shaped polymers about 50 residues long that are spaced by oligomers of four or more contiguous (1→4)Glc units.

Other, much less abundant noncellulosic polysaccharides, such as **glucomannans, galactoglucomannans,** and **galactomannans,** potentially interlock the microfibrils in some primary walls (Fig. 2.15). These mannans are found in virtually all angiosperms examined.

2.2.3 Pectin matrix polymers are rich in galacturonic acid.

Pectins—a mixture of heterogeneous, branched, and highly hydrated polysaccharides rich in D-galacturonic acid—have been defined classically as material extracted from the cell wall by Ca^{2+}-chelators such as ammonium oxalate, EDTA, EGTA, or cyclohexane diamine tetraacetate. They are thought to perform many functions: determining wall porosity and providing charged surfaces that modulate wall pH and ion

Table 2.1 Single-letter designators of xyloglucan side groups based on the nonreducing terminal sugar

Single-letter designator	Terminal sugar	Side group on the glucan chain
G	D-Glucose	None
X	D-Xylose	α-D-Xyl-(1→6)-
L	D-Galactose	β-D-Gal-(1→2)-α-D-Xyl-(1→6)-
F	L-Fucose	α-L-Fuc-(1→2)-β-D-Gal-(1→2)-α-D-Xyl-(1→6)-
A	L-Arabinose	α-L-Ara-(1→2)-α-D-Xyl-(1→6)-

(A) **(Fucogalacto)Xyloglucans**

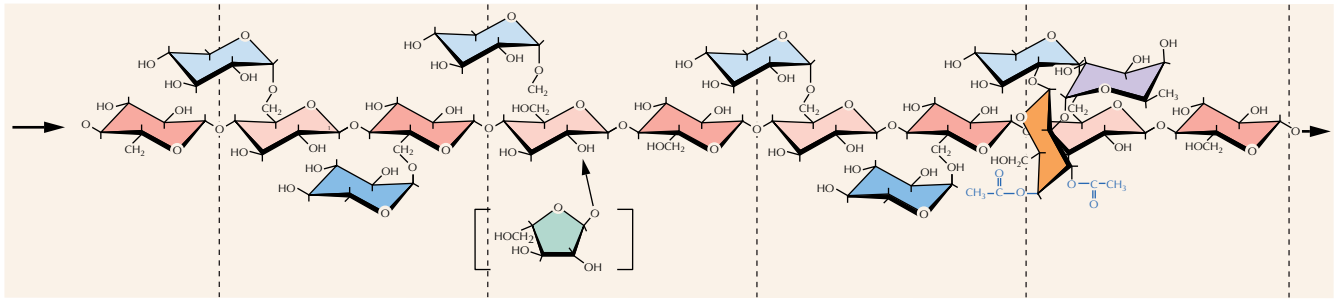

α-L-Fuc-(1→2)β-D-Gal-(1→2)α-D-Xyl-(1→6)
(3-O-Ac)
(4-O-Ac)
α-D-Xyl-(1→6)
α-D-Xyl-(1→6)
α-D-Xyl-(1→6)
→4)β-D-Glc-(1→4)β-D-Glc-(1→4)β-D-Glc-(1→4)β-D-Glc-(1→4)β-D-Glc-(1→4)β-D-Glc-(1→4)β-D-Glc-(1→4)β-D-Glc-(1→
α-D-Xyl-(1→6)
α-D-Xyl-(1→6)

XXXG XXFG

(B) **Solanaceous (arabino)xyloglucans**

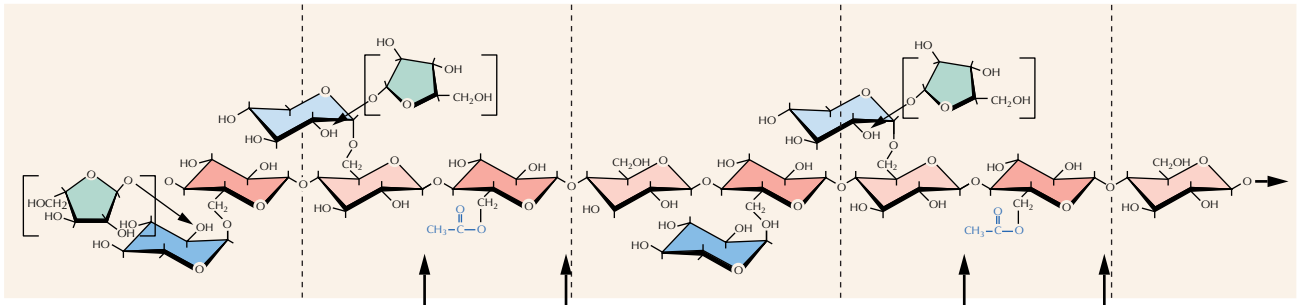

[α-L-Ara-(1→2)]α-D-Xyl-(1→6)
[α-L-Ara-(1→2)]α-D-Xyl-(1→6)
→4)β-D-Glc-(1→4)β-D-Glc-(1→4)β-D-Glc-(1→4)β-D-Glc-(1→4)β-D-Glc-(1→4)β-D-Glc-(1→4)β-D-Glc-(1→4)β-D-Glc-(1→
(6-O-Ac)
(6-O-Ac)
[α-L-Ara-(1→2)]α-D-Xyl-(1→6)
α-D-Xyl-(1→6)

(A)(A)G X(A)G

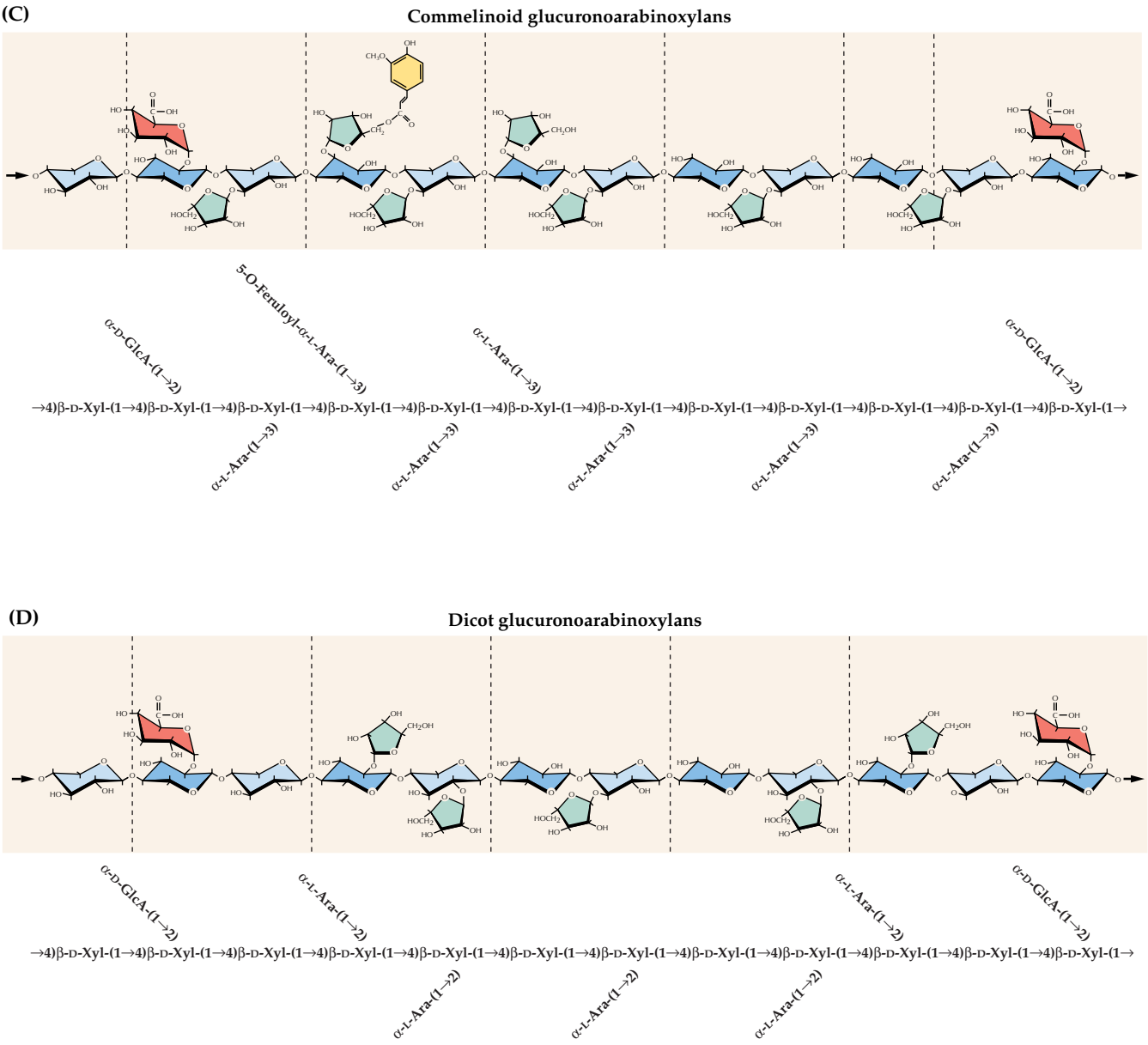

Figure 2.12

The chemical structures of the major cross-linking glycans of the primary walls of flowering plants. The dotted lines delineate the β(1→4)-disaccharide units of glucose and xylose inherent in all the cross-linking glycans. Such a linkage requires the sugars to be oriented about 180° from each other. (A) Fucogalactoxyloglucans. In most xyloglucans, the α-D-xylosyl units are added to three contiguous glucosyl units of the backbone to produce a heptasaccharide unit structure. On about one-half of these unit structures, a *t*-α-L-Fuc-(1→2)β-D-Gal- is added to the O-2 of the Xyl side group nearest the reducing end, forming a nonasaccharide unit. Attachment of an α-L-Ara unit to the O-2 position of the backbone glucose unit at a few positions along the backbone blocks hydrogen bonding of the XyG to cellulose at those sites. The arrows denote the only linkages able to be cleaved by the *Trichoderma* endo-β-D-glucanase. According to the single-letter designator convention (Table 2.1), these two oligomers are XXXG and XXFG. (B) Arabinoxyloglucans. In the Solanales and Lamiales, the major repeating unit is a hexamer, rather than a heptamer, with one or two α-L-Ara units added directly to the O-2 position of the Xyl units. The Solanaceae XyG units are separated by two unbranched Glc units rather than one, and the penultimate Glc contains an acetyl group at the O-6 position. The arrows denote the linkages that can be cleaved by the *Trichoderma* endo-β-D-glucanase. In the single-letter designator convention (Table 2.1), these two oligomers are AAG or XAG, if the Ara units are attached; both are XXG if no Ara units are attached. (C) Commelinoid glucuronoarabinoxylans. In the GAX from commelinoid monocot walls, the α-L-Ara units are added strictly to the O-3 position of the xylosyl units of the backbone polymer. Feruloyl groups (and sometimes other hydroxycinnamic acids) are esterified to the O-5 position of the α-L-Ara units and are spaced about every 50 Xyl units of the backbone. The α-D-GlcAs are added to the O-2 position of the xylosyl units. (D) Other glucuronoarabinoxylans. The noncommelinoid monocots and all dicots also contain GAX in addition to the more abundant XyG. However, the α-L-Ara units of these GAXs are attached to the O-2 position as well as to the O-3 position. As with the commelinoid GAX, the α-D-GlcA units are attached only at the O-2 position. XLFG can be a significant decasaccharide in some species.

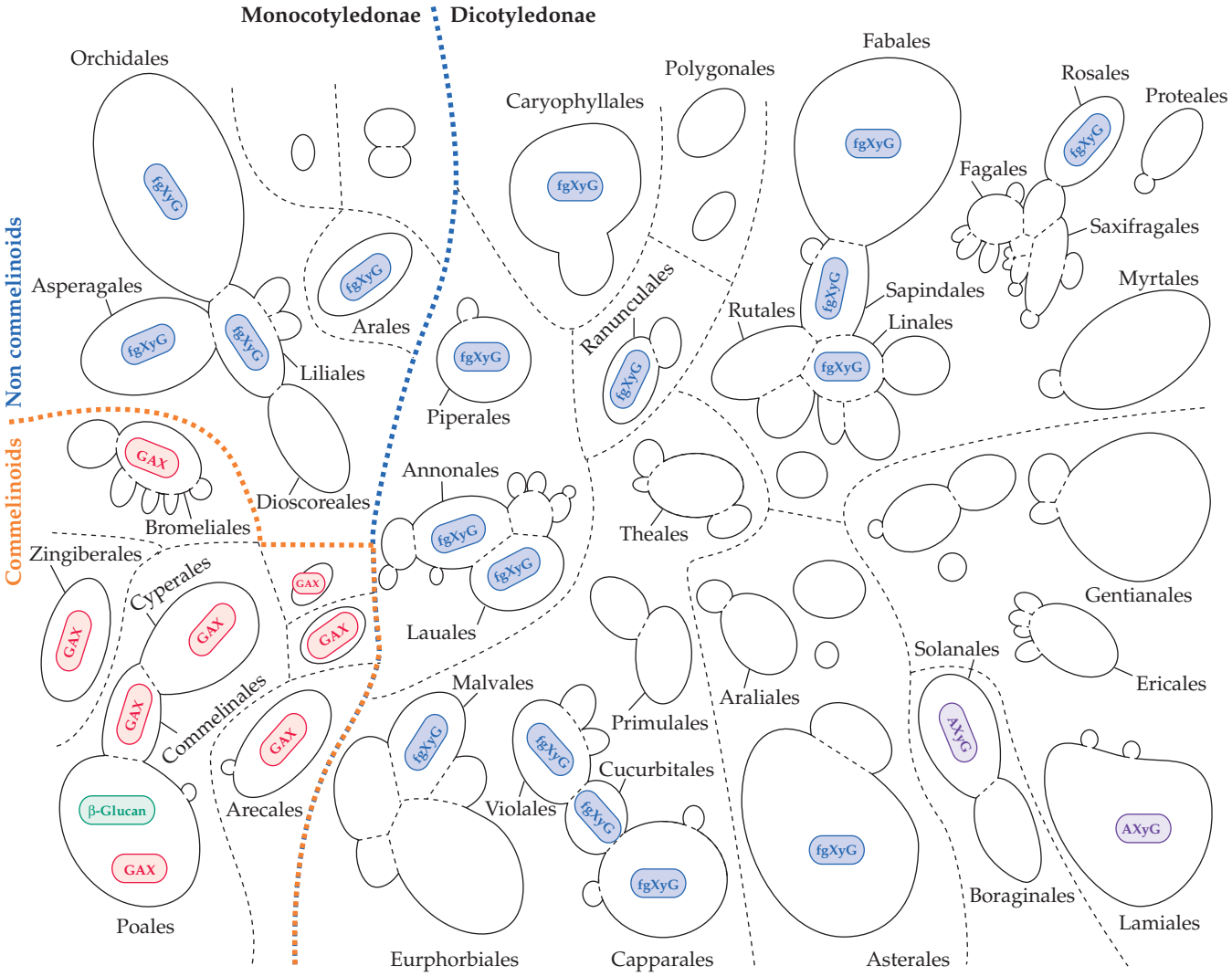

Figure 2.13
Orders of the flowering plants, dicot and monocot, with symbolic descriptions of the major cross-linking glycans and major distinctions illustrated between grasses, commelinoids, and noncommelinoid monocots, and between Solanales and Lamiales and the other dicot orders. fgXyG, fucogalactoxyloglucan; AXyG, arabinoxyloglucan; GAX, glucuronoarabinoxylan (see Fig. 2.12); β-glucan, (1→3),(1→4)β-D-glucan (see Fig. 2.14).

balance; regulating cell–cell adhesion at the middle lamella; and serving as recognition molecules that alert plant cells to the presence of symbiotic organisms, pathogens, and insects. Particular cell wall enzymes may bind to the charged pectin network, constraining their activities to local regions of the wall. By limiting wall porosity, pectins may affect cell growth, regulating the access of wall-loosening enzymes to their glycan substrates (see Section 2.5.7).

Two fundamental constituents of pectins are **homogalacturonan** (HGA; Fig. 2.16A) and **rhamnogalacturonan I** (RG I; Fig. 2.16C). HGAs are homopolymers of (1→4)α-D-GalA that contain as many as 200 GalA units and are about 100 nm long. There are two kinds of structurally modified HGAs, **xylogalacturonan** (Fig. 2.16B) and **rhamnogalacturonan II** (RG II; Fig. 2.17A). RG II has the richest diversity of sugars and linkage structures known, including apiose, aceric acid (3-C′-carboxy-5-deoxy-L-xylose), 2-*O*-methyl fucose, 2-*O*-methyl xylose, Kdo (3-deoxy-D-*manno*-2-octulosonic acid), and Dha (3-deoxy-D-*lyxo*-2-heptulosaric acid). Its very highly conserved structure among flowering plants suggests an important

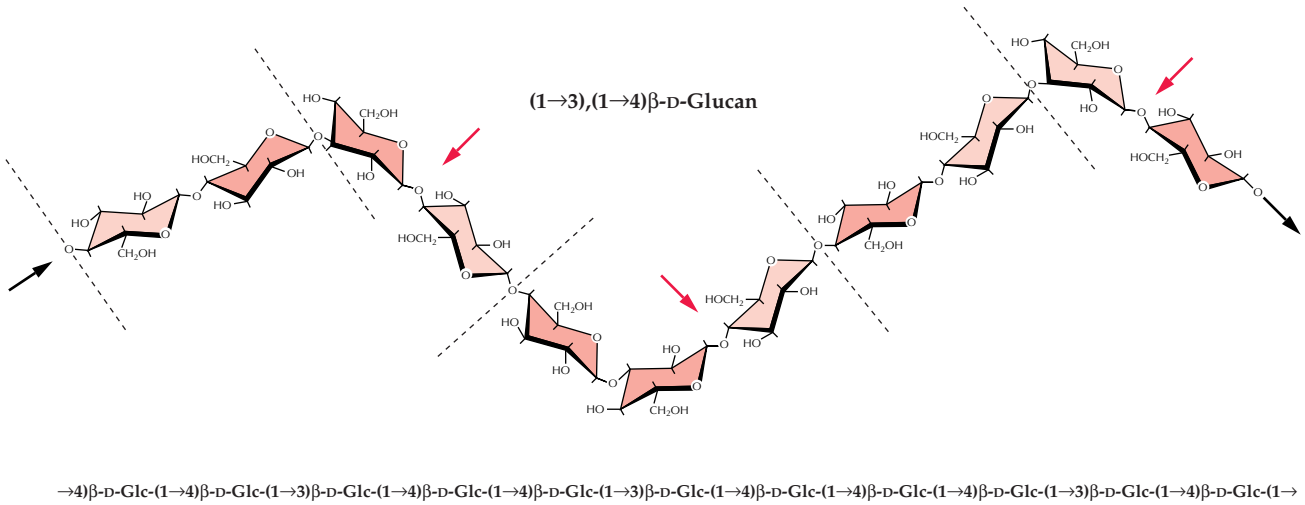

Figure 2.14
The mixed-linkage (1→3),(1→4)β-D-glucan unique to the Poales. The red arrows indicate cleavage sites by the *Bacillus subtilis* endoglucanase. The dotted lines demonstrate cellobiose units within the polymer.

function despite its low abundance in cell walls. Dimers of RG II have been found to be cross-linked by two diester bonds per boron atom between apiose units in the complex side groups (Fig. 2.17B).

RG I is a rod-like heteropolymer of repeating (1→2)α-L-Rha-(1→4)α-D-GalA disaccharide units. The best-documented RG I forms are isolated from the cell walls by enzymatic digestion with **polygalacturonase** (PGase), but the length of RG I is unknown because there may be runs of HGA on the ends of the molecule.

Other polysaccharides, composed mostly of neutral sugars—such as **arabinans, galactans,** and highly branched type I **arabinogalactans (AGs)** of various configurations and sizes—are attached to the O-4 of many of the Rha residues of RG I (see Fig. 2.16D). In general, about half of the Rha units of RG I have side chains, but this ratio can vary with cell type and physiological state. There are two types of AG structures. Type I AGs are found associated only with pectins and are composed of (1→4)β-D-galactan chains with mostly *t*-Ara units at the O-3 of the Gal units. Type II AGs constitute a broad group of short (1→3)- and (1→6)β-D-galactan chains connected to each other by (1→3,1→6)-linked branch point residues and are associated with specific proteins, called **arabinogalactan proteins** (AGPs) (see next section).

2.2.4 Structural proteins of the cell wall are encoded by large multigene families.

Although the structural framework of the cell wall is largely carbohydrate, structural proteins may also form networks in the wall. There are four major classes of structural proteins, three of them named for their uniquely enriched amino acid: the **hydroxyproline-rich glycoproteins** (HRGPs), the **proline-rich proteins** (PRPs), and the **glycine-rich proteins** (GRPs) (Fig. 2.18). All of them are developmentally regulated, their relative amounts varying among tissues (Fig. 2.19) and species. Like other secretory proteins destined for the cell wall, the structural proteins are cotranslationally inserted into the endoplasmic reticulum (ER). Thus, all mRNAs for cell wall proteins encode signal peptides that target the proteins to the secretory pathway (see Chapter 4).

Extensin, encoded by a multigene family, is one of the best-studied HRGPs of plants. Extensin consists of repeating Ser-$(Hyp)_4$ and Tyr-Lys-Tyr sequences that are important for secondary and tertiary structure (see Fig. 2.18). The repeating Hyp units predict a "polyproline II" rod-like molecule.

Another large multigene family codes for PRPs. The conformational structure of PRPs is unknown, but their similarity to extensin suggests that they also may be rod-shaped proteins.

(A) (Galacto)Glucomannan

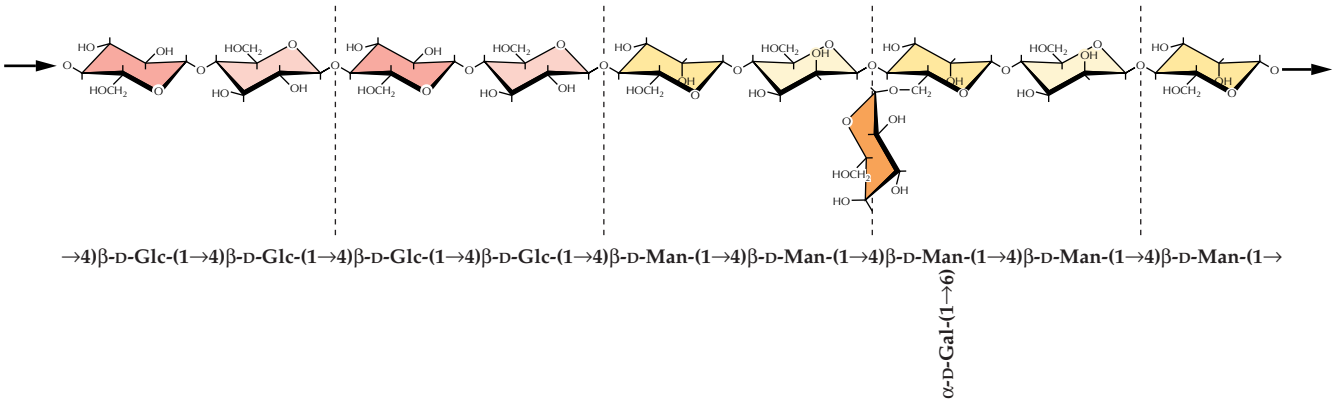

→4)β-D-Glc-(1→4)β-D-Glc-(1→4)β-D-Glc-(1→4)β-D-Man-(1→4)β-D-Man-(1→4)β-D-Man-(1→4)β-D-Man-(1→4)β-D-Man-(1→

α-D-Gal-(1→6)

(B) Galactomannan

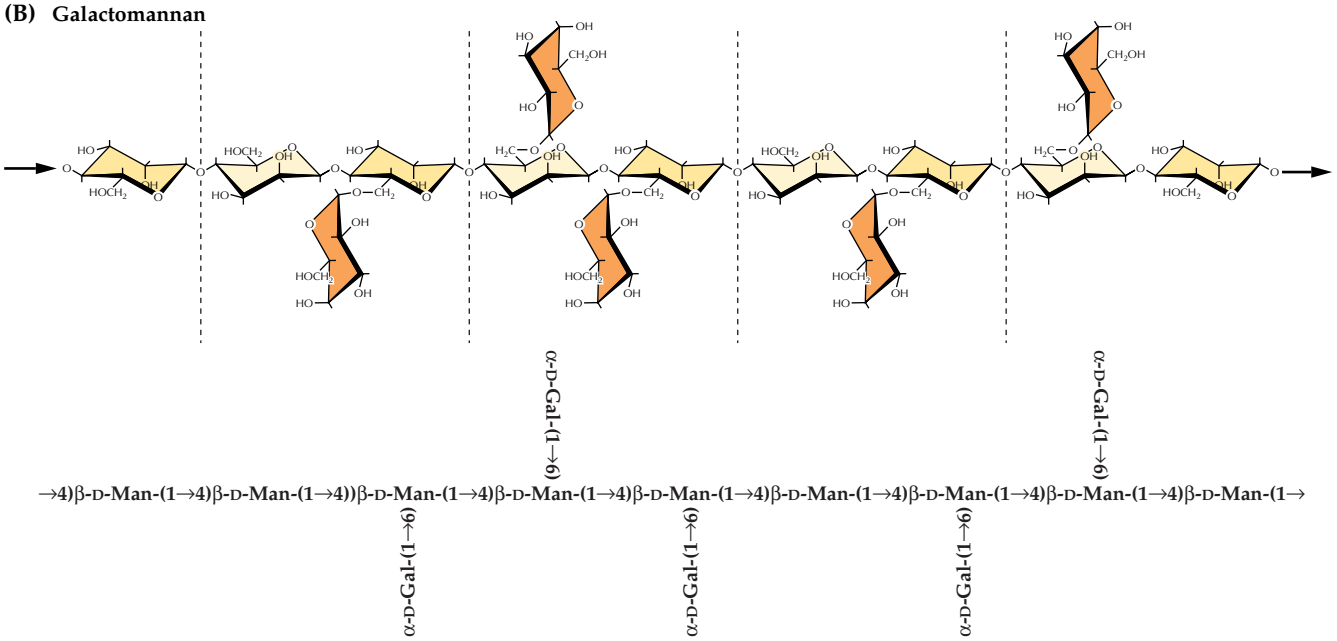

α-D-Gal-(1→6) α-D-Gal-(1→6)

→4)β-D-Man-(1→4)β-D-Man-(1→4))β-D-Man-(1→4)β-D-Man-(1→4)β-D-Man-(1→4)β-D-Man-(1→4)β-D-Man-(1→4)β-D-Man-(1→

α-D-Gal-(1→6) α-D-Gal-(1→6) α-D-Gal-(1→6)

(C) Mannan

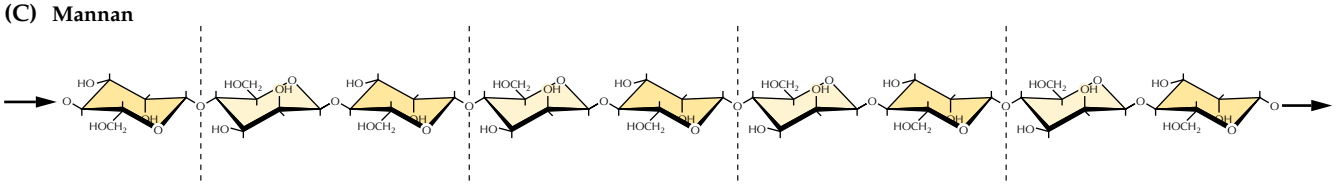

→4)β-D-Man-(1→4)β-D-Man-(1→4))β-D-Man-(1→4)β-D-Man-(1→4)β-D-Man-(1→4)β-D-Man-(1→4)β-D-Man-(1→4)β-D-Man-(1→4)β-D-Man-(1→

Figure 2.15

Cross-linking glycans that contain mannose. The dotted lines mark (1→4)β-disaccharide unit structures (see Fig. 2.12). (A) (Galacto)Glucomannans are roughly equimolar mixtures of (1→4)β-D-Man and (1→4)β-D-Glc units, with various amounts of terminal α-D-Gal units added to the O-6 position of the Man units. (B) Galactomannans have backbones composed exclusively of (1 →4)β-D-Man with the α-D-Gal units added at the O-6 positions. (C) Pure mannans can hydrogen bond into paracrystalline arrays, which are similar in structure to cellulose.

GRPs, some of which contain more than 70% glycine, are predicted to be β-pleated sheets rather than rod-shaped molecules. GRPs are thought to form a plate-like structure at the plasma membrane–cell wall interface. The cell wall face of the pleated sheet contains an arrangement of aromatic amino acids, the function of which is not known (see Fig. 2.18). Like HRGPs, cell wall GRPs are difficult to extract and may become cross-linked into the wall. In one example, bean GRPs are synthesized in xylem parenchyma cells but are targeted and exported to the walls of neighboring cells. GRPs constitute

Box 2.3 Polysaccharide sequences can be inferred by analyzing the cleavage products of sequence-specific glycanases.

A direct method for determining the sequence of sugars in a complex carbohydrate is not available. However, much like the restriction endonucleases that recognize and cleave specific sequences of DNA, **sequence-dependent glycanases** that cleave polysaccharides can be used to generate small oligosaccharides, for which the structure can be determined. Glycanases obtained from fungi and bacteria cleave specific glycosidic linkages. For example, the activity of an endo-β-D-glucanase from the fungus *Trichoderma viride* is blocked by appendant groups of the glucan chain; the enzyme can hydrolyze only unsubstituted (1→4)β-D-glucosyl linkages. This feature makes the enzyme useful in determining the frequency of contiguous attachment of xylosyl units onto the (1→4)β-D-glucan chain of xyloglucan.

Sequence-dependent glycanases either require or are restricted by structural features of the polysaccharide. A *Bacillus subtilis* endoglucanase cleaves a (1→4)β-D-glucosyl linkage only if preceded by a (1→3)β-D-linkage, and a *B. subtilis* xylanase cleaves (1→4)β-D-xylosyl linkages only at sites with appendant glucuronic acid units. Several of these enzymes have been used to yield oligomers characteristic of repeating unit structures, which provides a reasonable approximation of the general sequence of very large polymers.

In general, sugars and oligosaccharides are not well resolved by conventional **high-performance liquid chromatography** (HPLC) systems. However, special alkali-resistant HPLC apparatus can support **high-pH anion-exchange HPLC** (HPAE-HPLC), a useful new tool for analyzing the oligosaccharide products of sequence-dependent glycanases. The hydroxyl groups of sugars are weak acids and become negatively charged at high pH. This property may be exploited, given that the relative retention on an anion-exchange column depends on the number, positions, and degrees of freedom of the hydroxyl groups of the oligomer. The oligosaccharides become charged when introduced into a stream of NaOH solution as concentrated as 0.5 M. The anionic oligosaccharides bind to the column and are eluted in a gradient of increasing sodium acetate in NaOH. As the sugars elute, they are detected by an electrochemical cell called a **pulsed amperometric detector** (PAD). A small proportion of the sugars are oxidized as they pass over the gold-plated detector, and when these oxidized sugars bind to the detector plate, the concentration is measured as the relative decrease in the standing potential of the detector. A brief pulse of reversed polarity repels the oxidized sugar from the plate. This pulse-cycle is repeated every 300 ms or so. The measuring pulses are summed to provide a chromatogram that is digitally integrated. The PAD is reasonably specific for sugars, in that few other compounds are oxidized by comparable electrical pulses. Because most of the sample is not oxidized by the PAD, peak fractions can be collected individually, neutralized, and deionized before being subjected to nuclear magnetic resonance, methylation analysis, or other mass spectrometry techniques to determine the linkage structure (see Boxes 2.1 and 2.2).

In the HPAE-HPLC chromatographs shown here, xyloglucans from seed flours of *Tamarindus* and from leaves of *Arabidopsis* and tobacco (a solanaceous plant) are digested to their respective oligosaccharide units by endo-β-D-glucanase and separated by HPAE-HPLC. For *Tamarindus,* peak 7 is XXXG, peaks 8 and 8′ are XLXG and XXLG, respectively, and peak 9 is XLLG; for *Arabidopsis,* peak 7 is the same as for *Tamarindus,* peak 9 is XXFG, and peak 10 is XLFG. The single broad peak for tobacco (combined peaks 6 and 7) contains both XAG and AAG (the fourth glucosyl unit at the reducing end is hydrolyzed from the oligomer by the endo-β-D-glucanase).

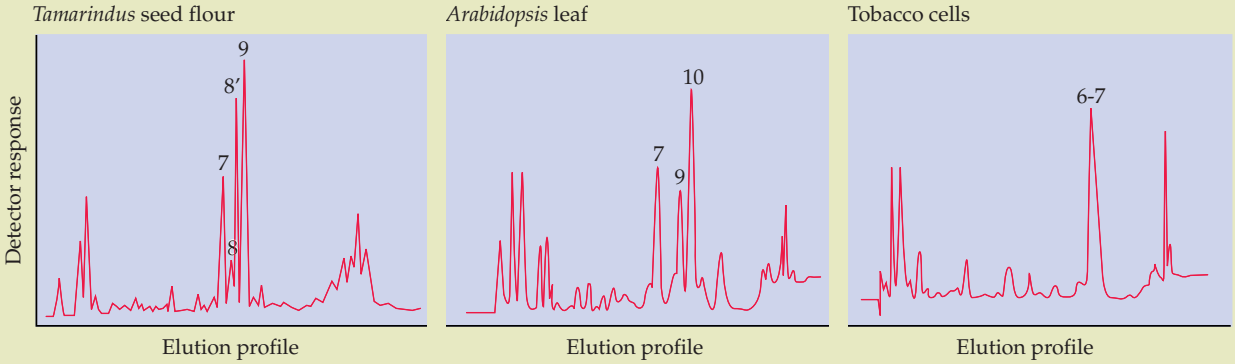

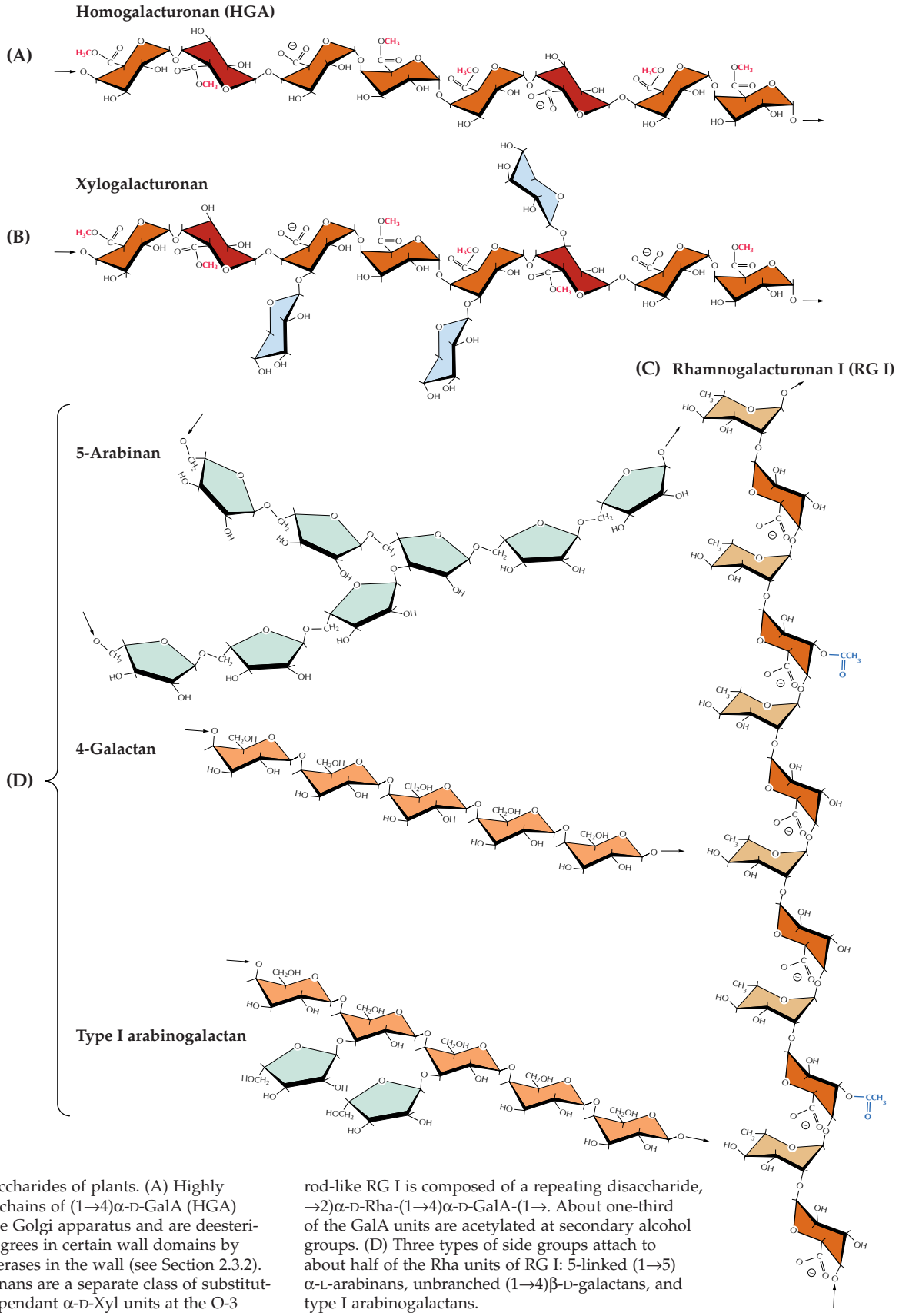

Figure 2.16
The pectic polysaccharides of plants. (A) Highly methyl-esterified chains of (1→4)α-D-GalA (HGA) are secreted by the Golgi apparatus and are deesterified to various degrees in certain wall domains by pectin methyl esterases in the wall (see Section 2.3.2). (B) Xylogalacturonans are a separate class of substituted HGA, with appendant α-D-Xyl units at the O-3 position of about half of the GalA units. (C) Contorted, rod-like RG I is composed of a repeating disaccharide, →2)α-D-Rha-(1→4)α-D-GalA-(1→. About one-third of the GalA units are acetylated at secondary alcohol groups. (D) Three types of side groups attach to about half of the Rha units of RG I: 5-linked (1→5) α-L-arabinans, unbranched (1→4)β-D-galactans, and type I arabinogalactans.

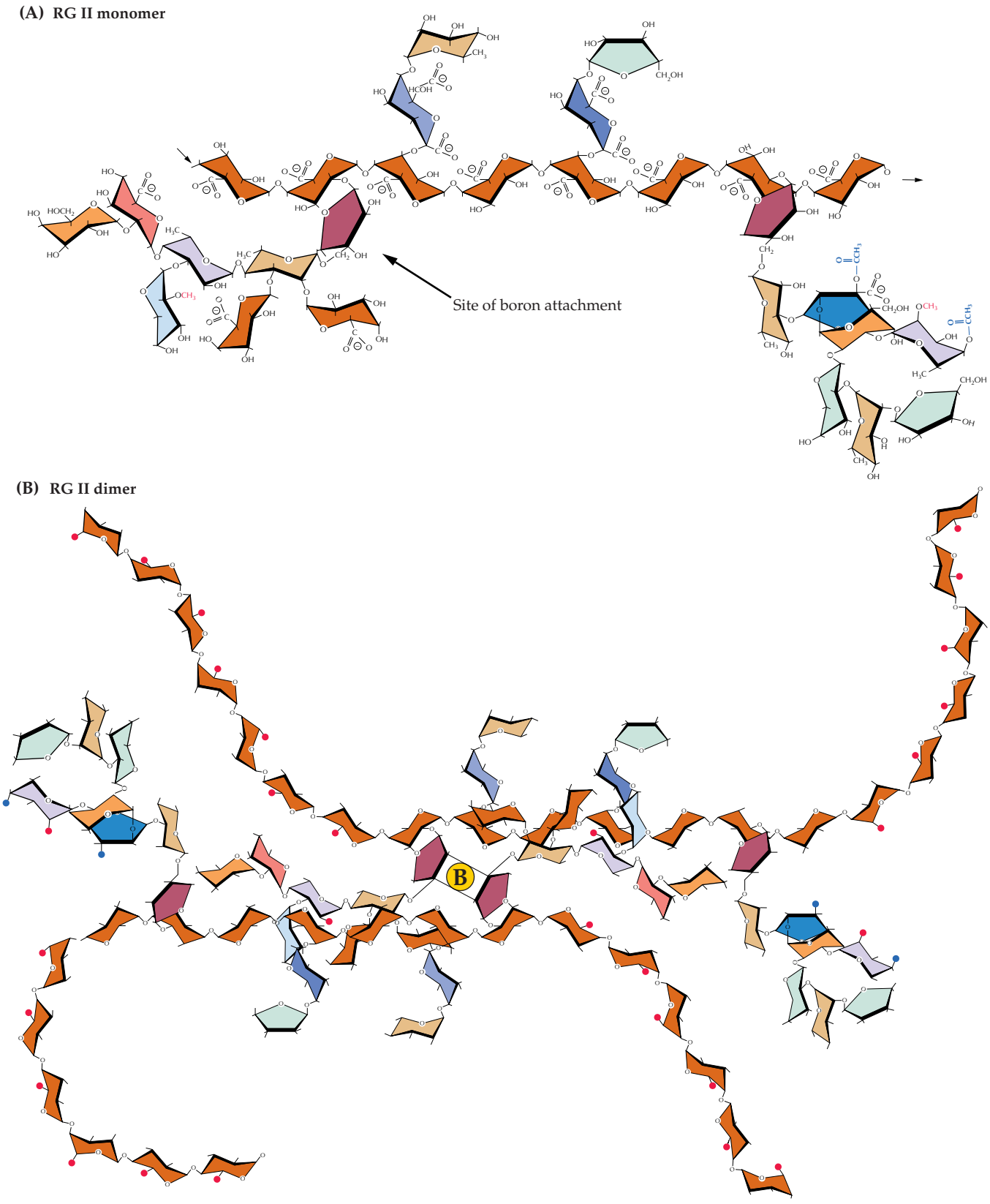

Figure 2.17
(A) RG II is a complex HGA with four distinct side groups containing several different kinds of sugar linkages. (B) RG II monomers of about 4200 kDa can dimerize as boron di-diesters of the apiose residues. Red dots indicate methyl groups, blue dots acetyl groups.

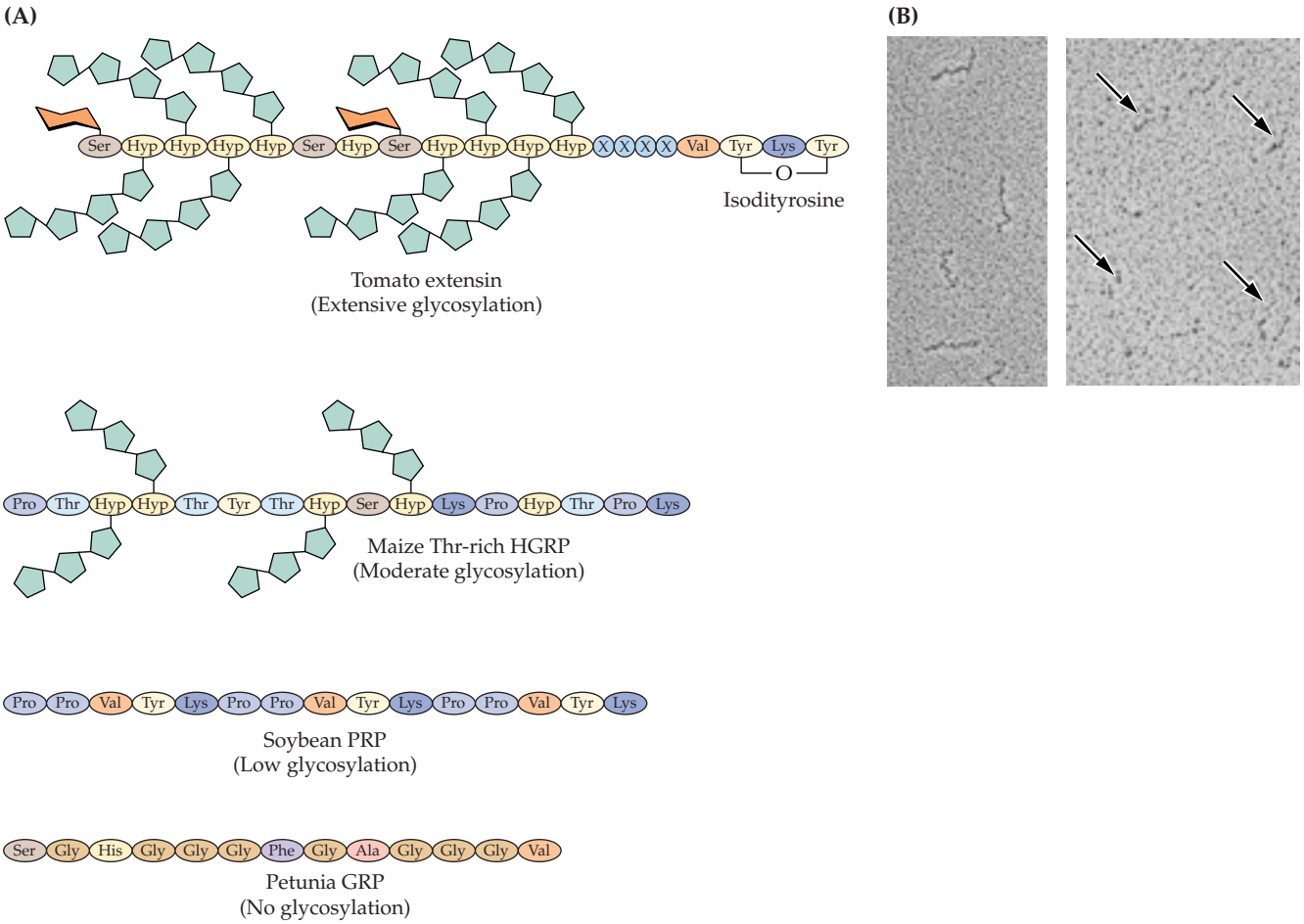

Figure 2.18
Comparisons of repeated motifs of extensins, maize Thr-rich proteins, PRPs, and GRPs. (A) A Ser-$(Hyp)_4$ or related motif found in many flowering plants is heavily glycosylated with mono-, di-, tri-, and tetraarabinosides that associate with the polyproline helix to reinforce a rod-shaped structure of tomato extensin molecules. A Gal unit is attached to the Ser residue. The Tyr-Lys-Tyr motif is the likely position of the intramolecular isodityrosine linkage. An extensin-like Thr-rich protein from maize is moderately glycosylated. The repeated motifs of PRP lack many contiguously hydroxylated Ser, Thr, and Hyp residues—a signal for glycosylation with arabinosides—so PRPs are not as heavily glycosylated. (B) Rotary-shadowed replicas of isolated extensin precursors reveal their rod-shaped structure (left). Removal of the arabinosides (right) results in loss of the rod-like conformation (arrows). (C) In contrast to the rod-shaped extensins, the GRPs may form β-sheet structures and are not glycosylated. A petunia GRP has 14 repeats of the motif shown in (A). The aromatic residues align on one face of the β-sheet.

a diverse group of glycoproteins that may function as structural elements inside the cell as well as in the cell wall, and genes for GRPs have now been found in many species.

The fourth major class of structural proteins, AGPs (Fig. 2.20), are more aptly named proteoglycans because they can be more than 95% carbohydrate. AGPs constitute a broad class of molecules located in Golgi-derived vesicles, the plasma membrane, and the cell wall. The site of glycosylation of the AGPs remains unknown but is likely to occur in the Golgi apparatus because it involves the attachment of large, highly branched galactan chains and subsequent decoration with Ara units. Characterization of the polysaccharide contents of the Golgi apparatus and secretory vesicles—including their glycosylated proteins—shows that a majority of the material present is AGP. Another characteristic of all AGPs is their ability to bind the Yariv reagent, a β-D-Glc derivative of phloroglucinol (Fig. 2.20).

Only recently have the genes encoding a few of the AGPs of flowering plants been cloned and the proteins' amino acid sequences deduced. Like GRPs, the AGPs are a diverse family of proteins, many of which are unrelated except for the glycan structures. The few proteins that have been identified can be characterized as enriched in Pro(Hyp), Ala, and Ser/Thr. They possess no distinguishing common motifs but do contain domains with similarity to some PRPs, extensins, and the solanaceous lectins (Fig. 2.20). No clear-cut function has been described for AGPs, or indeed for any of the structural proteins. Some proteins may have more subtle architectural roles (e.g., as nucleation sites for wall assembly) or may directly bind polymers together like the clamps that interlock scaffolding poles.

2.2.5 Aromatic substances are present in the nonlignified walls of commelinoid species.

The primary walls of the commelinoid orders of monocots and the Chenopodiaceae (such as sugar beet and spinach) contain significant amounts of aromatic substances in their nonlignified cell walls—a feature that makes them fluorescent under ultraviolet (UV) light. A large fraction of plant aromatics consists of **hydroxycinnamic acids,** such as ferulic and *p*-coumaric acids (Fig. 2.21; see also Chapter 24). In grasses, these hydroxycinnamates are attached as carboxyl esters to the O-5 position of a few of the Ara units of GAX. A small proportion of the ferulic acid units of neighboring GAXs may cross-link by phenyl–phenyl or phenyl–ether linkages to interconnect the GAX into a large network (Fig. 2.22). In the Chenopodiaceae, ferulic acids are attached to Gal or Ara units on side chains subtending some RG I molecules. Hydroxycinnamic acids are also reduced in the plant to hydroxycinnamoyl alcohols, which form the common precursors for lignin and lignan structures (see Chapter 24).

2.3 Cell wall architecture

2.3.1 The primary wall consists of structural networks.

Buildings come in many styles. So, too, does the architecture of cell walls. Any wall model is generic, and in the following subsections, we establish architectural principles rather than detail a specific cell wall.

The primary cell wall is made up of two, sometimes three, structurally independent but interacting networks. The fundamental framework of cellulose and cross-linking glycans lies embedded in a second network of matrix pectic polysaccharides. The third independent network consists of the structural proteins or a phenylpropanoid network. Evidence for these networks comes partially from direct imaging of walls (Box 2.4). Subsequent sections of the chapter will address two distinct cell wall types, Type I and Type II, which differ in chemical composition and are associated with distinct plant taxa (see Fig. 2.13).

2.3.2 Walls of angiosperms are arranged in two distinct types of architecture.

The walls of most dicots and the noncommelinoid monocots contain about equal amounts of XyGs and cellulose. These kinds of wall we denote as **Type I walls.** XyGs

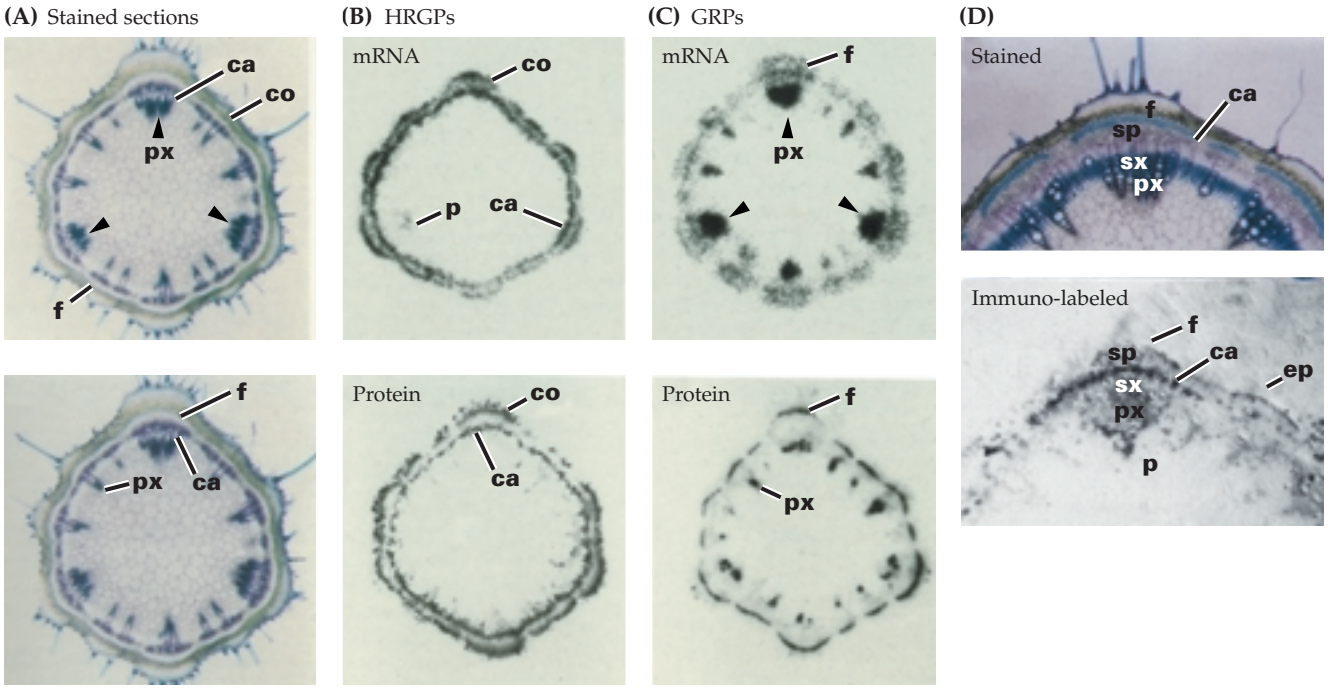

Figure 2.19
When cleanly sliced sections of a plant are pressed firmly for a few seconds to a nitrocellulose sheet, molecules of soluble carbohydrate, protein, and nucleic acids are left behind, imprinted on the nitrocellulose in a nearly cell-specific pattern. Coined **tissue printing** by Joe Varner, this technique has been instrumental in providing biologists with an extremely simple experimental tool of many uses. (A) Stained sections of the elongating second internode of soybean stem are provided for comparison with the other pairs of sections. (B) In situ hybridization with an HRGP cDNA probe and immuno-localization with an HRGP-specific antibody reveal that HRGPs and the mRNA transcripts that encode them are colocalized in cortical (co) and cambial (ca) cells. (C) The same techniques show that GRP mRNA transcripts and their protein products are enriched in the phloem (f) and protoxylem (px). Thus, the GRP proteins and transcripts are found primarily in vascular or lignified cells, whereas the HRGP proteins and transcripts are located in meristematic cells and cells around the cambium. (D) Magnification of the stained section and tissue print shows that HRGP can be immunolocalized to the cellular level. ep, epidermis; p, pith; sp, secondary phloem; sx, secondary xylem.

occur in two distinct locations in the wall. They bind tightly to the exposed faces of glucan chains in the cellulose microfibrils, and they lock the microfibrils into the proper spatial arrangement by spanning the distance between adjacent microfibrils or by linking to other XyGs. With an average length of about 200 nm, XyGs are long enough to span the distance between two microfibrils and bind to both of them. Such spanning XyGs have been observed by electron microscopy (see Box 2.4).

In Type I walls (Fig. 2.23A), the cellulose-XyG framework is embedded in a pectin matrix that controls, among other physiological properties, wall porosity. HGA is thought to be secreted as highly methyl-esterified polymers, and the enzyme **pectin methylesterase** (PME), located in the cell wall, cleaves some of the methyl groups to initiate binding of the carboxylate ions to Ca^{2+}. The helical chains of HGAs can condense by cross-linking with Ca^{2+} to form "junction zones," thereby linking two antiparallel chains (Fig. 2.24A). The strongest junctions occur between two chains of at least seven unesterified GalA units each. If sufficient Ca^{2+} is present, some methyl esters can be tolerated in the junction, and the HGAs can bind in both parallel and antiparallel orientation (Fig. 2.24B). The spacing of the junctions is postulated to create a cell-specific pore size. Rha units of RG I and their side chains interrupt the Ca^{2+} junctions and contribute to the pore definition (Fig. 2.25).

Other properties of the pectin network also regulate porosity. The extent of methyl esterification may remain high in the walls of some cells, and a type of gel may form

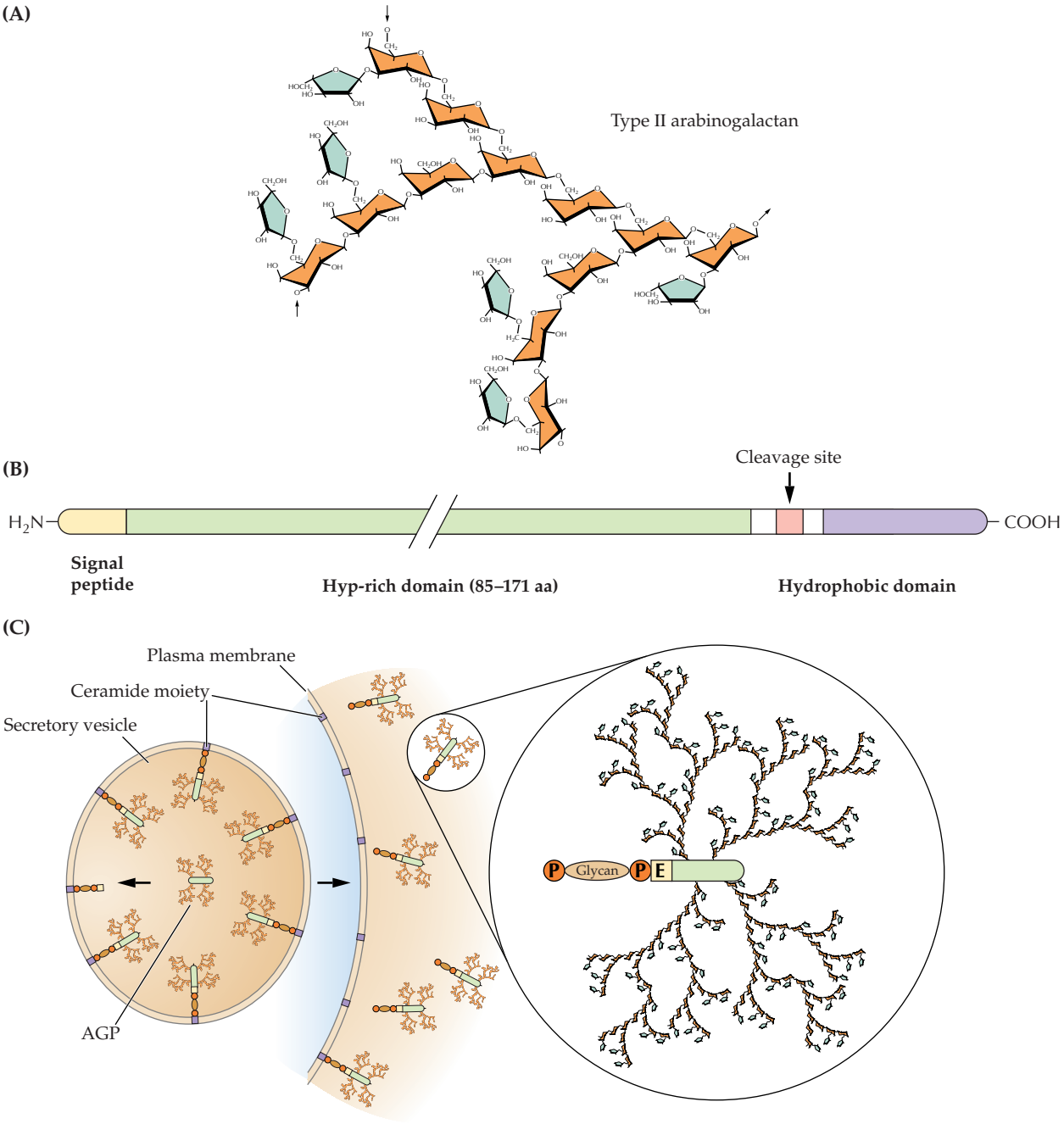

(D)

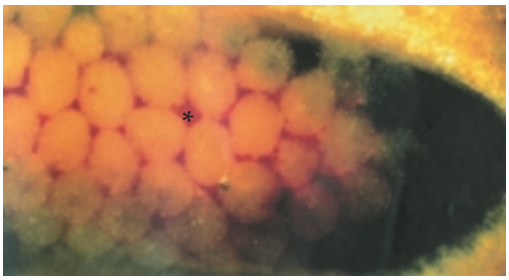

Figure 2.20

(A) The arabinogalactan proteins (AGPs) are proteoglycans, many of which are glycosylated with type II AG structures. (B) The few AGP genes that have been identified encode proteins enriched for Hyp, Ala, and Ser/Thr residues. The domains are thought to contain the AG chains but, as with the GRPs, there are no clear-cut unifying motifs. Some of the AGPs contain domains that are homologous to extensins or PRPs and contain Cys-rich domains. Each of these domains is glycosylated in different ways. (C) Some AGPs, after cleavage of the C terminus, covalently attach to glycosylphosphatidyl inositides (called GPI anchors) during synthesis and secretion in the ER and Golgi apparatus. Note that the GPI anchor and its attached protein are enlarged relative to the AG carbohydrates. Once at the exterior of the cell, the AGP portion may be cleaved from the ceramide moiety of the GPI anchor and serve as a signal molecule. E, ethanolamine. (D) The Yariv reagent, a reddish phloroglucinol derivative with three β-linked galactosyl units, specifically stains AGPs (see asterisk for example). AGPs are particularly enriched in the styles of many flowers, such as this one from *Nicotiana alata.*

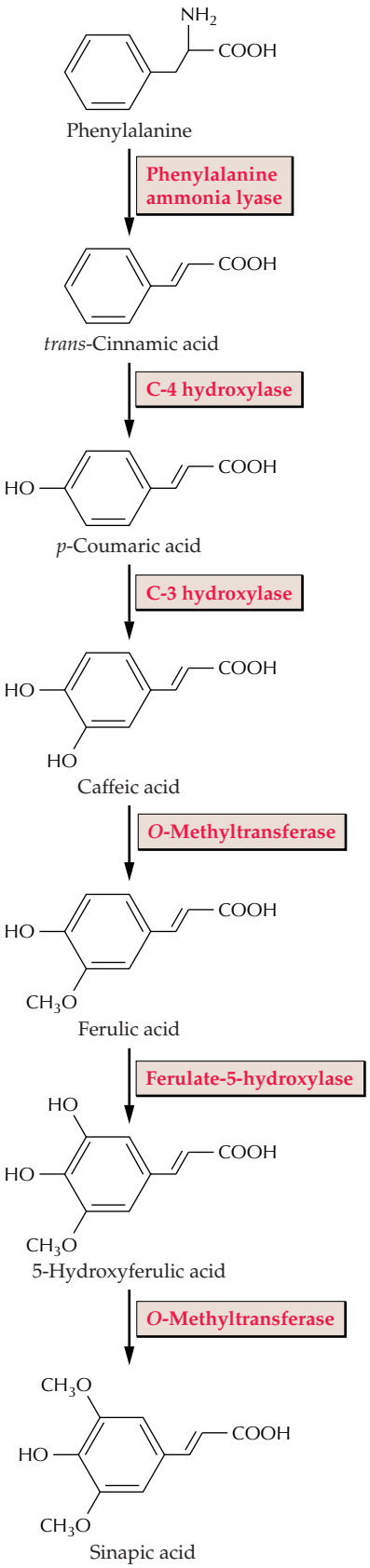

Figure 2.21
Conversion pathway from phenylalanine to the hydroxycinnamic acids of grasses and chenopods. The hydroxycinnamic acids are esterified to the Ara units of Type II arabinoxylans and to Gal and Ara units of some pectic polysaccharides. These hydroxycinnamic acids are the basis for the UV fluorescence observed in nonlignified walls of the commelinoid species. They also may be reduced to their respective cinnamoyl alcohols, which then are precursors of lignin.

that contains highly esterified parallel chains of HGAs. Some HGAs and RGs are cross-linked by ester linkages to other polymers that are held more tightly in the wall matrix and can be released from the wall only by the action of deesterifying agents. Other pectic polymers may separate the sites of borate di-diester cross-linking along the pectic backbone (see Fig. 2.17). Neutral polymers (arabinans or galactans) are pinned at one end to the pectic backbone but extend into, and are highly mobile in, the wall pores (Fig. 2.25). At some stages of cell development, hydrolases are released that trim these neutral polymers, potentially increasing the pore size in the walls. In meristems and elongating cells, where Ca^{2+} concentrations are kept quite low, significant deesterification of HGA can occur without Ca^{2+} binding. Although this may not contribute to pore size dynamics, it alters charge density and local pH.

Some Type I walls contain large amounts of protein, including basic proteins that can interact with the pectin network. In these instances, various structural proteins can form intermolecular bridges with other proteins without necessarily binding to the polysaccharide components.

Type II walls of commelinoid monocots contain cellulose microfibrils similar to those of the Type I wall; instead of XyG, however, the principal polymers that interlock the microfibrils are GAXs. Unbranched GAXs can hydrogen-bond to cellulose or to each other. The attachment of the α-L-Ara and α-L-GlcA side groups to the xylan backbone of GAXs prevents the formation of hydrogen bonds and therefore blocks cross-linking between two branched GAX chains or from GAX to cellulose. In contrast, the α-D-Xyl units attached at the O-6 of XyG, away from the binding plane, stabilize the linear structure and permit binding to one side of the glucan backbone. Despite the predominance of GAX, small amounts of XyG also are present in Type II walls and bind tightly to cellulose.

In general, Type II walls are pectin-poor, but an additional contribution to the charge density of the wall is provided by the α-L-GlcA units on GAX. These walls have very little structural protein compared with dicots and other monocots, but they can accumulate extensive interconnecting networks of phenylpropanoids, particularly as the cells stop expanding (see Fig. 2.23B).

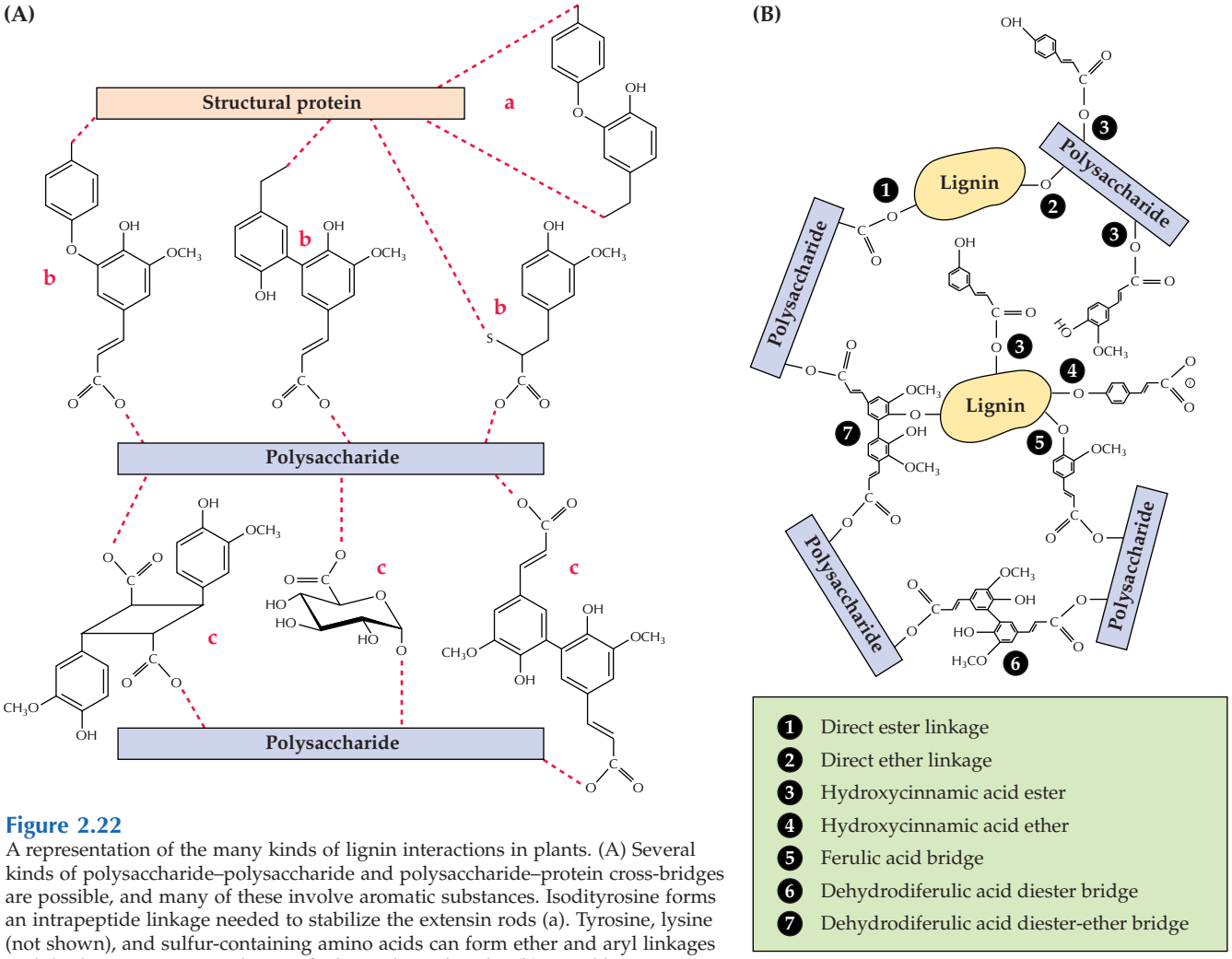

Figure 2.22
A representation of the many kinds of lignin interactions in plants. (A) Several kinds of polysaccharide–polysaccharide and polysaccharide–protein cross-bridges are possible, and many of these involve aromatic substances. Isodityrosine forms an intrapeptide linkage needed to stabilize the extensin rods (a). Tyrosine, lysine (not shown), and sulfur-containing amino acids can form ether and aryl linkages with hydroxycinnamic acids esterified to polysaccharides (b). Neighboring polysaccharides may contain cross-bridges esterified directly to sugars (c). (B) A summary of the kinds of aromatic ester and ether cross-links between carbohydrate and lignin.

2.3.3 Polymers remain soluble until they can be cross-linked at the cell surface.

Many polymers are modified by esterification, acetylation, or arabinosylation for solubility during transport. Later, extracellular enzymes deesterify, deacetylate, or dearabinosylate at free sites along the polymers for cross-linking into the cell wall. These sites are determined by the long-range binding order of polysaccharides, permitting their assembly into very precise cell wall architectures. A range of cross-linking possibilities exists, including hydrogen-bonding, ionic bonding with Ca^{2+} ions, covalent ester linkages, ether linkages, and van der Waals interactions. AGPs, because they constitute a majority of the material of secretory vesicles but never accumulate to a comparable extent in the wall, may function as a chaperone-like matrix that prevents premature associations and keeps enzymatic functions in a quiescent state until the secretory materials are assembled in the wall.

Assembly processes occur in an aqueous environment, and one of the major components of cell walls is water. This is of structural importance from the viewpoint of maintaining polymers in their proper conformations. Water is the medium that permits the passage of ions and of signaling molecules through the apoplast; it also

Box 2.4

Cell walls and their component polymers can be visualized directly by novel microscopy techniques.

More than 300 years ago, Robert Hooke recorded the first images of plant cell walls in this *camera lucida* print of sections of the bark of cork oak (panel A).

(A)

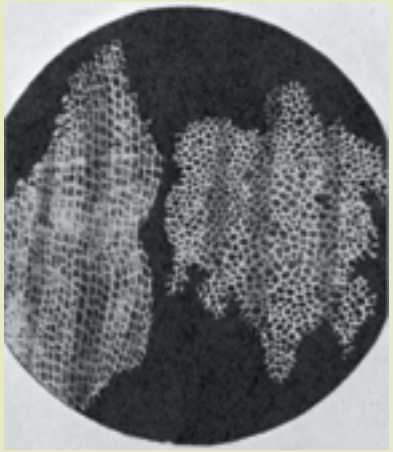

However, many years passed before the structural details of cell walls could be resolved by microscopy. When conventional techniques are used to stain plant tissues for electron microscopy, the cell wall appears as a fuzzy zone with little structural information (see Fig. 2.3B for an example). However, an alternative method of preparing samples, **fast-freeze, deep-etch, rotary-shadowed replica,** allows visualization of cell walls at high resolution and with good preservation of the three-dimensional spatial relationships of the polymers (panel B; scale bar represents 200 nm). This technique requires four steps:

(B)

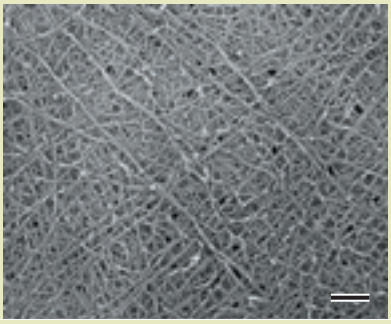

- Wall material is frozen rapidly with liquid nitrogen or helium.
- Surface ice is removed under vacuum.
- The exposed surface is coated with a thin film of platinum and carbon to produce a replica, essentially a three-dimensional contour map of the cell wall polymers in their proper orientation.
- The underlying tissue is dissolved away, and the replica is viewed in the electron microscope.

Because the walls are frozen so quickly, little ice damage occurs, and because no chemical fixatives or dehydrants are used, the normal spacing of components remains. Gentle extraction of pectic polysaccharides from cell walls before freezing can reveal the fine, thread-like cross-linking glycans spanning the larger microfibrils (panel B). This technique has allowed more accurate determinations of microfibril diameters and their spacing. A glancing fracture through an onion epidermal wall prepared by this technique reveals the individual strata of the wall, called lamellae (panel C).

(C)

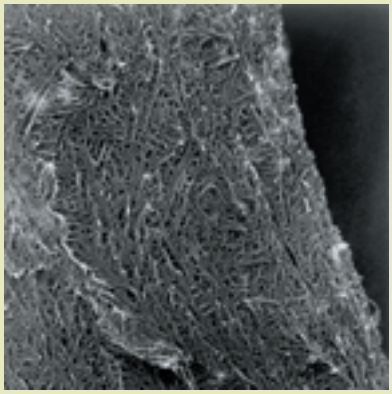

An alternative technique uses acid-etching of material fixed and sectioned for conventional transmission electron microscopy. A glancing section through the thick outer wall of an epidermal cell wall, which was then acid-etched and viewed by conventional transmission electron microscopy, reveals an iterative pattern of microfibril orientation in the individual lamellae (panel D).

Isolated cell wall molecules can also be imaged with the replica technique. The molecules are mixed in glycerol and sprayed onto a freshly cleaved sheet of mica. After the glycerol has been dried under vacuum, a rotary-shadowed replica is made, and the mica is dissolved by strong acid. Length measurements can be made directly from electron micrographs. For example, homogalacturonans isolated from cell walls of onion parenchyma can be as long as 400 nm (panel E). Minimum molecular mass can then be estimated from length data.

(D)

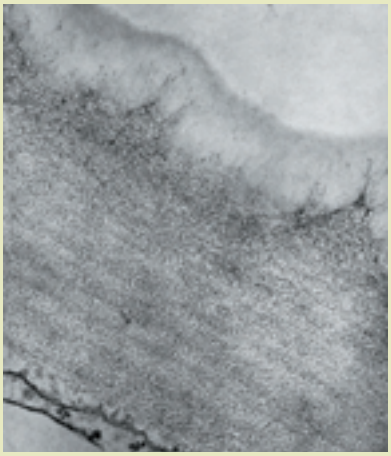

(E)

Another technique, **atomic force microscopy,** is now being used to image cell walls in even greater detail (panel F). This method is sensitive enough to resolve the spacing of individual glucose molecules in a microfibril.

(F)

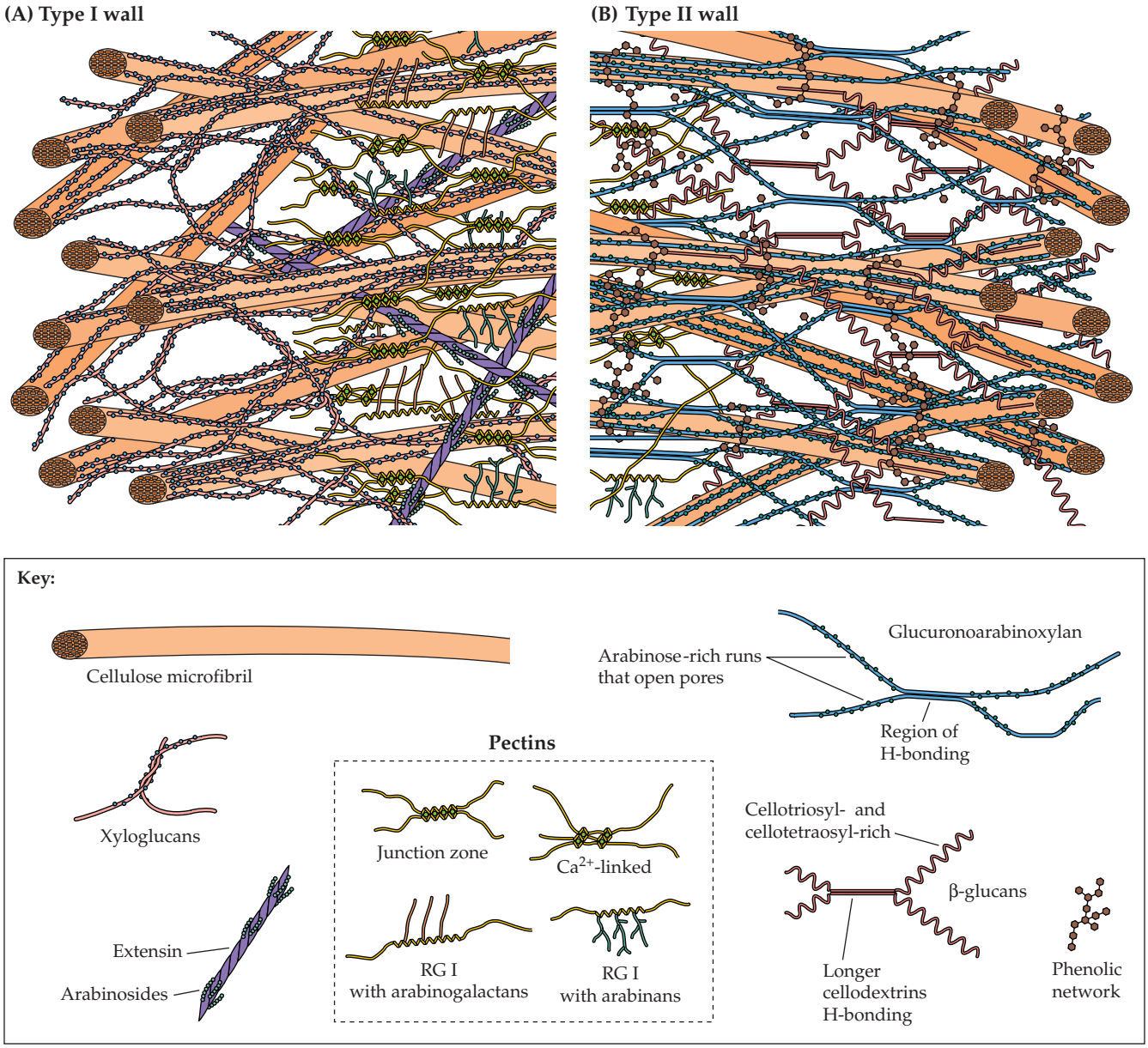

Figure 2.23
(A) A three-dimensional molecular model of the Type I wall shows the molecular interactions between cellulose, XyG, pectins, and wall proteins. The framework of cellulose microfibrils and XyG polymers is embedded in a matrix of pectic polysaccharides, HGA, and RG I, the latter being substituted with arabinan, galactan, and arabinogalactan. Because XyGs have only a single face that can hydrogen bond to another glucan chain and can self-associate, we depict several XyGs as woven to interlace the microfibrils. Many other associations are possible, including bridging of two microfibrils by a single XyG. With microfibril diameters of 5 to 10 nm and a spacing of about 20 to 30 nm, a primary wall 80 nm thick can contain only about 5 to 10 strata (only three lamellae of microfibrils are shown for clarity). During growth, cleavage or dissociation of XyGs by enzymes loosens the cellulose–XyG network, allowing microfibrils to separate in the long axis of the page. After growth, extensin molecules may interlock the separated microfibrils to reinforce the architecture. Additional proteins may also be inserted to cross-link extensin, forming a heteropeptide network. Formation of intramolecular covalent bonds among the individual wall proteins may help to terminate cell elongation. (B) A three-dimensional molecular model of the Type II wall shows the molecular interactions between cellulose, GAX, pectins, and aromatic substances. The microfibrils are interlocked by GAXs instead of XyGs. Unlike XyGs, the xylans are substituted with Ara units, which block hydrogen bonding. The xylans are probably synthesized in a highly substituted form, and dearabinosylated in the extracellular space to yield runs of the xylan that can bind on either face to cellulose or to each other. Porosity of the GAX domain could be determined by the extent of removal of the appendant units. Some highly substituted GAX remains intercalated in the small amount of pectins that are also found in the primary wall. Unlike the Type I wall, a substantial portion of the noncellulosic polymers are "wired on" to the microfibrils by alkali-resistant phenolic linkages. Depicted here is the special Type II wall of the grasses (Poales), which synthesize β-glucans during cell enlargement. These corkscrew-shaped molecules contain linear runs of cellodextrins about every 50 glucosyl units or so; these runs are targets for endo-β-D-glucanases, which cleave them.

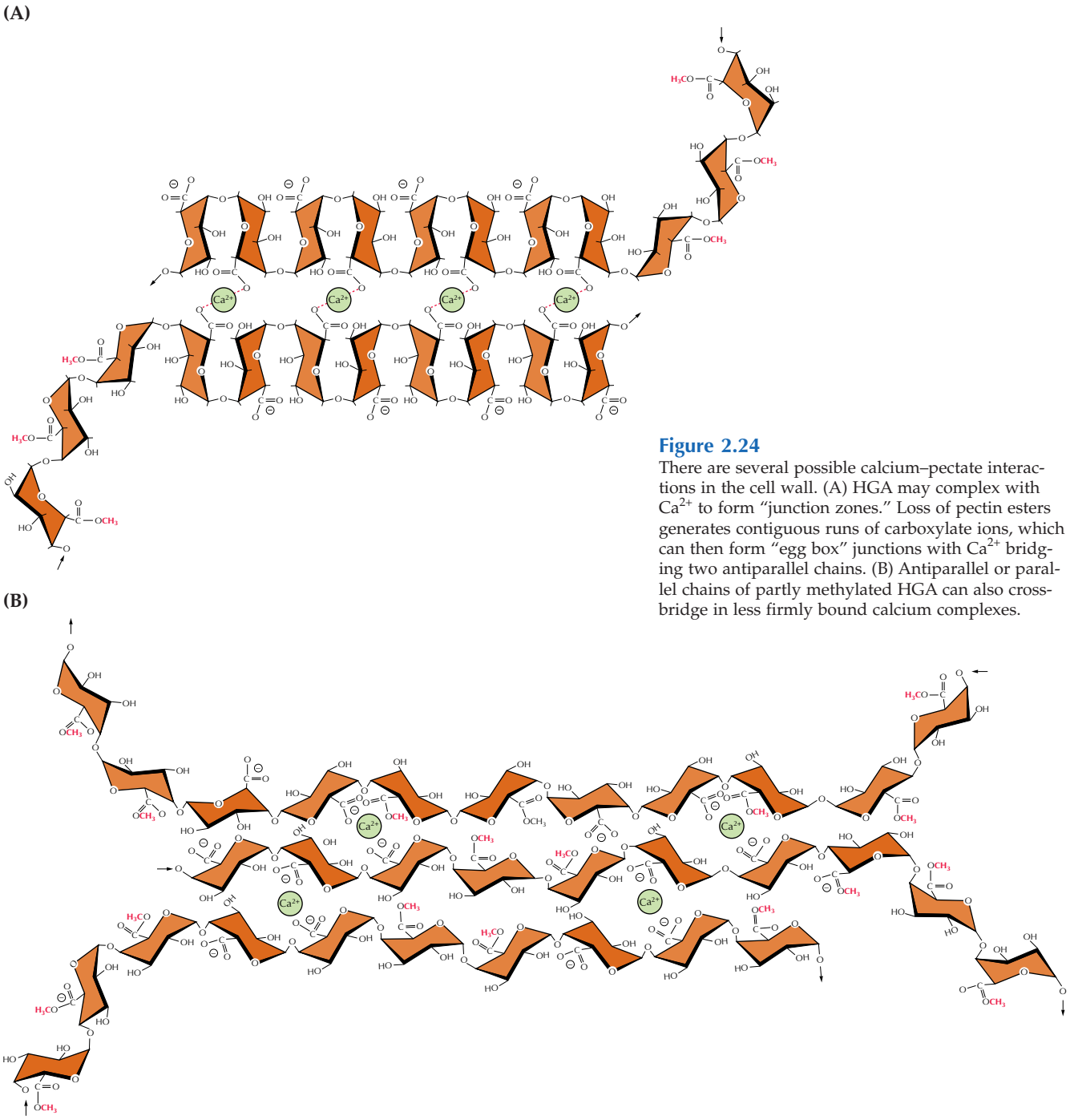

Figure 2.24
There are several possible calcium–pectate interactions in the cell wall. (A) HGA may complex with Ca^{2+} to form "junction zones." Loss of pectin esters generates contiguous runs of carboxylate ions, which can then form "egg box" junctions with Ca^{2+} bridging two antiparallel chains. (B) Antiparallel or parallel chains of partly methylated HGA can also cross-bridge in less firmly bound calcium complexes.

provides an environment for enzymes to function. The pH of apoplastic space is thought to be 5.5; whether this pH changes appreciably during growth is not yet resolved. The pore diameter that limits diffusion of molecules through the primary wall is about 4 nm, but some molecules larger than this can pass through the wall to the plasma membrane, perhaps by way of a small number of larger pores or because they are rod-like rather than globular.

2.4 Cell wall biosynthesis and assembly

2.4.1 Cell walls are born in the developing cell plate.

Cell walls originate in the developing cell plate. As plant nuclei complete division during telophase of the mitotic cell cycle, the **phragmosome,** a flattened membranous vesicle containing cell wall components, forms across the cell within a cytoskeletal array

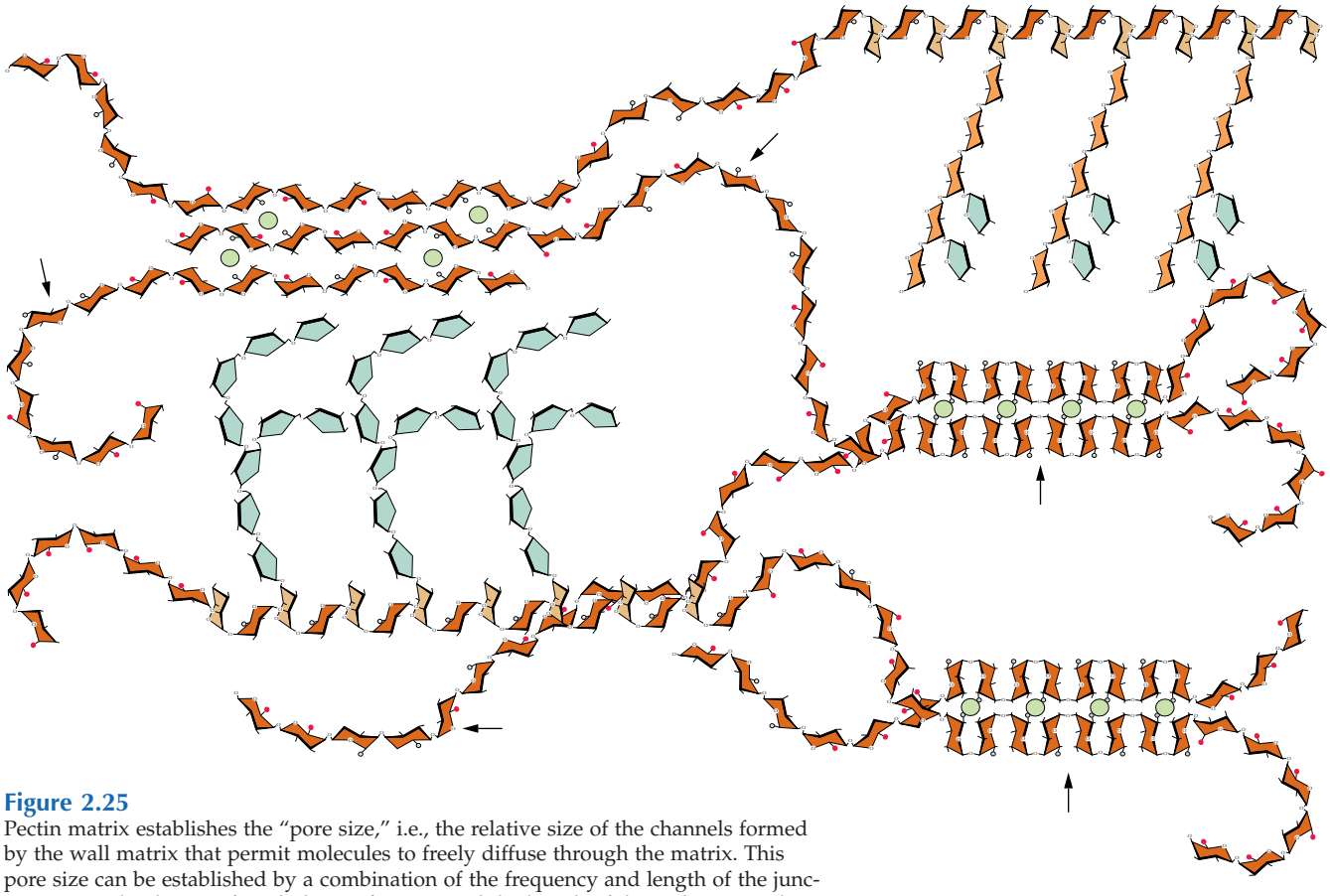

Figure 2.25
Pectin matrix establishes the "pore size," i.e., the relative size of the channels formed by the wall matrix that permit molecules to freely diffuse through the matrix. This pore size can be established by a combination of the frequency and length of the junction zones, the degree of methyl-esterification, and the length of the arabinans, galactans, and arabinogalactans attached to RG I that extend into the pores. Additional factors that influence pore size are the frequency of RG II and its dimerization by boron (not shown). The charge density depends on the extent of deesterification of the HGA to yield carboxyl acids unbound to Ca^{2+}. Arrows denote domains of negative-charge density in HGAs.

called the **phragmoplast.** The noncellulosic cell wall polysaccharides synthesized in the Golgi apparatus and packaged in vesicles fuse with the growing cell plate. The plate grows outward until the edges of the membranous vesicle fuse with the plasma membrane, creating two cells. Finally, the new cell wall fuses with the existing primary wall (see Chapter 5).

The plant Golgi apparatus is a factory for the synthesis, processing, and targeting of glycoproteins (Fig. 2.26). The Golgi apparatus also has been shown by autoradiography to be the site of synthesis of noncellulosic polysaccharides. Thus—except for cellulose—the polysaccharides, the structural proteins, and a broad spectrum of enzymes are coordinately secreted in Golgi-derived vesicles and targeted to the cell wall.

2.4.2 Golgi-localized enzymes interconvert the nucleotide sugars, which serve as substrates for polysaccharide synthesis.

The reactions that synthesize noncellulosic cell wall polysaccharides in the Golgi apparatus utilize several nucleotide sugars as substrates. Beginning with formation of UDP-glucose and GDP-glucose (Fig. 2.27), pathways for **nucleotide sugar interconversion** produce various nucleotide sugars de novo in enzyme-catalyzed reactions (Figs. 2.28 and 2.29). Many of these interconversion enzymes (e.g., epimerases and dehydratases) appear to be membrane-bound and localized to the ER-Golgi apparatus. Guanosine-based nucleotide sugars (Fig. 2.29), such as GDP-Glc and GDP-Man, are used in the synthesis of glucomannan, and GDP-Fuc

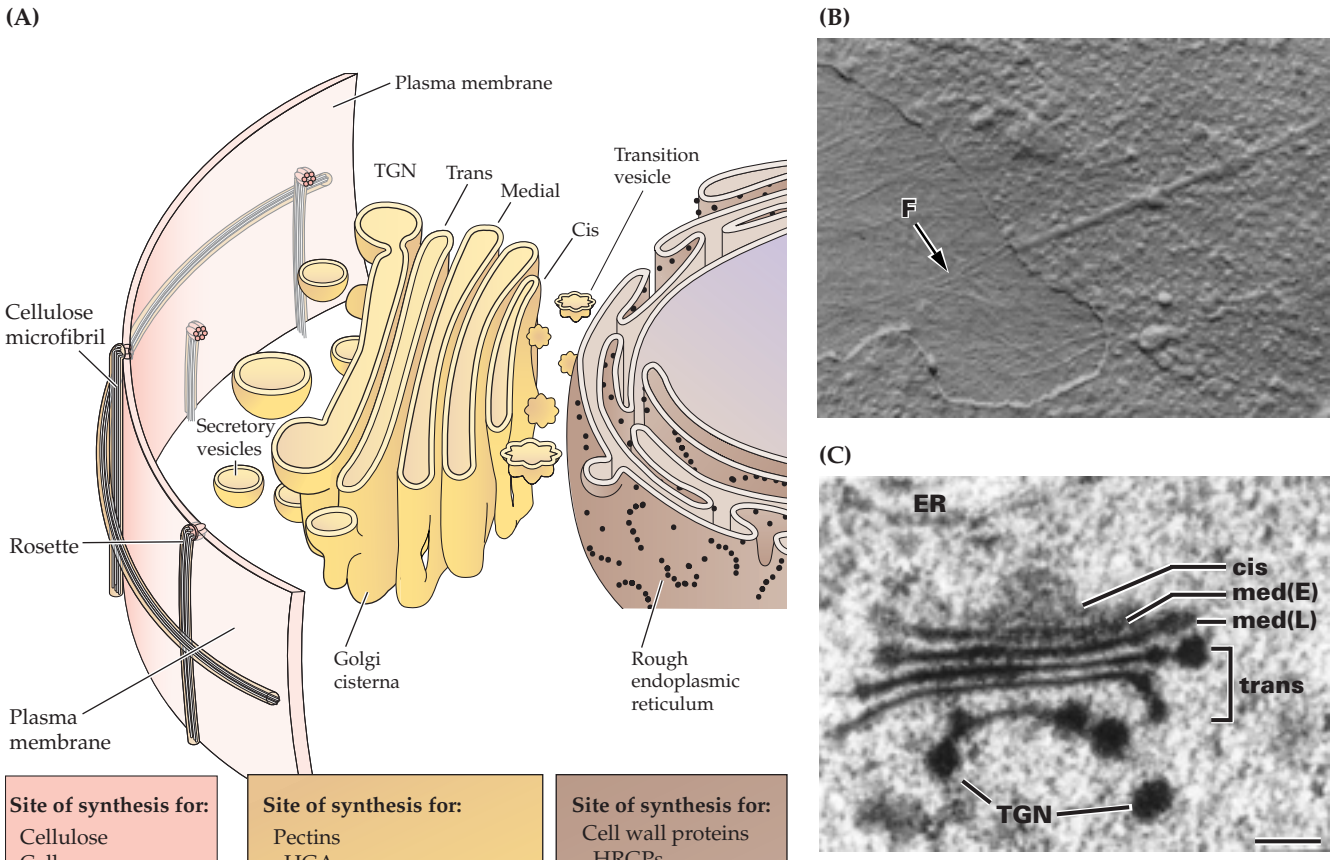

Figure 2.26
(A) Biosynthesis of the wall requires a coordination of the synthesis of cellulose microfibrils at the plasma membrane surface, with the synthesis and glycosylation of proteins and wall-modifying enzymes at the rough ER and the synthesis of all noncellulosic polysaccharides at the Golgi apparatus. Material destined for the cell wall is packaged into secretory vesicles, transported to the cell surface, and integrated with the newly synthesized microfibrils. Assembly of the new wall stratum is estimated to begin when no more than 10 glucose residues of a cellulose chain are made. (B) A replica of an E-face (exterior leaf of a fractured membrane bilayer). The numerous vesicles aggregating at the surface resemble small craters. A portion of the membrane has torn away to reveal the underlying microfibrils (F). (C) A cross-section of a single dictyosome body of the Golgi apparatus shows the characteristic development of several membrane sheets, from the cis face nearest the ER to the trans face; these develop into the distinct *trans*-Golgi network (TGN), the principal vesicle-secreting body. E and L, early and late *medial*-Golgi stacks, respectively.

is a substrate in the fucosylation of complex glycoproteins, pectins, and some cross-linking glycans.

One of the more intriguing questions yet to be answered is how arabinofuranosyl units are made. L-Arabinose is in the furanose ring conformation in most plant polymers containing this sugar, including GAX, 5-linked arabinans, AGP, and extensin, whereas UDP-Ara (see Fig. 2.28) is exclusively in the pyranose form. An arabinosyltransferase may differ from other glycosyltransferases in its ability to permit ring rearrangement before the sugar is added to the polymer.

The precise topographic location of the polysaccharide synthase enzymes on or within the Golgi membranes has not been established. For branched polysaccharides, the nucleotide sugar substrate used for synthesis of the backbone may be donated from either the cytosolic or the lumenal side of the Golgi, but the branch units probably are added only from the lumenal side.

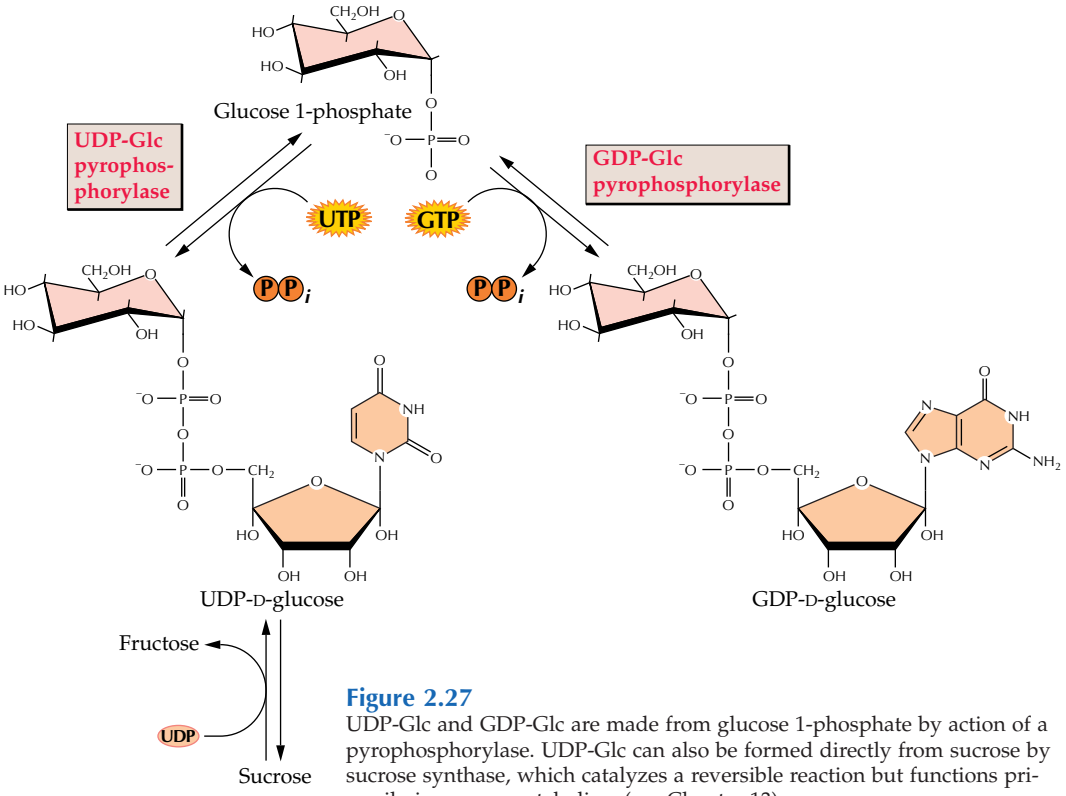

Figure 2.27
UDP-Glc and GDP-Glc are made from glucose 1-phosphate by action of a pyrophosphorylase. UDP-Glc can also be formed directly from sucrose by sucrose synthase, which catalyzes a reversible reaction but functions primarily in sucrose catabolism (see Chapter 13).

Hence, synthesis of complex polysaccharides must be coordinated with transport of some of the nucleotide sugars into the Golgi apparatus.

Formation of nucleotide sugars occurs via two distinct pathways. The de novo synthesis pathways initially produce the full array of nucleotide sugars, which are then used as substrate for the synthesis of polysaccharides, glycoproteins, and several other glycosylation reactions. However, several monosaccharides other than Glc may be incorporated into nucleotide sugars via salvage pathways involving C-1 kinases and nucleotide diphosphate (NDP)–sugar pyrophosphorylases (see Figs. 2.28 and 2.29). The salvage pathways are essential for reuse of these monosaccharides after their hydrolysis from polymers during cell wall assembly and during turnover of the cell wall. Some sugars, such as Rha and Xyl, do not have C-1 kinases (see Fig. 2.28), and their carbons must be reused via other pathways. Xyl carbons are returned by way of the pentose phosphate pathway after isomerization to xylulose.

2.4.3 Membrane fractions enriched for Golgi membranes can synthesize many noncellulosic polysaccharides in vitro.

Many reports of the synthesis of noncellulosic wall polysaccharides in vitro include use of membrane preparations enriched in Golgi membranes. In mixed-membrane preparations containing plasma membrane, Golgi, and UDP-Glc as a substrate, the predominant product is the (1→3)β-D-glucan, callose—a polymer thought to be made as a default product by damaged cellulose synthase. This reaction is activated by calcium ions, the concentrations of which increase markedly in cells that have been damaged. Thus, the other noncellulosic polysaccharides of interest must be detected and quantified in the presence of a huge background of callose.

By treating polysaccharides with sequence-dependent glycanases, researchers can detect the characteristic unit structures despite the presence of the wound-induced callose. This technique, which verifies that isolated membranes are capable of

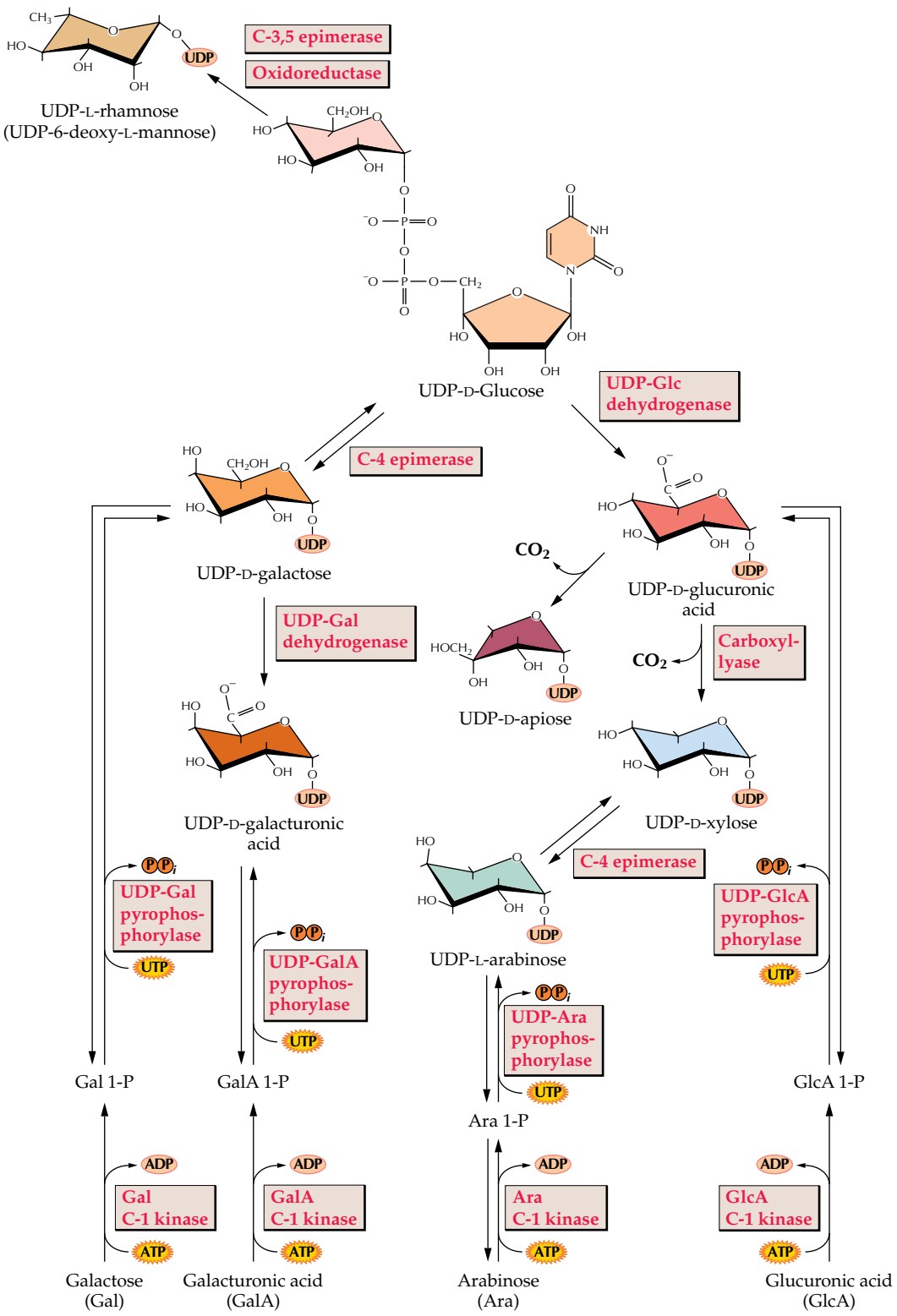

Figure 2.28
Synthesis of UDP-sugars. UDP-Gal is made from UDP-Glc in an equilibrium reaction catalyzed by a C-4 epimerase. UDP-Xyl and UDP-L-Ara are interconverted similarly by a C-4 epimerase. A C-3,5 epimerase and a hypothetical oxidoreductase are thought to convert UDP-Glc to UDP-Rha. Oxidation of UDP-Gal or UDP-Glc by a dehydrogenase yields UDP-GalA or UDP-GlcA, respectively. Decarboxylation of UDP-GlcA by a carboxyl-lyase constitutes another pathway to UDP-Xyl. Finally, Gal, GalA, Ara, and GlcA can be uridinylated via salvage pathways, in which the sugars are phosphorylated by C-1 kinases to generate sugar 1-phosphates, which in turn act as substrates for the pyrophosphorylases that generate nucleotide sugar end-products.

synthesizing unit structures identical to those made in vivo, has been particularly useful for studying in vitro synthesis of XyG.

The isolated Golgi apparatus of plants with Type I walls can synthesize very short (1→4)β-D-glucan chains from either UDP-Glc or GDP-Glc, but the synthesis of XyG is greatly enhanced by addition of nearly millimolar amounts of both UDP-Glc and UDP-Xyl, with Mn^{2+} or Mg^{2+} as cofactor. Cleavage of the XyG reaction products yields substantial amounts of the diagnostic XXXG heptasaccharide unit, verifying that the cellular machinery needed to make a complete unit structure can be preserved in a cell-free system. Because only very short chains of (1→4)β-D-glucan backbone can be made from UDP-Glc in the absence of UDP-Xyl, the glucosyl- and xylosyltransferases appear to be tightly coupled, catalyzing the formation of the repeating heptasaccharide units cooperatively. The attachment of additional sugars to the Xyl units may occur coordinately as well, but additional elaboration involving galactosyl- and fucosyltransferases continues during later stages of transit through the Golgi apparatus (see Fig. 2.26). These types of coordinated glycosyl transfers are observed in the synthesis of glucomannans with GDP-Glc and GDP-Man, galactomannans with GDP-Man and UDP-Gal, and arabinoxylans with UDP-Xyl and UDP-Ara. In addition, the synthesis of HGA in vitro appears to be coordinated with its methyl-esterification.

UDP-Glc is the substrate for the mixed-linkage β-glucan synthase of grass species, and either Mg^{2+} or Mn^{2+} is required as a cofactor. The preservation of β-glucan synthase activity is demonstrated by digestion of the β-glucan product with a *Bacillus subtilis* endoglucanase into characteristic tri- and tetrasaccharides (G_4G_3G and $G_4G_4G_4G$, respectively) in the correct ratio (Fig. 2.30).

None of the genes encoding the polysaccharide synthases that make the backbone chains have been identified, but numerous candidates are potential homologs of cellulose synthases, in particular within sequences encoding the UDP-Glc–binding domains (see Section 2.4.5). In contrast, the genes of several fucosyl- and galactosyltransferases, which add single sugars subtending the backbone as side groups, have now been identified. These genes encode

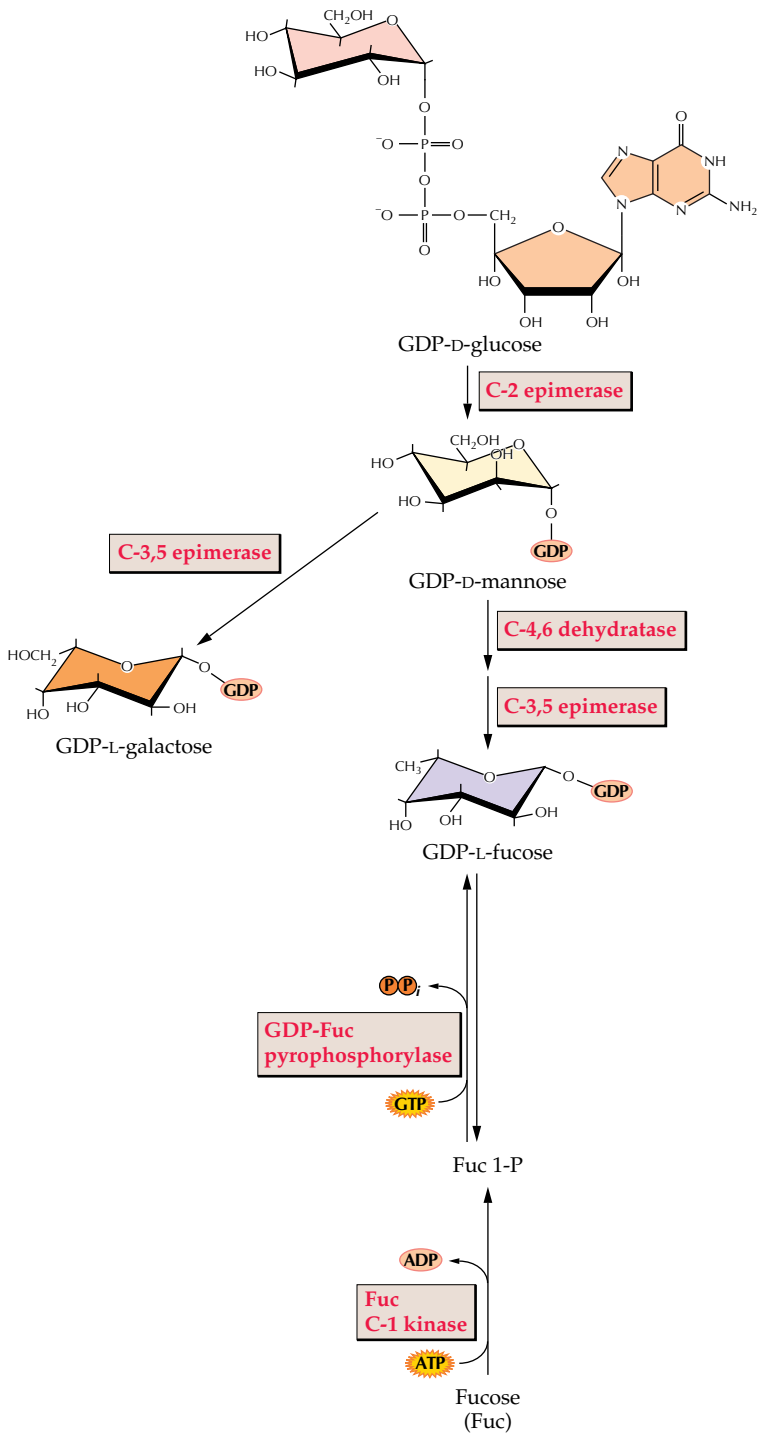

Figure 2.29
Synthesis of GDP-sugars. GDP-Glc is converted to GDP-Man by a C-2 epimerase. GDP-Man yields GDP-L-Gal in a reaction catalyzed by a C-3,5 epimerase. Two enzymes, a C-4,6 dehydratase and the C-3,5 epimerase active in GDP-L-Gal biosynthesis, participate sequentially in the conversion of GDP-Man to GDP-L-Fuc. A salvage pathway generates GDP-L-Fuc from glucose.

a special class of proteins with single-membrane spans that extend the transferase activity into the lumen of the Golgi membranes.

2.4.4 Cellulose microfibrils are assembled at the plasma membrane surface.

The only polymers known to be made at the outer plasma membrane surface of plants are cellulose and callose. Cellulose synthesis is catalyzed by multimeric enzyme complexes located at the termini of growing cellulose microfibrils (Fig. 2.31). These **terminal complexes** are visible in freeze-fracture replicas of plasma membrane. In some algae, terminal complexes are organized in linear arrays, whereas in others—and in all angiosperms—they form **particle rosettes** (Fig. 2.31). Terminal complexes appear in the plasma membrane coincident with the activity of cellulose synthesis. Kinetic studies monitoring the pathway of glucose to cellulose have established that UDP-Glc is the primary substrate for cellulose synthase. Isoforms of sucrose synthase, an enzyme that produces UDP-Glc directly from sucrose (see Fig. 2.27), also are associated with the plasma membrane; here, in close association with cellulose synthase, these isoforms may contribute substrate directly into the catalytic site of the enzyme.

Although callose synthesis in isolated membranes may have resulted from damage to the cellulose synthase, callose is a natural component of the initial cell plate, the pollen tube wall, and transitional stages of wall development of certain cell types. Unlike the wound polymer, pollen tube callose is synthesized by enzymes that do not require Ca^{2+} as cofactors; moreover, these synthases must be enzymes distinct from cellulose synthases.

Although cellulose synthase generates one of the most abundant biopolymers on earth, this plant enzyme has proven curiously difficult to purify in active form. Cellulose synthase activity from plants disappears even under conditions of gentle plasma membrane isolation, and no terminal complexes have been found in isolated membranes. The complex may require cytoskeletal or cell wall components for it to stabilize in the membrane.

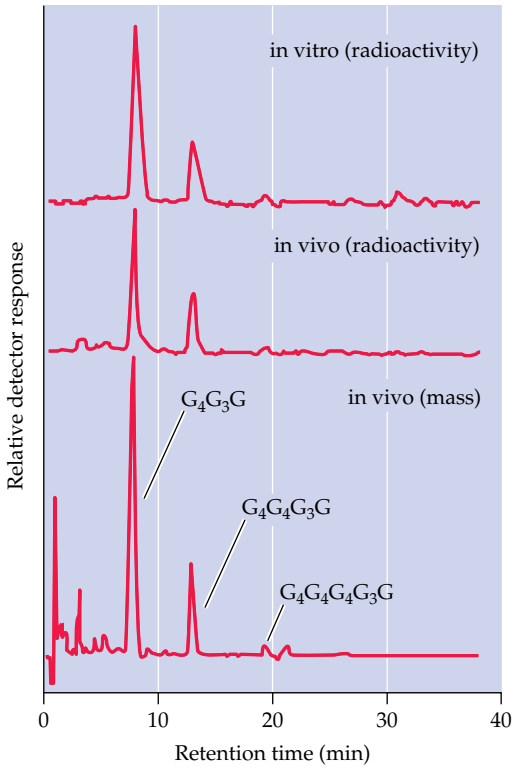

Figure 2.30
The *Bacillus subtilis* endoglucanase has the unusual ability to hydrolyze a (1→4)β-D-glucosyl linkage only if the penultimate linkage is (1→3)β-D-glucosyl linkage. Because 90% of cereal β-glucans are composed of cellotriosyl and cellotetraosyl units in a ratio of about 2.5:1, the enzyme generates cellobiosyl-(1→3)-glucose (G_4G_3G) and cellotriosyl-(1→3)-glucose ($G_4G_4G_3G$) oligosaccharides in this ratio also. When the radioactive products of such a digest are separated by HPAE-HPLC, the ratio of these oligomeric units is the same whether from β-glucan synthesized in vivo by living plants fed [^{14}C]glucose or from isolated Golgi membranes treated with UDP-[^{14}C]glucose. Characterization of polysaccharide synthase reaction products in such a way confirms that synthesis in vitro parallels that in vivo. $G_4G_4G_4G_3G$, cellotetraosyl-(1→3)-glucose.

2.4.5 Cellulose synthase genes from plants have been cloned on the basis of sequence identity with bacterial enzymes.

After a search spanning nearly four decades, several genes encoding cellulose synthases of plants have been identified. The molecular groundwork for this research was laid by identifying cellulose synthase genes in the bacteria *Acetobacter xylinum* and *Agrobacterium tumefaciens*, which extrude extracellular ribbons of cellulose. These synthase genes and those of other enzymes requiring nucleotide sugars encode four highly conserved domains thought to be critical for binding and catalysis of UDP-Glc (and

certain other UDP-sugars) (Fig. 2.32). So far, all other kinds of synthases able to make contiguous (1→4)β-glycosyl linkages, such as chitin synthases and hyaluronate synthases, contain these four highly homologous sequences of amino acids.

Searching sequences in a cDNA library made from cotton fibers at the onset of secondary wall cellulose formation (see Section 2.6.3), Deborah Delmer and colleagues found two plant sequences homologous to the *Acetobacter* cellulose synthase gene, sharing all four UDP-Glc binding sequences. The plant *Ces*A genes are highly expressed in fibers at the time of active synthesis of secondary wall cellulose. The polypeptides they encode (size about 110 kDa) are predicted to have eight transmembrane domains, to bind the substrate UDP-Glc, and to contain two large domains unique to plants.

Genetic proof of the function of a *Ces*A homolog has been obtained by complementing an *Arabidopsis* mutant unable to make cellulose at a high temperature. Transformation of the temperature-sensitive mutant with the wild-type *Ces*A gene restores the normal phenotype, providing the first evidence that a plant *Ces*A gene functions in the formation of cellulose microfibrils. However, direct proof of the function of the gene product is still lacking, because cellulose cannot at present be synthesized to any great extent in vitro.

The discovery of *Ces*A genes has now opened the door for the identification of many other cell wall polysaccharide synthase genes. The *Arabidopsis* genome contains several homologs of cotton *Ces*A, and other sequences share significant identity with one or more of the suspected UDP-Glc binding domains.

Why do plants have so many different *Ces*A and related genes? Almost all plant cell types can be identified by unique features of their cell wall, so the large family of *Ces*A genes may represent the diversity of cellulose synthases needed to build specialized walls. In addition, some of the related genes may encode other kinds of synthases that make a broad range of noncellulosic polysaccharides. Of all of the polymers built from pyranosyl sugars, those that possess runs of (1→4)β-linkages of either glucose, xylose, or mannose invert the orientation of one sugar unit with respect to its neighbor (see Figs. 2.12, 2.14, and 2.15). The steric problem is the same as for cellulose synthase, and it is tempting to speculate that an ancestral cellulose synthase may have been modified to confine the location of the synthase to the Golgi apparatus and to alter the nucleotide sugar substrate.

2.5 Growth and cell walls

2.5.1 The cell wall is a dynamic structure.

Cell expansion involves extensive changes in the mass and composition of the cell wall. Cell growth, an irreversible increase in cell volume, can occur by expansion (increase in cell size in two or three dimensions) or by elongation (expansion constrained to one dimension). Variety in cell shape may result if either of these two processes occurs at specific regions of the cell surface.

During elongation or expansion, existing cell wall architecture must change to incorporate new material, increasing the surface area of the cell and inducing water uptake by the protoplast. The osmotic pressure (turgor) exerted by the protoplast is necessary to drive cell expansion, and this pressure usually remains a relatively constant driving force for expansion. The regulation of **wall loosening** is considered the primary determinant of rates of cell expansion. The cell wall architecture must be extensible; that is, mechanisms must exist that allow discrete biochemical loosening of the cell wall matrix, permitting microfibril separation and insertion of newly synthesized polymers. Cells may extend to tens, hundreds, or even thousands of times their original length while maintaining a constant wall thickness. Thus, wall loosening and continued deposition of new material into the wall must be tightly integrated events (Fig. 2.33).

2.5.2 Most plant cells grow by uniform deposition of cell wall materials, whereas some demonstrate tip growth.

In the vast majority of plant cells, growth and the deposition of new wall material occur uniformly along the entire expanding wall. However, **tip growth,** the growth and deposition of new wall material strictly at

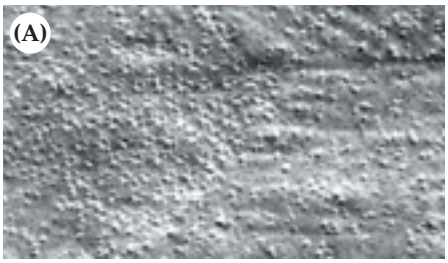
(A)

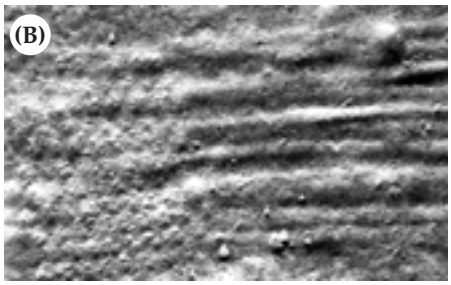
(B)

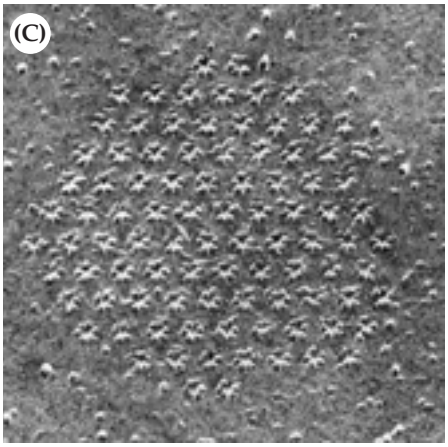
(C)

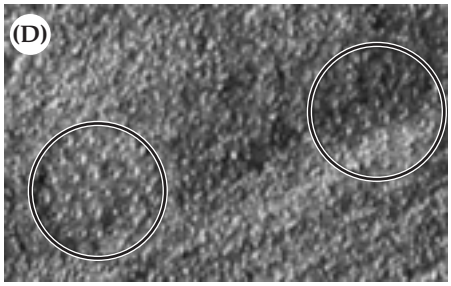
(D)


(E)

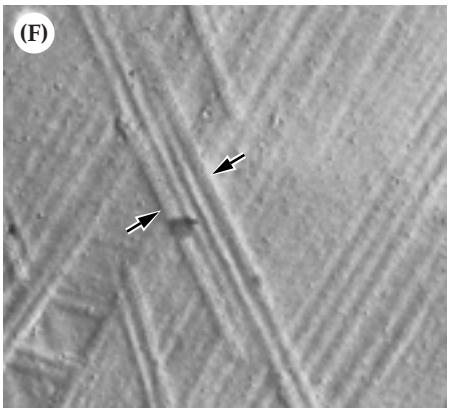
(F)

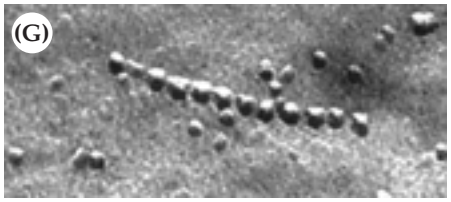
(G)


(H)

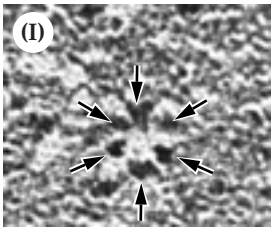
(I)

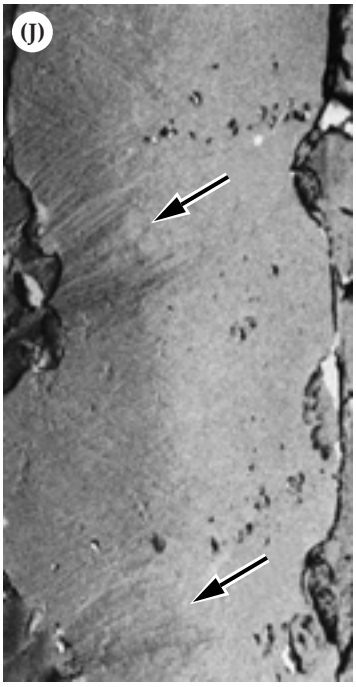
(J)

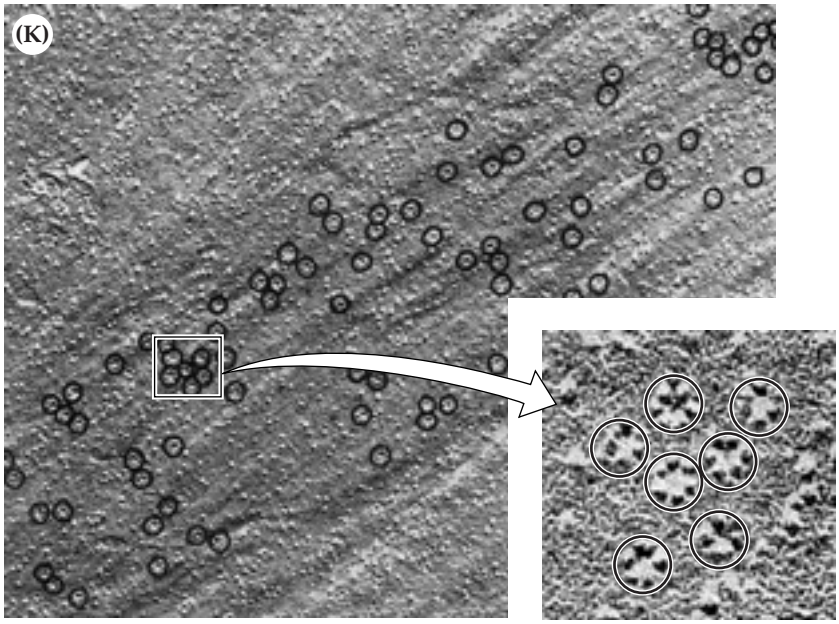
(K)

Figure 2.31 ***(Facing page)***
The terminal complexes associated with cellulose microfibril biosynthesis are imaged by freeze-fracture and rotary-shadowing of membranes. The six-membered particle rosettes were first seen in the desmid *Micrasterias* (A–C). The rosettes are seen on the "P-face," the inner leaf of the plasma membrane bilayer (A), whereas the impression of the microfibrils and larger particles that apparently fit into the center of each rosette are located in the outer leaf, or "E-face" (B). In this alga, the individual rosettes aggregate in the membrane to form even larger hexagonal arrays that are associated with formation of flat ribbons of cellulose (C). The green alga *Spirogyra* also assembles aggregates of rosettes (D), but some algae, such as *Oocystis,* have linear arrays of particles (E). These terminal complexes often pair up at the plasma membrane and initiate synthesis of microfibrils in opposite directions (see arrows) (F). The cellular slime mold, *Dictyostelium discoideum,* forms two kinds of terminal complexes: A linear array is associated with the extracellular ribbon of cellulose formed by streaming cells (G), whereas the cell wall of the stalk cells is made by aggregate arrays that appear to be rudimentary rosettes (H). In contrast to algae, all flowering plants examined contain single rosette structures (I); arrows point to each of the six particles. Such single rosettes are abundant during the formation of the secondary wall thickenings (arrows) visible in this longitudinal section of a vessel element of cress (*Lepidium sativum* L.) (J). The rosettes (circled) are found in great abundance only in the membrane underlying the developing thickening (K); individual rosettes are magnified in the inset.

the tip of a cell, occurs in some plant cells, notably root hairs and pollen tubes (Fig. 2.34).

Plant cells possess arrays of **cortical microtubules** underlying and connected to the plasma membrane (see Chapter 5). The orientation of the cortical microtubule array often predicts the orientation of cellulose microfibril deposition. The cortical array may align the cellulose synthase complexes, either by direct protein-mediated connection or by defining channels in the membrane in which the synthase can move. In turn, cellulose microfibril orientation controls whether cells expand or elongate and determines the plane of elongation. In cells that grow by uniform expansion, layers of microfibrils lie unaligned in the wall matrix, but in cells that elongate, microfibrils align in transverse or helical orientations to the axis of elongation (see Fig 2.11).

2.5.3 The multinet growth hypothesis has been developed to explain axial displacement of cellulose microfibrils during growth of the cell wall.

From studies of developing cotton fibers, the **multinet growth hypothesis** was developed to explain how cellulose microfibrils that have been deposited in a transverse or slightly helical orientation are displaced axially as elongation proceeds (Fig. 2.35A). New microfibrils deposited in strata on the inner surface of the wall in a generally transverse orientation functionally replace older microfibrils. The older microfibrils are pushed into the outer layers of the wall and are passively reoriented in a longitudinal direction as the cell elongates. Consistent with this hypothesis, the changes in the diffraction patterns of polarized light by algal cells, induced by reorientation of the parallel

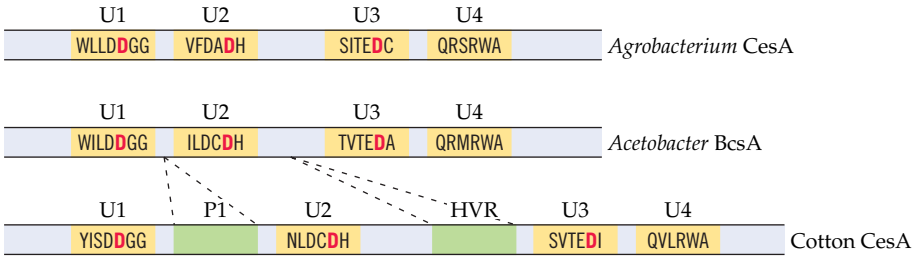

Figure 2.32
Cellulose synthases from *Acetobacter xylinum, Agrobacterium tumefaciens,* and *Gossypium hirsutum* (cotton) are characterized by four motifs (called U-motifs) critical for binding the substrate UDP-Glc. Three of the four domains demonstrate absolute conservation of an aspartyl residue (in red) predicted to be necessary for catalysis of glycosidic bond formation. In addition to the three aspartyl residues, the QxxRW motif in U4 also is conserved in every synthase of a polysaccharide with contiguous (1→4)β–linked units in which one sugar is inverted with respect to its neighbors. Two sequences, P1 and HVR, are plant specific.

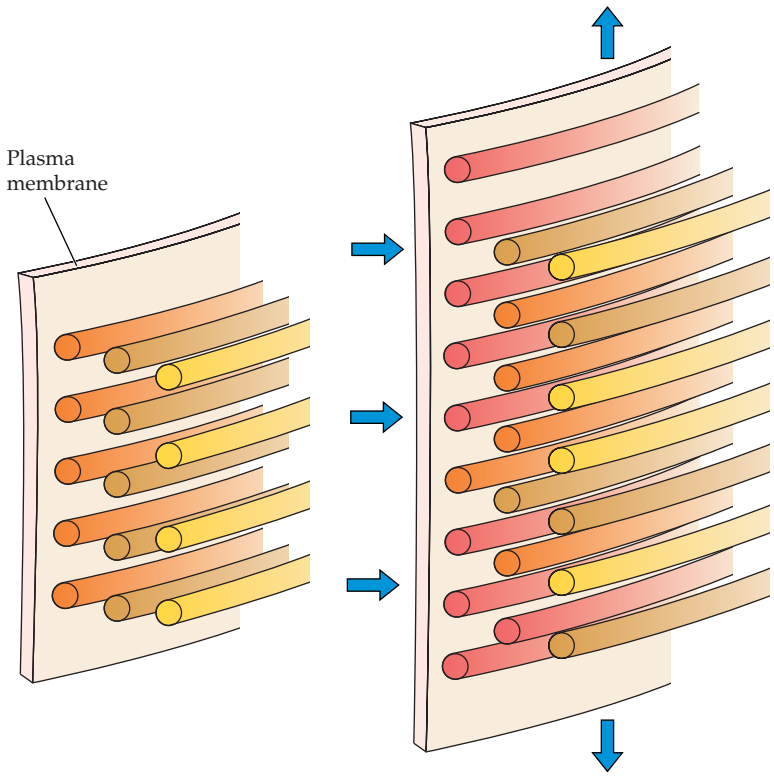

Figure 2.33
Wall loosening and incorporation of new wall polymers are integrated with each other so that wall thickness is maintained during cell expansion. Because the walls are only a few strata thick, loosening of the wall with no insertion of new wall material would very quickly thin the wall during growth and cause rupture. In contrast, deposition without loosening would increase wall thickness, because the walls would not expand. Vertical arrows denote the direction of expansion, and horizontal arrows show the addition of new microfibrils (red) on the inner surface of the wall.

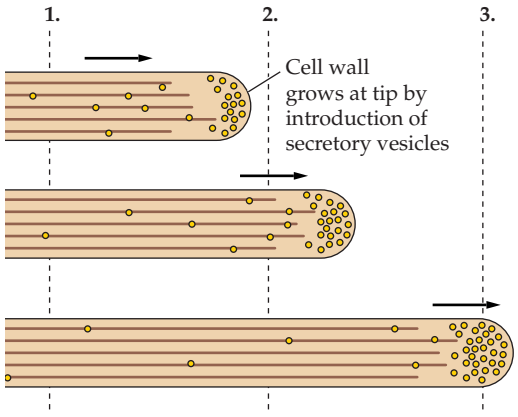

Figure 2.34
In tip growth, the rate of vesicle delivery and deposition at the tip determines the rate of growth. Vesicles are delivered to the tip via actin microfilaments (see Chapter 5).

microfibrils, occur primarily in the inner layers of the wall close to the plasma membrane. The driving force for wall extension is generally viewed to be the turgor generated by the protoplast, but it is the tension created on the microfibrils 90° perpendicular to the outward push of the protoplast that leads to separation of the microfibrils (Fig. 2.35B). A turgor pressure of 1 MPa can generate several hundred megapascals of tension because the volume of a relatively large protoplast is resisted by a very thin cell wall.

The essence of the multinet growth hypothesis is descriptive for many kinds of cells, but microfibrils do not necessarily reorient axially, and substantial extension is possible with little reorientation if many wall strata contribute to the direction of expansion. Cellulose microfibrils woven in a shallow helix around the cell prevent the growing cell from becoming spherical. By analogy, a spring-like toy such as Slinky or Flexi stretches easily along its longest axis but resists attempts to increase its diameter (Fig. 2.35C); when stretched, the spring extends substantially with only a small change in the helical angle but a wide separation of the coils. Extension of a cell wall might be viewed as a series of tightly interacting concentric Slinkys in both right-handed and left-handed orientations that reorient at crossed angles during separation (Fig. 2.35A). Given the estimated thickness of the primary wall (80 to 100 nm in meristematic and parenchymatous cells) and the dimensions of the matrix components (see Box 2.4, panel C), only about 5 to 10 strata make up the wall. Moreover, microfibrils from several strata may merge somewhat to fill in gaps as new strata are deposited onto the inner surface (see Fig. 2.33).

2.5.4 The biophysics of growth underpins cell wall dynamics.

Several different classes of cell wall polymers constitute nearly independent determinants of strength in elongating cells. These include (*a*) microfibrils arranged in the transverse axis, which are interconnected to the cross-linking glycans; (*b*) putative networks involving structural proteins or phenylpropanoid compounds; and (*c*) elements of the pectin network. When plant growth

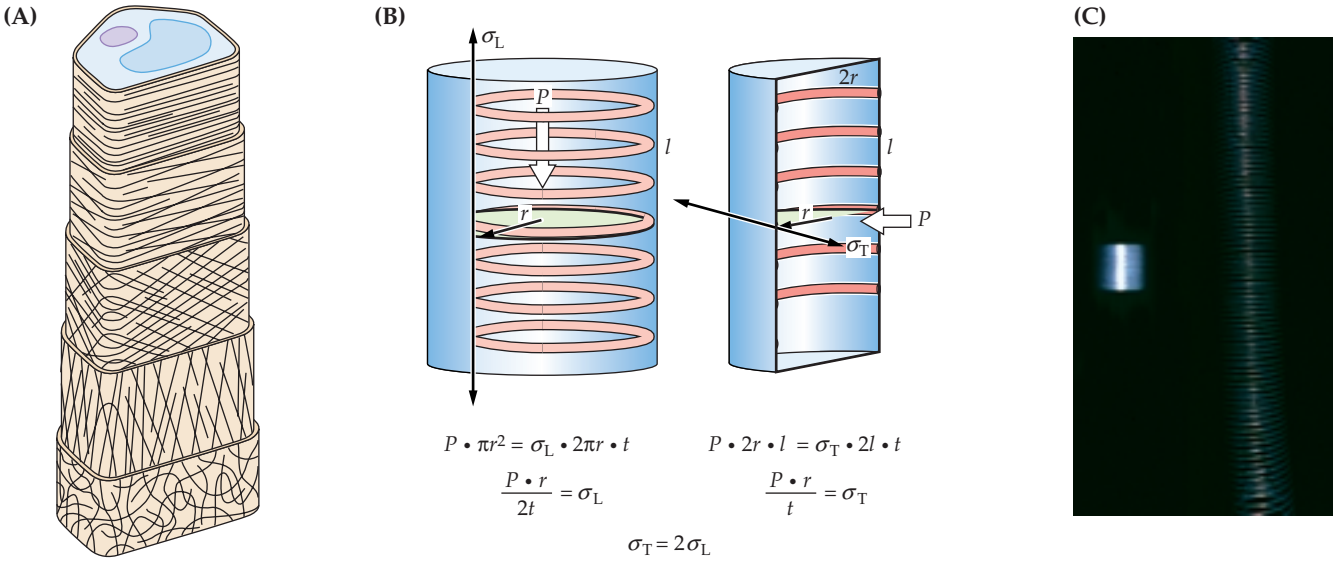

Figure 2.35
(A) The original multinet growth hypothesis explains that as walls stretch during growth, the microfibrils reorient passively from a transverse direction on the inner wall to a longitudinal direction at the outer wall. (B) The hydrostatic pressure developed by the protoplast is resisted by a relatively thin cell wall, and the tensile force pulling the microfibrils apart is several orders of magnitude higher than cell turgor pressure. For example, a spherical cell with a radius *(r)* of 50 µm and 1 MPa of turgor pressure *(P)*, enveloped by a cell wall only 0.1 µm thick *(t)*, develops 250 MPa of tension in the wall. This enormous tension changes as the cell geometry changes. When this cell begins to elongate and become cylindrical, the tension increases to 500 MPa tangentially because of the change in cell dimension. *l*, length; σ_L, longitudinal stress; σ_T, tangential stress. (C) Although a Slinky is difficult to extend radially because of the orientation of the coils, it is easily extended lengthwise. Cell shape in plants is controlled similarly. Altering the interaction between the tethering cross-linking glycans and cellulose is the principal determinant of the rate of cell expansion.

regulators such as auxin and gibberellin change the *direction* of growth, they do so through changing the orientation of cortical microtubules and cellulose microfibrils. When they change the *rate* of growth, their mechanisms include dissociation or breakage of the tethering molecules from microfibrils. Mathematical formulations that describe the growth rate of plant cells allow us to define the cell wall properties that must be modified to permit growth.

Equation 2.1

$$dl/dt = L_p (\Delta\psi_w)$$

Equation 2.2

$$dV/dt = A \bullet L_p (\Delta\psi_w)$$

Equation 2.3

$$\text{Rate} = m (\psi_p - Y)$$

The rate of cell elongation can be quantified by Equation 2.1, where dl/dt is the change in length per unit time, L_p is hydraulic conductivity (i.e., the rate at which water can flow across the membrane), and $\Delta\psi_w$ is the water potential difference between the cell and the external medium. The difference in water potential is the driving force for water movement and has two components, $\psi_s + \psi_p$, the osmotic potential and pressure potential (turgor), respectively. Revising the equation to include any change in cellular volume (V) yields Equation 2.2, where growth is defined as a change in volume per unit time and depends on the surface area (A) of the plasma membrane available for water uptake. Thus the rate of growth is proportional to membrane surface area, the conductivity of the membrane, and the water potential difference driving water uptake. In nongrowing cells, $\Delta\psi_w$ (and thus dV/dt) = 0, because the rigid cell wall prevents water uptake, and the turgor pressure rises to a value equal to that of the osmotic potential of the cell. By contrast, in growing cells, $\Delta\psi_w$ does not reach zero because the wall tethers have been loosened. As a result, cell volume increases irreversibly. This

wall-localized event, called **stress relaxation,** serves as the fundamental difference between growing and nongrowing cells (Fig. 2.36).

When turgor is reduced in growing cells by an increase in the external osmotic potential, growth ceases at some pressure before the turgor reaches zero. This value, called the **yield threshold,** defines the pressure potential that must be exceeded before expansion can occur. The increment of growth rate change above the yield threshold is dependent not only on turgor but also on a factor called wall **extensibility,** which is the slope (m) of the general equation shown as Equation 2.3, where *Y* is the yield threshold. Much of the work remaining in the study of cell wall growth involves assessing the biochemical determinants of yield threshold and extensibility (see Section 2.5.6).

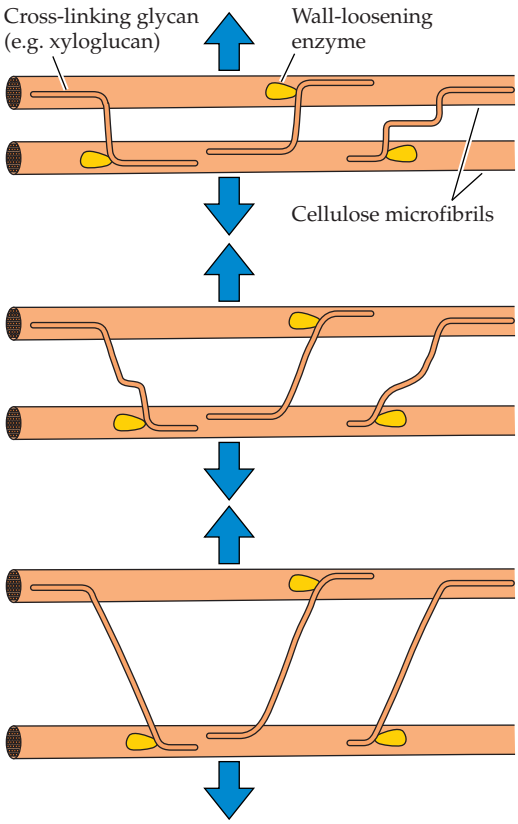

Figure 2.36
Stress-relaxation is considered the underlying basis of cell expansion. When an elongating cell is stretched by turgor, the longitudinal stress (indicated by arrows) is borne more or less equally by the glycans tethering the cellulose microfibrils. If some of the tethers are dislodged from the microfibrils, or hydrolyzed, they temporarily "relax" and the yield threshold is breached because the other tethers are strained. Water uptake results in expansion of the microfibrils to take up the slack of the relaxed glycans, which are once again placed under tensile stress.

2.5.5 The acid-growth hypothesis postulates that auxin-dependent acidification of the cell wall promotes wall extensibility and cell growth.

Despite the marked differences in the composition of Type I and Type II walls, the biophysics of growth of grasses and other flowering plants are similar. Although the chemical complexity of the wall is daunting, the similarity of the physiological responses of all flowering plants to acid, auxin, and light of different qualities indicates that a few common mechanisms of wall expansion exist, regardless of the kinds of molecules that tether the microfibrils.

The extraction of several kinds of polysaccharide hydrolases from the cell walls of tissues rich in growing cells raised the possibility that the regulation of these enzymes was a mechanism by which auxin could cause wall expansion. A major breakthrough came with the discoveries that auxin caused acidification of the medium in which elongating tissue sections were bathed and that H^+ could substitute effectively for the auxin hormone (Fig. 2.37A). This **acid-growth hypothesis** proposes that auxin activates a plasma-membrane proton pump, which acidifies the cell wall. The low pH, in turn, activates apoplast-localized growth-specific hydrolases, which cleave the load-bearing bonds that tether cellulose microfibrils to other polysaccharides. Cleavage of these bonds results in loosening of the cell wall, and the water potential difference causes uptake of water. Relaxation of the wall (i.e., separation of the microfibrils) passively leads to an increase in cell size.

The basic tenets of the acid-growth hypothesis have stood the test of time, but three problems persist. First, no enzymes have been found that hydrolyze cell wall cross-linking glycans exclusively at pH conditions lower than 5.0. Second, no reasonable explanation exists for how growth is kept in check once the hydrolases are activated. Third, no hydrolases extracted from the wall and added back to the isolated tissue sections, regardless of external pH, cause extension in vitro.

2.5.6 At present, two kinds of enzymes are being evaluated as having possible wall-loosening activities.

Two candidate wall-loosening enzymes are currently being studied. One of these, **xyloglucan endotransglycosylase** (XET), carries out a transglycosylation of XyG in which one chain of XyG is cleaved and reattached to the nonreducing terminus of another XyG chain. Given such a mechanism, microfibrils could undergo a transient slippage but the overall tensile strength of the interlocking XyG matrix would not diminish (Fig. 2.38). XETs may also function in the realignment of XyG chains in different strata during growth and in the assembly of the wall as newly synthesized XyGs are incorporated. In some cases, the correlation between growth and XET activity is not clear, and some XETs appear to function hydrolytically.

Other proteins catalyze wall extension in vitro without any detectable hydrolytic or transglycolytic events. Called **expansins,** these proteins probably catalyze breakage of hydrogen bonds between cellulose and the load-bearing cross-linking glycans. Such an activity could disrupt the tethering of

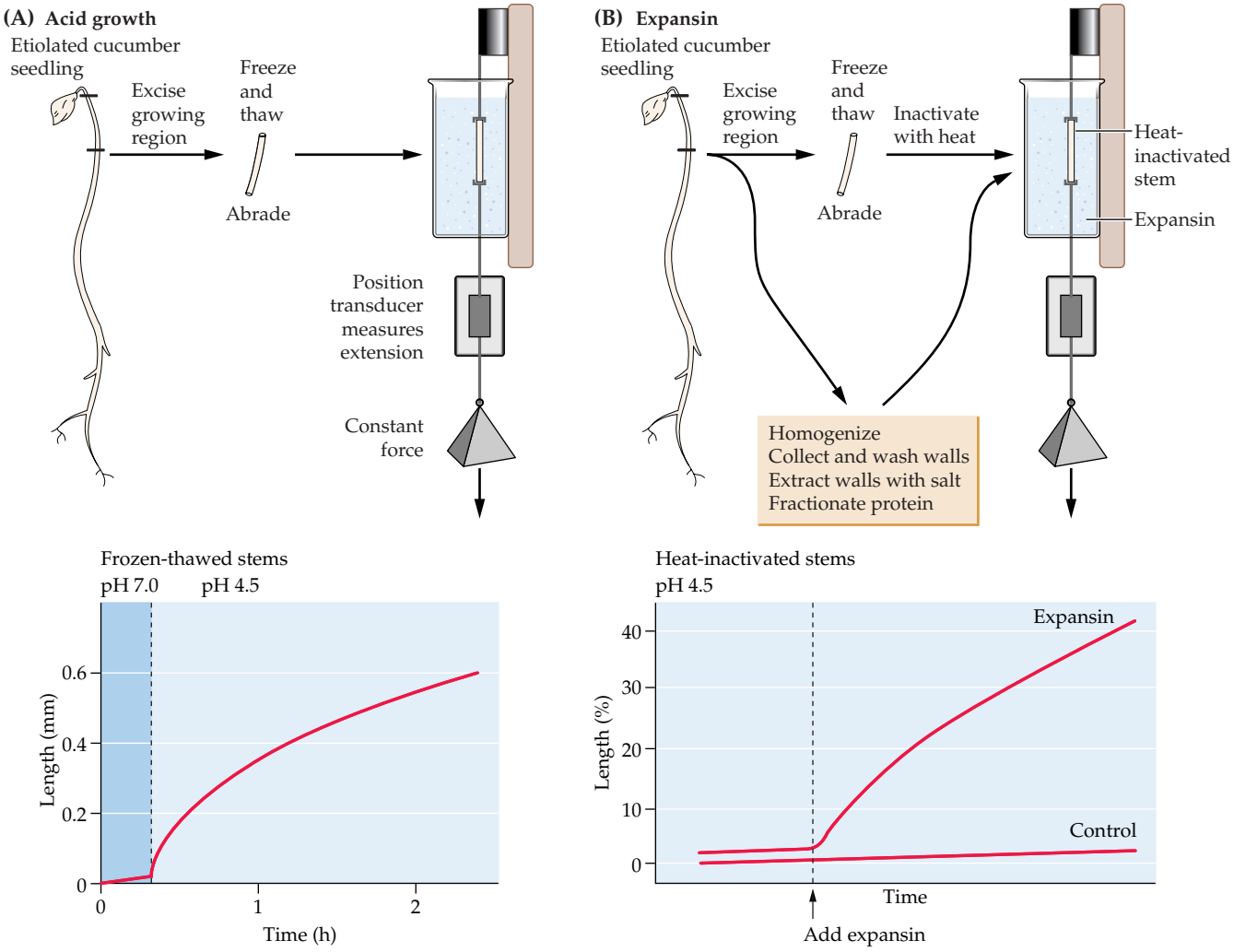

Figure 2.37
Sections of growing epicotyl, hypocotyl, or coleoptile are frozen, thawed, and placed under a constant stress. A position transducer measures elongation continuously. (A) When the bathing solution of the frozen-thawed sections is changed from pH 7 to 4.5, extension occurs almost immediately. (B) If the sections are heat-inactivated, no extension occurs at any pH. However, when expansins are added, extension is restored at acidic pH. Neither plant hydrolases nor xyloglucan endotransglycosylase is able to cause this effect in vitro.

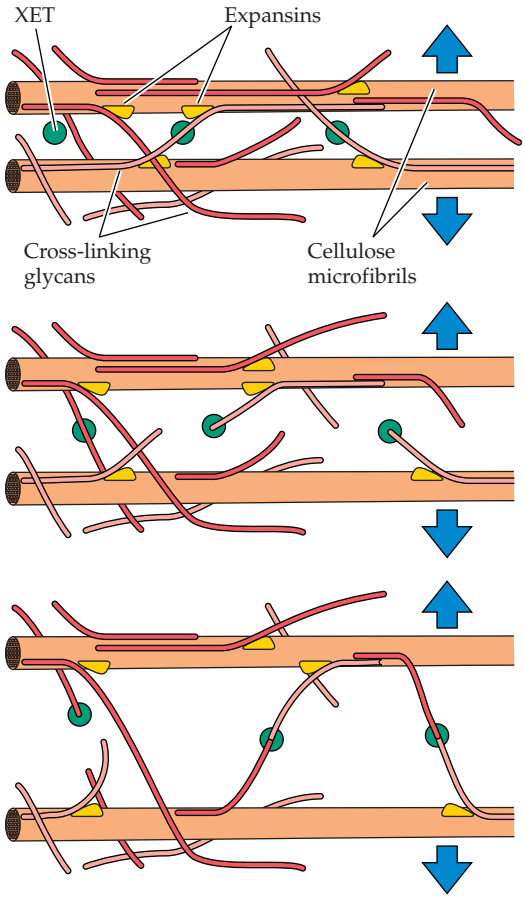

Figure 2.38
Microfibril separation driven by osmotic pressure of the cell is facilitated by loosening of the cross-linking glycans that tether them. This may be accomplished by coordinate action of expansins, which break the steric interactions between the cross-linking glycans and cellulose, and XET, which hydrolyzes a glycan and reattaches one part of the chain to the nonreducing terminus of another. This action by XET may also function in forming new tethers because microfibrils from inner lamellae merge with microfibrils of the outermost lamellae as they are pulled apart during wall extension (see Fig. 2.33).

cellulose by XyGs in Type I walls, by GAXs in Type II walls, and by GAXs or β-glucans in grass walls (Fig 2.38).

Expansins are the only proteins shown to produce wall expansion in vitro (see Fig. 2.37B). They are ubiquitous in growing tissues of all flowering plants, and they appear to break hydrogen bonds between cellulose and several kinds of cross-linking glycans regardless of their chemical structure. Also, because grass expansins induce extension of tissues with Type I walls, it is attractive to think that expansins are ubiquitous enzymes involved in the rapid growth responses of both Type I and Type II walls. However, further studies show that a second multigene family of β-expansins, found predominantly in the grasses, have no appreciable activity on Type I cell walls. Exogenous application of expansins to a meristem induces bulging of the meristem at the sites of application—bulges that develop into leaf primordia.

The genes of several XETs and expansins have been cloned, and experiments designed to reduce the amounts of each in transgenic plants are being tested to determine their relative significance. XET and expansin may not be the only wall-loosening agents, and work continues to determine the roles played by hydrolases.

Because the wall composition of grass Type II cell walls differs from that of all other flowering plant species, researchers also are investigating the involvement in cell wall loosening of the exo- and endo-β-D-glucanases that hydrolyze grass β-D-glucans to glucose. Addition of purified exo- and endoglucanases to heat-killed coleoptiles cannot induce extension growth. However, when antibodies directed against these enzymes are added to enzyme-active walls, wall growth is inhibited, suggesting that these glucanases also play a role in extension growth in grasses.

2.5.7 In Type I walls, cell growth is associated with subtle biochemical changes in the pectin network.

If XET and expansin activities are indeed growth-inducing factors in the cell wall, then how are they regulated? The cellulose/cross-linking glycan network lies embedded in a pectin network that may control access of these enzymes to their substrates. The self-hydrolysis of isolated walls by nascent enzymes, termed **autolysis,** yields substantial amounts of Ara and Gal from Type I walls, suggesting that changes in the arabinan and galactan side-branches of RG I (see Fig. 2.16) or AGPs (see Fig. 2.20) occur during growth.

The most marked change revealed by biochemical analysis is the increase in the degree of methyl-esterification of the wall HGAs when the newly synthesized pectins are deposited during elongation. The

deposition of highly esterified HGAs is succeeded by a deesterification event that can remove a large proportion of methyl ester groups from the wall when growth stops. The ionized carboxyl groups can form Ca^{2+}-HGA junction zones, causing the wall to become more rigid (see Fig. 2.24). The cell walls of meristematic and elongation zones are characteristically low in Ca^{2+}, and Ca^{2+}-HGA junction zones are observed more frequently after cell elongation has stopped.

2.5.8 More obvious biochemical changes occur in growing Type II walls than in Type I walls.

More obvious chemical changes occur with the cross-linking glycans of the Type II walls of commelinoid monocots. A highly substituted GAX (HS-GAX), in which six of every seven Xyl units bears an appendant group, is associated with the maximum growth rate of coleoptiles. The number of side groups of Ara and GlcA along the GAX chains varies markedly, from GAXs for which Xyl units are nearly all branched to those with only 10% or less of the Xyl units bearing side groups. Side groups not only prevent hydrogen bonding but also render the GAX water-soluble. In dividing and elongating cells, highly branched GAXs are abundant, whereas after elongation and differentiation, more and more unbranched GAX polymers accumulate. Cleavage of the Ara and other side groups from contiguously branched Xyl units can yield runs of unbranched xylan capable of binding to other unbranched xylans or to cellulose microfibrils.

Type II walls also have a low pectin content. Chemically, pectins of the Type II wall include both HGA and RG, and HS-GAX is closely associated with these pectins. Interactions between the HS-GAX, HGA, and RG could control wall-loosening activities, as suggested for the Type I wall. The spacing of the appendant Ara and GlcA units of GAXs could determine porosity and surface charge, functionally replacing the predominant pectic substances in the Type I cell wall, as illustrated in Fig. 2.23B. The HGAs of maize pectins, which are methyl-esterified (see Fig. 2.16A), also contain nonmethyl esters, the formation and disappearance of which coincide with the most rapid rate of cell elongation. We do not yet know the chemical nature of the nonmethyl esters. Some arabinans, particularly the 5-linked arabinans, are found in the walls of dividing cells but are not made during cell expansion.

When grass cells begin to elongate, they accumulate the mixed-linkage **β-glucans** in addition to GAX (see Fig. 2.14). β-Glucans are unique to the Poales (see Fig. 2.13) and are one of the few known developmental stage–specific polysaccharides. Absent from meristems and dividing cells, β-glucans accumulate to almost 30% of the noncellulosic cell wall material during the peak of cell elongation and then are largely hydrolyzed by the cells during differentiation. Because synthesis and hydrolysis of the β-glucans occur simultaneously throughout elongation, the amount that accumulates is a small fraction of the total synthesized. The appearance of β-glucans during cell expansion and the acceleration of their hydrolysis by growth regulators all implicate direct involvement of the polymer in growth.

2.5.9 Once growth has ceased, cell wall shape must be locked in place by wall components.

Once elongation is complete, the primary wall locks the cell into shape by becoming much less extensible. One component of the locking mechanism for Type I walls may be HRGPs, such as extensin. The flexible regions of these proteins could wrap around cellulose microfibrils, and the rod-like regions could serve as spacers. However, we do not yet know how extensins are cross-linked in the wall. Extensin units, and perhaps other proteins, may covalently bind to each other, forming an independent interlocking network, as illustrated in Figure 2.23A. The loss of solubility of extensins in Type I walls is associated with an increase in the tensile strength of the wall.

Other proteins may be necessary to actually lock the extensins together. One candidate is a 33-kDa PRP. Greater quantities of PRP are synthesized later in cell development and particularly in the same vascular cells as extensin. One hypothesis holds that extensin precursors accumulate in the cell

wall during cell division and elongation but cannot cross-link wall components without the presence of PRPs.

Just as in Type I walls, Type II walls are locked into form during differentiation; unlike Type I walls, however, they do not use Hyp-rich extensin. Instead, Type II walls contain a threonine-rich protein with sequences reminiscent of the typical extensin structure; cross-linking phenolic compounds are also present. As with extensin, soluble precursors of the threonine-rich protein accumulate early in the cell cycle and become insoluble during cell elongation and differentiation. This polymer is prevalent in vascular tissue and in special, reinforced wall structures, such as the pericarp. However, much of the cross-linking function in Type II walls probably rests with the esterified and etherified phenolic acids, and formation of these cross-linkages accelerates at the end of the growth phase. Once the phenolic cross-bridges are in place, they may account for a substantial part of the load-bearing role in the fully expanded cells.

2.6 Cell differentiation

2.6.1 The plant extracellular matrix is a coat of many colors.

At the light microscopy level, traditional histochemical stains reveal a broad diversity in the distribution of various polysaccharides in different cells. The complexity of polysaccharide structure is resolved even more effectively when highly specific probes are used. This has been achieved by using the natural specificity of enzymes for their substrates and that of antibodies for particular antigens (Box 2.5). More recently, the advent of microspectroscopy, in which a microscope with modified optics is attached to a spectrometer, has made **chemical imaging** possible. The distribution of a particular functional group of a molecule can be mapped at the single-cell level (Box 2.5).

Even in a single cell, modifications occur that distinguish between transverse and longitudinal walls. For example, a preferential digestion of end walls occurs in sieve tube members. Some substances, such as waxes, are secreted only to a cell's outer epidermal face. Within a single wall there are zones of different architectures—the middle lamella, plasmodesmata, thickenings, channels, pit-fields, and the cell corners—and there are domains within the thickness of a wall in which the degree of pectin esterification and the abundance of RG I side chains differ (Fig. 2.39).

The size of such microdomains in the wall, compared with the sizes of the polymers that must fit in these domains, implies that mechanisms must exist for packaging and positioning of large molecules. For example, unesterified pectins can be as long as 700 nm and yet, in some cell types, are accommodated in a middle lamella 10 to 20 nm wide and so must be constrained at least to lie parallel to the plasma membrane. This microdiversity within walls is now changing our view of the wall—from that of a homogeneous and uniform building material to

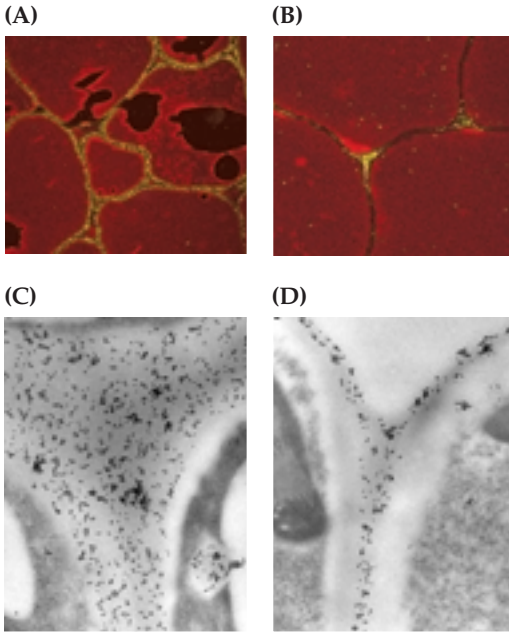

Figure 2.39
Potato cell walls labeled with immunogold and silver-enhanced to reveal the localization of pectin galactan side chains and calcium pectate junctions, with use of the monoclonal antibodies LM5 and 2F4, respectively, in the light microscope. The green color shows where light is reflected from silver-enhanced gold particles in the confocal microscope. The galactan side chains are localized to the primary wall (A), whereas calcium pectate is predominantly in cell corners (B). A methyl-esterified pectic epitope is present throughout the cell walls of vascular cells (C) but restricted to an outer layer of the walls of palisade cells (D) in electron micrographs of a *Zinnia* leaf immunogold-labeled with the JIM7 monoclonal antibody.

one of a mosaic of different wall architectures in which the various components contribute to the multifunctional properties of the apoplast.

2.6.2 Fruit-ripening involves developmentally regulated changes in cell wall architecture.

Most fruits in which the pericarp or endocarp softens during ripening develop thickened primary walls that are markedly enriched in pectic substances, primarily HGA and RG I. The texture of the ripe fruit pulp is governed by the extent of wall degradation and loss of cell–cell adhesion. For example, the walls of the apple cortex undergo little change in rigidity and exhibit little separation, whereas the walls of the peach and tomato pericarp soften considerably through wall swelling and loss of cell adhesion (Fig. 2.40). In tomato, the locules containing the seeds dissolve completely, in a process called **liquefaction.**

Pectins often constitute more than 50% of the fruit wall. The softening process in tomato parenchyma tissue is associated with loss of methyl esters of HGA, a consequence of the activity of PME, which removes methyl ester groups from the GalA residues of pectic polysaccharide backbones. The deesterified HGA backbone then is susceptible to the activity of PGase. PGase I, with a molecular mass of approximately 100 kDa, consists of 46-kDa PGase II tightly complexed with a β-subunit. The β-subunit is a unique **aromatic amino acid-rich protein** thought to function as an anchoring component for the PGase II subunit and is believed to be synthesized early in fruit development. The β-subunit may solubilize pectins from the cell wall, facilitating progressive hydrolysis by PGase II of the glycosidic bonds within the unbranched HGA backbone. Pectin modification within the wall during ripening is a tightly regulated process, the result of such mechanisms as substrate modification, which restricts enzyme access to the substrate, or the presence of enzyme inhibitors, as in the inhibition of PGase II activity by the diffusible products of pectin depolymerization.

However, despite extensive deesterification and depolymerization of the pectin polymers during ripening, fruit softening does not appear to result directly from these modifications to the pectic network. Using antisense inhibition of PGase, researchers were able almost completely to inhibit such activity, essentially preventing pectic depolymerization in transgenic fruit; however, little or no reduction in softening accompanied this achievement. Although the cross-linking glycans do not appear to undergo extensive ripening-related depolymerization, several glycan-modifying enzymes increase in activity, including XET, expansin, and glucan hydrolases. Thus these enzymes may be involved in restructuring the tethering by cross-linking glycans, thereby changing the properties of the network throughout the primary cell wall and contributing to the softening of the pericarp tissue and the whole tomato fruit.

2.6.3 Secondary walls are elaborated after the growth of the primary wall has stopped.

For many cell types, the differentiation process is associated with formation, on the plasma-membrane side of the primary wall, of a distinct secondary wall. Regardless of chemical composition, the primary wall is always defined as the structure that participates in irreversible expansion of the cell. When cells stop growing, the wall is cross-linked into its ultimate shape (see Section 2.5.9). At that point, deposition of the secondary wall begins.

Secondary walls often exhibit elaborate specializations. The cotton fiber, for example, consists of nearly 98% cellulose at maturity (Fig. 2.41A). In some cells, such as sclereids, vascular fibers, and the stone cells of pear, the secondary wall becomes uniformly thick, composed largely of cellulose microfibrils that can sometimes fill the entire lumen of the cell (Fig. 2.41B). The secondary wall may, however, contain additional noncellulosic polysaccharides, proteins, and aromatic substances such as lignin. In tracheids, secondary walls can form special patterns, such as annular or helical coils or reticulate and pitted patterns (Fig. 2.42). These walls typically contain glucuronoxylans or 4-*O*-methylglucuronoxylans in addition to cellulose. Unlike GAXs of grass walls, these xylans are devoid of Ara but contain a

Box 2.5 Heterogeneity of wall composition can be probed at the single-cell level.

Major monoclonal antibodies and other probes for components of the plant cell wall

Antibody	Antigen/epitope
Anti-pectin	
JIM5	Unesterified HGA
JIM7	Methyl-esterified HGA
PAM1/PAM2[a]	30 consecutive GalA units
2F4	Calcium-pectate
CCRC-M5	Sycamore RGI
CCRC-M7	AG epitope of RGI
LM5	(1→4)β-Galactan
LM6	Arabinan
Anti-xyloglucan	
CCRC-M1	(1→2)α-Linked fucosyl-containing epitope of XyG
Anti-glucan	
LAMP2H12H7	(1→3)β-Glucan
BG1	(1→3),(1→4)β-Glucan
Cellobiohydrolase[b]	Cellulose
Cellulose binding domain[b]	Cellulose
Anti-extensin	
11.D2	Tobacco extensin
MC-1	Maize extensin
JIM11	Carrot root
JIM12	Carrot root
JIM20	Carrot root
JIM19	Extensin
LM1	Rice extensin
Anti-AGP	
PCBC3	Tobacco-style AGPs
PN16.4B4	Plasma membrane AGPs
JIM4	Carrot PM AGPs
MAC207	PM AGPs
JIM13	PM AGPs
JIM15	PM AGPs
JIM8	PM AGPs
ZUM15	Carrot AGPs
ZUM18	Carrot AGPs
LM2	PM AGPs
Anti-cell wall enzymes	
mWP3	Cell wall peroxidases
αE1	(1→3),(1→4)β-Glucanase

[a]Recombinant phage library antibody; see Willats, W.G.T., Gilmartin, P. M., Mikkelsen, J. D., Knox, J. P. (1999) Cell wall antibodies without immunization: generation and use of de-esterified homogalacturonan block-specific antibodies from a naive phage display library. *Plant J.* 18: 57–65.
[b]Enzyme probes, commercially available.

A wide range of antibodies have been raised against cell wall epitopes, most commonly by using monoclonal antibody technology (see table at left). However, some antibodies have been generated from recombinant phage libraries. Difficulties encountered in the production of antibodies to polysaccharides arise from the different processing of polysaccharide antigens, as opposed to protein antigens, by cells of the immune system. The complexity of polysaccharide structure has also made the precise characterization of epitopes difficult.

These antibodies are used as "designer stains" to label cell walls (panel A), isolated polymers (panel B), or their sites of synthesis (panel C). In A, pericarp cell walls of orange tomatoes are labeled with the JIM5 antibody, which recognizes relatively unesterified pectin. The pectin within the wall of one cell (cell 1) has undergone deesterification, whereas domains of the neighboring cell wall (cell 2) remain methyl-esterified (scale bar represents 500 nm). In B, rhamnogalacturonans are negatively stained after

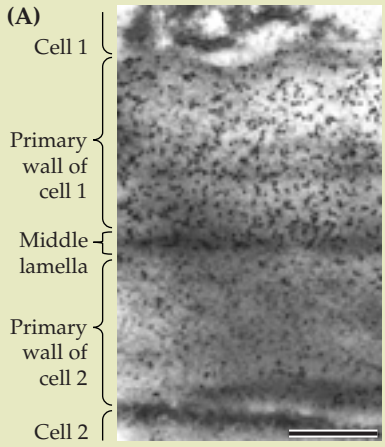

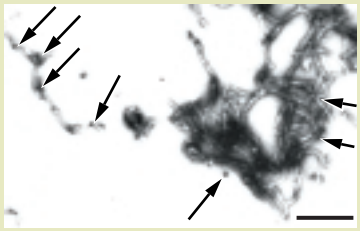

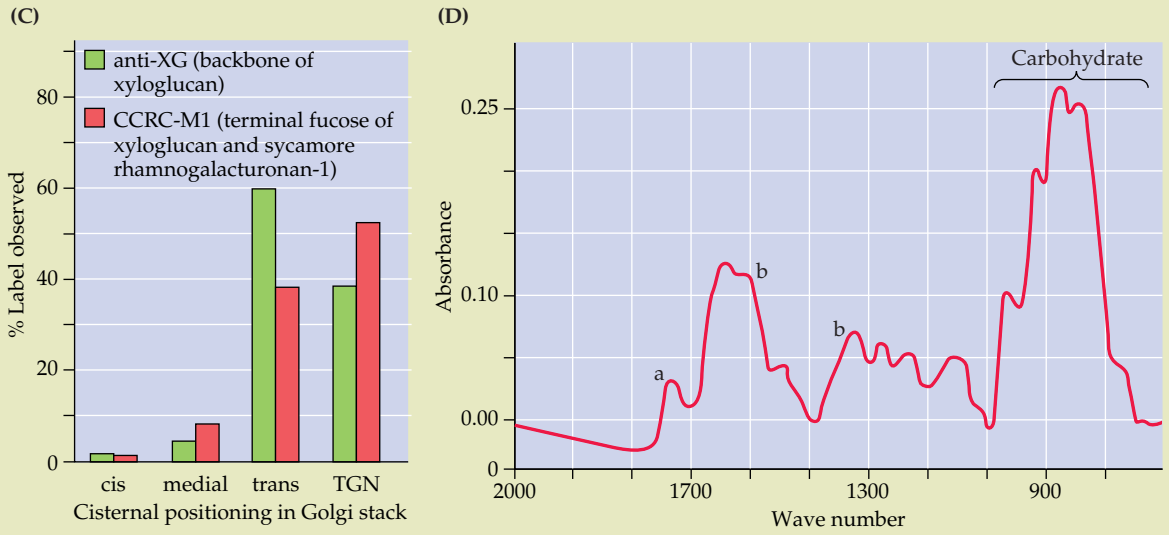

extraction from onion cell walls labeled with JIM5 immunogold. Arrows indicate 5-nm-diameter colloidal gold particles (scale bar represents 200 nm). In C, immunolabeling with two different antibodies shows that XyG synthesis is initiated in the medial to trans Golgi membranes, with addition of fucosyl units occurring primarily in the *trans*-Golgi network (TGN). The anti-XyG antibody recognizes the xylosyl unit on the glucan backbone, whereas antibody CCRC-M1 recognizes the *t*-Fuc unit of the nonasaccharide. By carefully counting the number of silver grains deposited over the individual Golgi membranes, we can see that the XyG unit structures are made predominantly in the trans membranes, whereas the fucosyl units become more prevalent slightly later, in the TGN. Some hydrolytic cell wall enzymes contain a polysaccharide-binding domain, such as the cellulose-binding domain of bacterial and fungal cellulases, and these enzymes can be conjugated directly with colloidal gold to produce probes for the electron microscope. The enzymes are denatured before coupling, which eliminates their catalytic activity, yet the binding specificity remains.

Another means of probing the chemical composition of single-cell walls is **Fourier transform infrared (FTIR) microspectroscopy.** FTIR spectroscopy is an extremely rapid, noninvasive vibrational spectroscopic method that can quantitatively detect a range of functional groups, including carboxylic esters, phenolic esters, protein amides, and carboxylic acids, and can provide a complex "fingerprint" of carbohydrate constituents that reflects not only the composition of the wall but also the molecular conformations and interactions of the wall polymers. Panel D shows the FTIR spectrum obtained from onion parenchyma cell walls. The ester peak (a) and the carboxylic acid peaks (b) are from the pectins. Several functional groups absorb IR radiation at characteristic frequencies, making assignments of some specific wall components possible (e.g., the methyl esters and carboxylate ions of pectins). The IR beam can be diverted via mirror optics to pass through a sample mounted on a stage of a microscope, and the area of sampling can be restricted to as little as 10 µm × 10 µm. Numerous individual spectra from areas of these dimensions can be collected over a large tissue area by using a computer-driven motorized stage to produce chemical images of the sample (panel E). Each frequency in the IR spectrum can be represented as a separate map. In plant organs, the presence of growth gradients and of different tissue types makes spectral mapping of the entire organ very desirable. Using a motorized stage, one can map an area from a transverse or longitudinal section at 5- to 10-µm intervals. Collection of hundreds of complete spectra takes a few hours, and the data can then be displayed as a series of functional group plots of the area mapped by aligning the IR map with the light micrograph of the sample. As an example, the ratio of the ester peak and carboxylic acid peak in a mashed *Arabidopsis* hypocotyl reveals that relatively more esterified pectin is localized in the vascular bundles. In the color map, blue represents a low ester-to-acid ratio whereas the white represents a much higher proportion of ester.

Another vibrational spectroscopy, **FT-Raman spectroscopy,** is used in combination with a microscope to image the cellular composition of cellulose and lignin in secondary walls, mostly of woods.

(A)

(B)

(C)

Figure 2.40
Cell walls are the principal textural elements of fresh fruits and vegetables. The walls of fruit change their architecture in different ways during ripening. (A) Apple walls may stiffen and maintain cell adhesions. The "mealy" texture of an overripe apple is a result of loss of cell–cell adhesion by dissolution of the middle lamella. The middle lamella is enriched in many pectic substances, but the mechanism of the cementing process for cell–cell adhesion is unknown. (B) The walls of the pericarp cells of peach swell and soften during ripening, whereas those of the seed coat become an exceptionally tough protective shield for the seed. (C) Like the peach, the tomato pericarp walls swell and soften during ripening, but some of the walls completely disintegrate, by a process called liquefaction, to create locules for the developing seed.

(1→2)α-D-GlcA residue about every 6 to 12 xylosyl residues. The collenchyma generally confines the secondary wall to thickened corners of these cells (see Fig. 2.41C).

The walls of many cells function long after the cells that produced them are dead and desiccated. For example, the orientation of the polymers assembled in the walls of living cells results in mechanical strains on desiccation, strains that result in abscission of plant parts and the dehiscence of fruit coats along defined planes. The paper-thin wings of a maple samara and the feathery tufts of hair cells of dandelion and willow fruits form only on drying: Each structure aids in the scattering of seeds (Fig. 2.43).

Many structural proteins are cell-specific, occurring only in the secondary wall. For example, some PRPs concentrate in the secondary walls of protoxylem elements of bean, whereas some of the GRP family members are synthesized in xylem parenchyma cells and exported to the primary walls of the neighboring protoxylem elements (see Fig. 2.19). Other GRPs are found in sclereids, associated with both the primary and secondary wall. HRGPs generally are found in the primary walls of all tissues, although in widely variable proportions, but a threonine-rich, extensin-like protein of maize is more abundant in the secondary walls of the firm pericarp of popcorn.

Not all cell wall secondary thickenings represent distinct secondary walls. Some thickened walls have a composition typical of a primary wall but simply contain many more strata. Guard cells and epidermal cells thicken the wall facing the environment to a much greater degree than they do the side walls or the inward-facing wall. Pairs of guard cells contain thickenings of radially arranged cellulose microfibrils, which are needed to withstand the enormous turgor pressures generated by the cell during stomatal opening (see Fig. 2.41D). Epidermal cells form specialized exterior layers of cutin and suberin (see next section) to prevent the loss of water vapor, and the contiguous side walls of endodermal cells are impregnated with suberin to force the water to move symplasmically into the stele.

2.6.4 Secondary deposition of suberin and cutin can render cell walls impermeable to water.

Suberin (see Chapters 10 and 24) material is found in specific tissues and cell types, notably, the root and stem epidermis, cork cells of the periderm, the surfaces of wounded cells, and parts of the endodermis and bundle sheath cells. It is recognized by lipid-specific stains such as Sudan IV, which detects the presence of long-chain fatty acids and alcohols, dicarboxylic acids, and hydroxylated fatty acids. The core of suberin is lignin-like, and the attachment of the long-chain hydrocarbons imparts a strongly hydrophobic characteristic to suberin that prevents water movement.

The polyester cutin and its associated waxes (see Chapter 10) also are found on leaf and stem surfaces, providing a strong barrier to the diffusion of water. Waxes generally are esters of long-chain fatty acids and alcohols but are better described as complex mixtures of these hydrocarbon esters with ketones, phenolic esters, terpenes, and sterols.

2.6.5 Lignin is a major component of some secondary walls.

The most obvious distinguishing feature of secondary walls is the incorporation of lignins, complex networks of aromatic compounds called phenylpropanoids. With a few exceptions, no lignin exists in primary walls. Synthesis of lignin is initiated solely when secondary wall deposition commences. The phenylpropanoids, hydroxycinnamoyl alcohols, and "monolignols"—*p*-coumaryl,

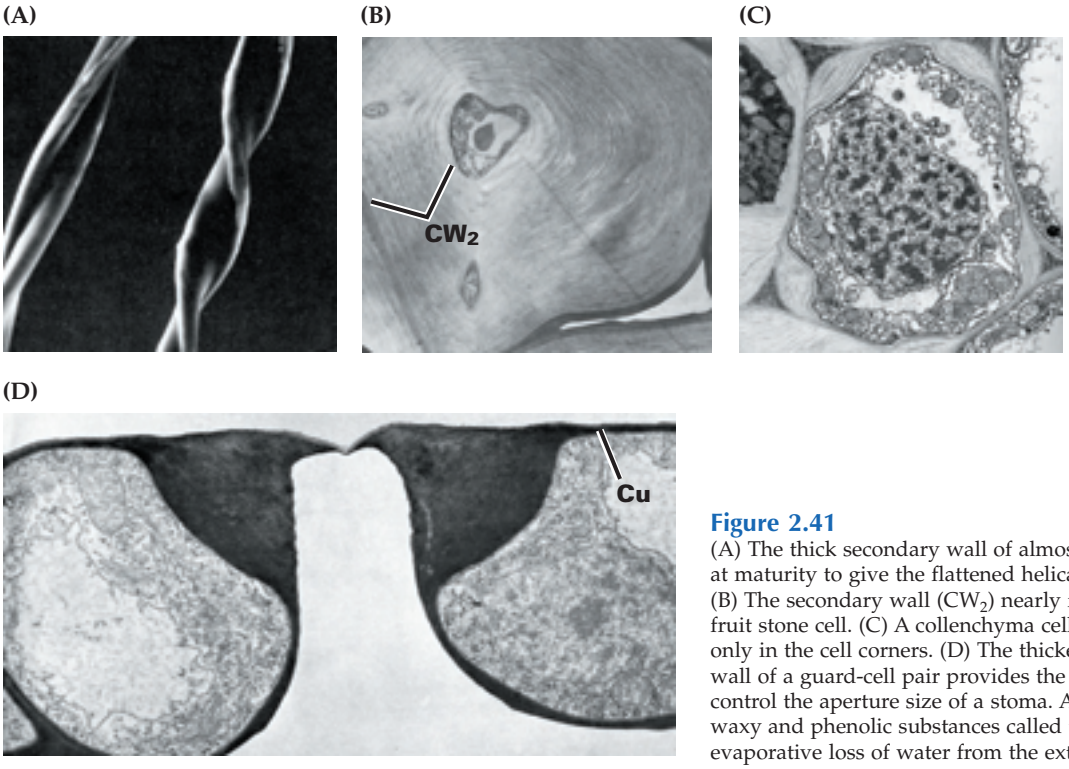

Figure 2.41
(A) The thick secondary wall of almost pure cellulose collapses at maturity to give the flattened helical form to a cotton fiber. (B) The secondary wall (CW_2) nearly fills the lumen of a pear fruit stone cell. (C) A collenchyma cell has reinforced thickenings only in the cell corners. (D) The thickened and elaborated inner wall of a guard-cell pair provides the physical form needed to control the aperture size of a stoma. A special wall outgrowth of waxy and phenolic substances called the cuticle (Cu) minimizes evaporative loss of water from the exterior surface.

coniferyl, and sinapyl alcohols—account for most of the lignin networks (see Chapter 24). The monolignols are linked by way of ester, ether, or carbon–carbon bonds. The diversity of monolignols and their possible intralignol linkages impart remarkable complexity of structure.

Lignins can be detected in tissue sections by specific stains, such as the Mäule reagent, acid fuchsin (Fig. 2.44A), and the Wiesner reagent (phloroglucinol; Fig. 2.44B and 2.44C). The Mäule reagent, a mixture of $KMnO_4$ and ammonia, is particularly useful because it distinguishes syringyl lignin and guaiacyl lignin, indicating the former by a bright red color and the latter by yellow (Fig. 2.44D and 2.44E). Total lignin is quantified by various methods, either chemically or by NMR and other spectroscopic methods. Degradative acidolysis and thioacidolysis, permanganate, nitrobenzene, and alkali/copper oxide oxidation all are used to detect lignin. The oxidation products from these reactions include *p*-hydroxybenzaldehyde, vanillin, and syringaldehyde from *p*-hydroxylphenyl, guaiacyl, and syringyl lignin, respectively. Because all plants contain *p*-hydroxylphenyl, lignins are classified strictly by their guaiacyl and syringyl content. Gymnosperms contain predominantly guaiacyl, whereas woody angiosperms and grasses exhibit a broad range of ratios of guaiacyl–syringyl residues.

The synthesis of monolignols is fairly well documented in plants, and all synthetic reactions appear to occur in the cytosol (see Chapter 24). How monolignols form lignin, however, is not clear. Lignols can be glycosylated in reactions associated with the ER and the Golgi apparatus, and this glycosylation may be necessary for membrane transport and targeting. The extent to which monolignols begin to condense and form associations with carbohydrates or other materials during secretion is unclear. Once in the wall, monolignols and their initial condensation products are polymerized by **peroxidases,** which utilize H_2O_2 as a substrate, or by **laccases,** which use O_2 and participate in the formation of dilignols.

As cells differentiate, many other kinds of ester, ether, and phenyl–phenyl bonds can tightly link an aromatic framework to carbohydrate (see Fig. 2.22). Even lignin is covalently linked to cellulose and xylans in ways that indicate the orientations of polysaccharides may serve as a template for the lignin patterning.

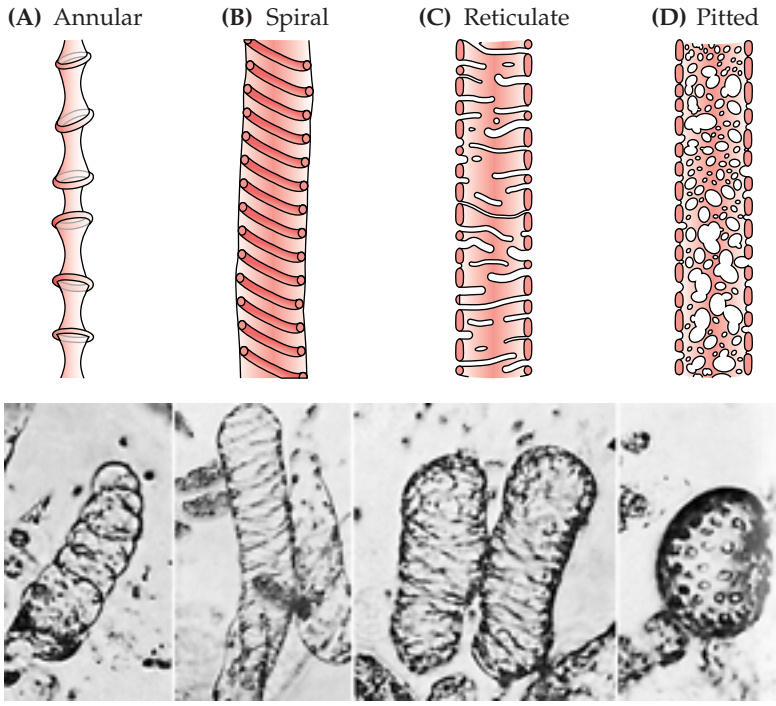

Figure 2.42
The secondary wall thickening patterns of vessel elements in a single plant may be annular, spiral, reticulate, or pitted. Each of these patterns is evident during formation of the tracheary elements in vitro by *Zinnia* mesophyll cells in liquid culture.

Figure 2.43
Cells that produce special walls can function long after death. The sycamore-maple uses the paper-thin walls of a samara as wings for seed dispersal (A). The hard fruit coat of a willow cracks open along a dehiscence zone on desiccation (B). The pattern of microfibril deposition creates a physical tension that causes the fruit to snap open. Like the dandelion (C), the feather tufts of willow trichomes are used for long-distance seed dispersal.

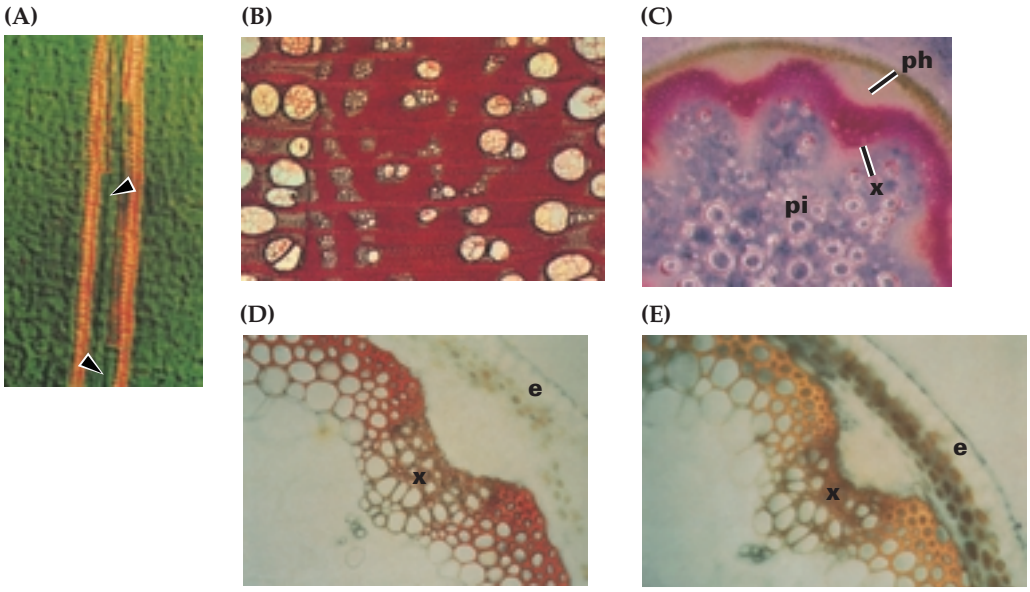

Figure 2.44
Several different procedures can be used to visualize lignin, including (A) acid fuchsin, which produces an orange fluorescence. In this *Arabidopsis* leaf, lignin can be seen in the spiral thickenings of the vessels. Phloroglucinol is a general stain for lignin, as seen in the cross-section of a *Robinia pseudoacacia* stem (B), or the xylem (x) and extraxylary fibers of an *Arabidopsis* floral stem (C). The Mäule reagent produces a red color with syringyl lignin, which is made predominantly from sinapyl alcohols, but forms a yellow color on reacting with guaiacyl lignin, which is made primarily from coniferols (D). This reagent here differentiates a mutant of *Arabidopsis* unable to make syringyl lignin (E). ph, phloem; pi, pith; e, endodermis.

2.6.6 Some secondary walls can serve as storage materials.

Another site of diversity among plant species is in the secondary walls of the cotyledon and the endosperm of developing seeds. These walls contain little or no cellulose but rather consist of a single noncellulosic polysaccharide typically found in the primary wall (see Figs. 2.12, 2.14, and 2.15). These secondary walls serve two functions. First, they provide a strong wall to protect the embryo or impose mechanical dormancy. Second, they contain specialized storage carbohydrates that are digested during germination and converted to sucrose for transport to the growing seedling.

The cotyledon walls of *Tamarindus* and similar legumes, as well as species of Primulaceae (primrose family), Linaceae (flax family), and Ranunculaceae (buttercup family) abound in a Gal-rich XyG. Glucomannans predominate in the cotyledon walls of some lilies and irises. Seeds of date (Fig. 2.45), coconut, and other palms; coffee bean; ivory nut; and seeds of some Apiaceae all contain a thick cotyledon or endosperm wall of almost pure mannan. The endosperm wall of lettuce seeds, which constitutes the mechanical determinant of dormancy, is more than 70% mannan. All endospermic legumes store galactomannans, but the Man:Gal ratio can vary markedly, yielding a variety of galactomannans with very different physical properties. For example, fenugreek *(Trigonella)* makes an almost fully branched galactomannan, whereas guar *(Cyamopsis)* galactomannans and those of the carob or locust bean *(Ceratonia)* are much less branched, which changes their viscosities. Seeds of yet other species accumulate neutral polysaccharides typically found associated with pectins. For example, lupines contain large amounts of (1→4)β-D-galactan, and some arabinan.

All of the grasses accumulate (1→3), (1→4)β-D-glucan in the walls of the endosperm at some stage in embryo development. Oat and barley brans are notably enriched in β-glucans, which make up as much as 30% of the aleurone layer cell walls at maturity.

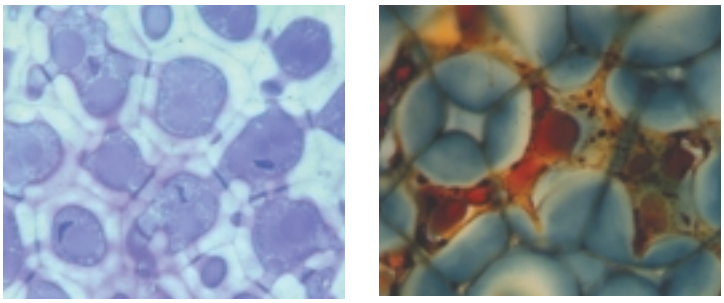

Figure 2.45
Endosperm cells of date *(Phoenix dactylifera)* have extremely hard and thick walls that accumulate mannans. (A) A low-magnification light micrograph of date endosperm shows that these mannans exclude the toluidine blue O dye. (B) Cotyledon walls of the Brazilian legume jatobá (*Hymanaea courbaril*) accumulate "amyloid" xyloglucans that stain lightly with iodine (B).

2.6.7 Walls can be modified experimentally by use of environmental adaptation, mutation, and genetic engineering.

Polysaccharides are not primary gene products, and it has proven difficult to discover precisely the role that each component (and its modifications) plays in the overall mechanical and functional properties of the cell wall or of the tissues that contain them. Cells in liquid culture (Fig. 2.46) have proved useful in a whole range of studies on cell wall metabolism in which wall modifications are induced in response to various environmental stresses. However, given the estimated 1000 gene products involved in cell wall biosynthesis, assembly, and turnover, genetically defined variation offers the most comprehensive approach to addressing function. *Arabidopsis* mutants with altered carbohydrate components in the primary wall have been detected by gas chromatography of alditol acetates of their neutral sugars. More than three dozen mutants have been classified by mapping to 11 different loci in which one or several specific sugars are over- or underrepresented compared with the sugar composition in wild-type plants. Of these, *mur*1 has been identified as a GDP-mannose-4,6-dehydratase, *mur*2 as a fucosyltransferase, and *mur*4 as a C-4 epimerase. However, many cell wall mutants also have been selected on the basis of a growth or developmental phenotype. A mutant in primary wall cellulose synthase, *rsw*1, was selected by a root radial swelling phenotype; a secondary wall cellulose synthase mutant, *irx*3, was selected by its collapsed xylem phenotype. A dwarf hypocotyl mutant, *korrigan,* results from a lesion in a membrane-bound endoglucanase, whereas another dwarf, *acaulis,* is an XET mutant. The *tch*4 mutant is an XET mutant but remains elongated rather than becoming dwarfed, as wild-type plants do, in response to a breeze or gentle touch. As the genes of many cell-wall–modifying enzymes and structural proteins become available, the function of their products will be tested in suppression and overexpression studies.

2.7 Cell walls as food, feed, and fibers

Cell walls directly affect the raw material quality of human and animal food, textiles, wood, and paper and may play a role in human medicine. Modification of various cell wall constituents is a goal in the food processing, agriculture, and biotechnology industries. Successful achievement of this goal depends on understanding the molecular basis for mechanical and textural properties of plant-derived materials.

At present, the food industry uses isolated AGPs and pectins as gums and gelling agents. Fungal and bacterial wall hydrolases are used to adjust food textures and states. The cell walls of fruits and vegetables are now recognized as important dietary components and may protect against cancer of the colon, coronary heart disease, diabetes, and other ailments. β-Glucans are the causal agents in the ability of oat and barley brans to lower serum cholesterol and reduce the insulin demand of people with diabetes. Some pectins may have antitumor activities, possibly by stimulating the immune system after uptake through particular cells of the gastrointestinal tract.

With the advent of biotechnology, agricultural researchers are investigating particular enzymes involved in cell wall metabolism in hopes of producing crops with desired characteristics by enhancing commercially valuable traits (e.g., fiber production in flax, cotton, ramie, and sisal) or abolishing costly ones (e.g., lignification of some plant tissues). For example, the pulp and paper industry, which processes trees into cellulose, and the livestock industry, which depends on the transformation of cell walls into muscle tissue, are striving to reduce the lignin content in their respective sources of fiber and fodder. Reducing lignin content would reduce organochlorine wastes and cut costs tremendously for the paper industry, which currently uses chemical

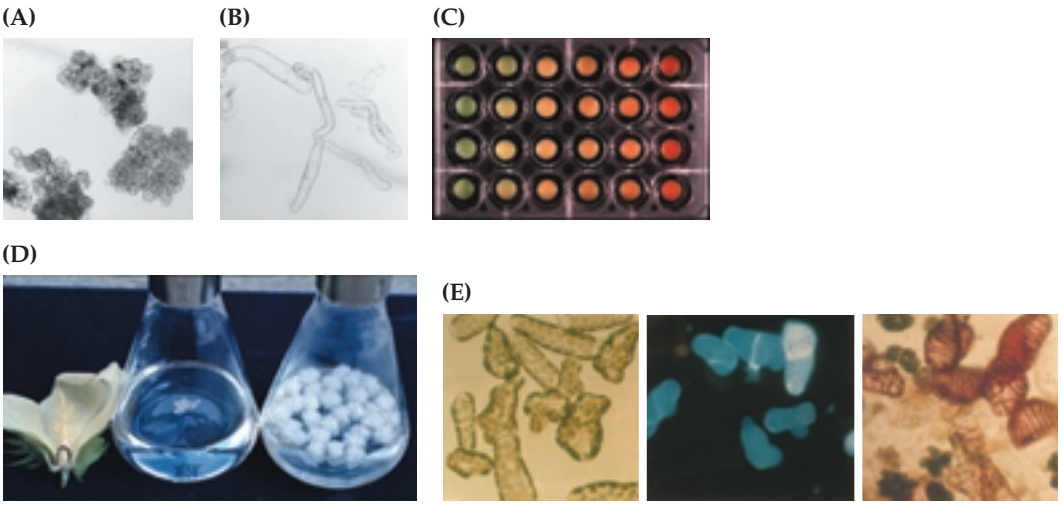

Figure 2.46
In addition to the many plant systems used in cell wall studies, cells in liquid (or suspension) culture are a very useful resource—abundant, homogeneous, and available at all times. Pioneering work with cells of the sycamore-maple *(Acer pseudoplatanus)* provided the first structures of XyG and RG I and II. Cell cultures are generally started by swirling pieces of tissue in flasks of culture medium until the cells break off. The culture is then propagated by diluting a sample of the culture into a fresh flask of medium every 7 days or so. (A) Most media are devised so that small clumps of dividing cells are produced, as shown with this carrot cell suspension culture. (B) The medium conditions can also be altered to induce cell elongation. (C) Sections of immature tomato pericarp will ripen in vitro if provided the proper developmental cues (e.g., ethylene). This system permits plant physiologists to study empirically the biochemical changes that occur in the cell wall during the swelling and softening events. (D) One of the more remarkable examples of cell development in vitro is the formation of cotton fibers by unfertilized ovules in liquid culture. The cotton fibers are epidermal hair cells that elongate for about 3 weeks, achieving a length of almost 3 cm. Toward the end of the elongation phase and primary wall formation, a thick secondary wall of almost pure cellulose is deposited, increasing the mass more than 20-fold and nearly filling the lumen of the fiber cell at maturity, about 2 weeks later. At maturity the fibers of the plant are more than 95% cellulose. (E) *Zinnia* mesophyll cells have been used to study the development of tracheary elements, including the deposition of secondary walls, in vitro. Intact single cells are obtained aseptically by gently mashing young leaves of *Zinnia* in a mortar and pestle and incubating them in a medium containing cytokinin and auxin (left panel). Culture conditions have been optimized so that more than 70% of the cells undergo xylogenesis synchronously. Like those in the plant, these tracheary elements develop thickened secondary walls, which yield a bright fluorescence when stained with Calcofluor (middle panel), and become lignified, as seen by staining with phloroglucinol (right panel).

extractions to purify cellulose from the wood. Lignin–carbohydrate interactions exert a great influence on digestibility of forage crops by animals, and the *kind* of lignin present, rather than the total amount, is often the critical factor. Hence, mutants with altered lignin type may yield new forage crops that exhibit greater digestibility without sacrifice of the strengthening function of lignin to the water-conducting cells of the plant.

Particular foods are being genetically engineered to maximize consumer appeal and to improve their storage characteristics. Target enzymes include PGase, PME, and several polysaccharide hydrolases. The results of attempts to change only one parameter of wall metabolism are rarely those predicted, because of the inherent complexity of the wall and the ability of plant cells to adapt to change. Such biotechnological applications will become ever more common as we understand more of the regulation of cell wall metabolism, particularly regulatory mechanisms for polymer synthesis and wall loosening. As we approach a revolution in the genetic engineering of the crops in our fields, the cell wall is a scientific frontier.

Summary

Cell walls are composed of polysaccharides, proteins, and aromatic substances. The primary wall of the cell is extensible but constrains the final size and shape of every cell. Facing walls of adjacent cells adhere to each other at the middle lamella. In some cells, secondary walls are deposited on the inner surface of the primary wall after growth has stopped. Cell walls become specialized for the function of the approximately 40 cell types that plants comprise.

The cellulose microfibrils form the scaffold of all cell walls and are tethered together

by cross-linking glycans; this framework is embedded in a gel of pectic substances. There are at least two types of primary walls. The Type I walls of dicots and non-commelinoid monocots have xyloglucan–cellulose networks embedded in a pectin-rich matrix and can be further cross-linked with a network of structural proteins. The Type II walls of commelinoid monocots have glucuronoarabinoxylan–cellulose networks in a relatively pectin-poor matrix. Ferulate esters and other hydroxycinnamic acids and aromatic substances cross-link the Type II walls.

The cell wall is born at the cell plate. Cellulose microfibrils are synthesized at the surface of the plasma membrane at terminal complexes called particle rosettes, whereas all noncellulosic cross-linking glycans and pectic substances are made at the Golgi apparatus and secreted. All cell wall sugars are synthesized de novo from interconversion of nucleotide sugars, which are the substrates for polysaccharide synthases and glycosyltransferases.

Cell enlargement depends on the activities of endoglycosidase, endotransglycosylase, or expansin, or some combination of these, but cell shape is largely governed by the pattern of cellulose deposition. Cell enlargement also is accompanied by numerous changes in the structure of the wall's cross-linking glycans and pectin matrix. Termination of cell growth is accompanied by cross-linking reactions involving proteins and aromatic substances.

In addition to their use in wood, paper, and textile products, cell walls are the major textural component in fresh fruits and vegetables and constitute important dietary fibers in human nutrition. Transgenic plants with altered cell wall structures will become an important factor in crop and biomass improvement.

Further Reading

Carpita, N. C. (1996) Structure and biogenesis of the cell walls of grasses. *Annu. Rev. Plant Physiol. Plant Mol. Biol.* 47: 445–471.

Carpita, N. C., Gibeaut, D. M. (1993) Structural models of primary cell walls in flowering plants: consistency of molecular structure with the physical properties of the walls during growth. *Plant J.* 3: 1–30.

Cosgrove, D. J. (1997) Relaxation in a high-stress environment: the molecular bases of extensible cell walls and cell enlargement. *Plant Cell* 9: 1031–1041.

Delmer, D. P. (1999) Cellulose biosynthesis: exciting times for a difficult field of study. *Annu. Rev. Plant Physiol. Plant Mol. Biol.* 50: 245–276.

Gibeaut, D. M., Carpita, N. C. (1994) The biosynthesis of plant cell wall polysaccharides. *FASEB J.* 8: 904–915.

Hadfield, K. A., Bennett, A. B. (1998) Polygalacturonases: many genes in search of a function. Plant Physiol. 117: 337–343.

Jarvis, M. C. (1984) Structure and properties of pectin gels in plant cell walls. *Plant Cell Environ.* 7: 153–164.

McCann, M. C. (1997) Tracheary element formation: building up to a dead end. Trends Plant Sci. 2: 333–338.

McCann, M. C., Roberts, K. (1991) Architecture of the primary cell wall. In *The Cytoskeletal Basis of Plant Growth and Form,* C. W. Lloyd, ed. Academic Press, London, pp. 109–129.

Meier, H., Reid, J.S.G. (1982) Reserve polysaccharides other than starch in higher plants. In *Encyclopedia of Plant Physiology,* Vol. 13A, F. A. Loewus and W. Tanner, eds. Springer-Verlag, Berlin, pp. 418–471.

Rees, D. A. (1977) *Polysaccharide Shapes.* Chapman and Hall, London.

Reiter, W.-D. (1998) *Arabidopsis thaliana* as a model system to study synthesis, structure, and function of the plant cell wall. *Plant Physiol. Biochem.* 36: 167–176.

Showalter, A. M. (1993) Structure and function of plant cell wall proteins. *Plant Cell* 5: 9–23.

Taiz, L. (1984) Plant cell expansion: regulation of cell-wall mechanical properties. *Annu. Rev. Plant Physiol.* 35: 585–657.